DISSECTING THE MOLECULAR BASIS OF BASIL-*PERONOSPORA BELBAHRII*

INTERACTIONS AND GENETIC ENGINEERING FOR DISEASE RESISTANCE

A DISSERTATION SUBMITTED TO THE GRADUATE DIVISION OF THE

UNIVERSITY OF HAWAIʻI AT MĀNOA IN PARTIAL FULFILMENT OF THE

REQUIREMENTS FOR THE DEGREE OF

DOCTOR IN PHILOSOPHY

IN

TROPICAL PLANT PATHOLOGY

DECEMBER 2019

BY

NATASHA NAVET

DISSERTATION COMMITTEE:

MIAOYING TIAN (CHAIRPERSON)

JOHN HU

BRENT S. SIPES

KOON-HUI WANG

DULAL BORTHAKUR (UNIVERSITY REP)

ACKNOWLEDGEMENT

My journey as a Ph.D. student has been a rollercoaster ride with remarkable as well as challenging experiences. In all these years, several people have contributed significantly in shaping my overall being, professionally and personally. Here is a tribute to all those people.

First and foremost, I express my deep sense of gratitude and profound respect to my advisor Dr. Miaoying Tian. It was only due to her valuable guidance, enthusiasm, patience, and extensive knowledge that I was able to complete my research in a credible manner. You have been more than my advisor, a life coach guiding me to improve at every step including, experimental skills, experiment designing, critical thinking, writing skills, confidence building, career advice, presentation skills, organization skills and above all introducing me to the 'world of phytopathology'. Thank you for all your support, persistence and efforts.

I would like to thank my dissertation committee member Dr. Dulal Borthakur for his unequivocal support and for conveying a spirit of optimism, determination for research and excitement in regards to teaching. I would like to thank my other committee members Dr. Brent Sipes and Dr. John Hu for your thoughtful feedback, support, never-ending encouragement, friendliness and most enlivening smile across the hallway. A very special thanks to my dissertation committee member Dr. Koon-Hui Wang, for providing her enduring support, sincerity, motivation and cheerfulness. Thank you, Dr. Janice Uchida, for all your helpful resources and knowledge.

Thank you, Dr. Dongliang Wu, for your assistance and guidance in research related matters. Heartfelt appreciation to my lab mates and friends Dandan Shao, Hannah Dose and Jeremiah Hasley for your help and discussions as well as for making my days brighter.
Thank you to all previous and current lab members whom I have worked with for all kinds of help.

DEDICATION

dedicated to my late grandfather Vijay Singh
&
Parents Sunita & Ashok Navet.

"The most pioneering personalities and anchors of my life"

Grandpa

Your legacy of knowledge, wisdom, principles and virtues will be forever be treasured.

Mom and Dad

Words won't do justice to convey how richfully blessed I am for your ceaseless devoted love, belief, support, care and affection for me that has made me a warrior. Thank you for standing by me in all the ups and downs of my life, yet motivating me to fight against all the odds and to believe in myself.

You have instilled in me the virtues of perseverance and commitment by relentlessly encouraging me to strive for excellence.

Thank you for the constant reminders that I carry the potential in me to achieve anything I set my mind to.

ABSTRACT

Oomycetes form a distinct phylogenetic lineage of eukaryotic microorganisms capable of causing diseases in numerous plants and animals. Downy mildews are among the most devastating phytopathogenic oomycetes that form an obligate biotrophic relationship with their specific host. *Peronospora belbahrii* causes basil downy mildew (BDM), which is considered one of the most threatening diseases of cultivated basil globally. Sweet basil is the most popular herb used extensively in culinary, cosmetic, and therapeutic industry holding a high economic status. However, its production is in jeopardy due to BDM as disease resistance is lacking in sweet basil varieties and introgression of resistant genes through traditional breeding has faced several challenges. Limited fungicides have shown efficacy on BDM disease with a high risk of evolving fungicide resistant pathogen strains. The obligate biotrophic lifestyle of *P. belbahrii* and tetraploidy of sweet basil has hindered the study of basil-*Peronospora belbahrii* molecular-interactions due to lack of effective functional genomic tools. Using two *Peronospora belbahrii* genes with a putative role in pathogenesis and two sweet basil genes with potential functions in host resistance/susceptibility, studies in this dissertation established a set of functional analysis tools for basil and *P. belbahrii* studies. With these tools, the roles of the above genes in disease resistance/susceptibility were defined genetically, which offers initial insights into the molecular basis of basil- *P. belbahrii* interactions. In addition, multiple lines of downy mildew resistant sweet basil plants were generated with potential use in commercial production.

Chapter 2 describes the functional characterization of a sweet basil L-type lectin gene, *Oblectin 1*. Plant lectins are carbohydrate-binding proteins, many of which have been shown to play essential roles in plant immunity. *Oblectin 1* expression was found highly induced in a resistant cultivar during infection by *P. belbahrii*, but not detected in a susceptible one, suggesting its role in resistance to BDM. Transgenic plants ectopically expressing *Oblectin* 1 in a susceptible cultivar Genoveser were successfully generated through *Agrobacterium*-mediated transformation with high transformation efficiency. Homozygous transgenic lines conferred partial resistance to *P. belbahrii*. Through this objective, we developed a highly efficient basil transformation system and genetically defined the role of *Oblectin 1* in resistance against *P. belbahrii*.

Chapter 3 demonstrates the applicability of using host-induced gene silencing (HIGS) approach to decipher the role of two candidate pathogenicity-related genes, *PbEC1* (*Peronospora belbahrii Effector Candidate 1*) and *PbORCER1* (*Peronospora belbahrii*

Oomycete RxLR-Containing Endoplasmic reticulum Resident 1). HIGS relies on an RNAi-based mechanism by which *in planta* generated small-interfering RNAs corresponding to a pathogen gene are transmitted to the pathogen during infection via cross-kingdom movement to silence the targeted gene. The candidate genes selected to test the efficacy of HIGS in basil were on the basis of effector features and sequence uniqueness. Transgenic basil plants, expressing inverted repeats of either *PbEC1* or *PbORCER1* partial coding-sequence flanking a pyruvate orthophosphate dikinase (PDK) intron, were generated. Upon infection, silencing of *PbORCER1* was observed in all tested homozygous lines expressing RNAi constructs of *PbORCER1*, however, silencing of *PbEC1* transcripts on homozygous transgenic plants expressing the *PbEC1* RNAi construct was not consistently observed likely because its expression was highly induced during infection, which masked the detection of silencing. The pathogen growth on homozygous transgenic plants expressing either RNAi construct was markedly reduced. The results suggest that HIGS is operational during sweet basil-*P. belbahrii* interactions, and therefore offers a promising tool for functional genomics studies of *P. belbahrii* and generation of basil downy mildew disease resistance.

Chapter 4 illustrates the establishment of an efficient *Agrobacterium*-delivered CRISPR/Cas9 system for targeted mutagenesis of a basil candidate susceptibility gene, *ObDMR1*. Two CRISPR/Cas9 constructs were developed, targeting different sites of the *ObDMR1* gene. 92% of the transgenic plants displayed successful mutagenesis of *ObDMR1* at one target site. *ObDMR1* editing in sweet basil was shown to be predominantly heterozygous, but a complete knockout of all alleles was successfully achieved in one line in the first generation of transgenic plants. Transgene-free homozygous plants were obtained in the second generation. Homozygous plants having 1-bp frameshift mutations displayed dwarfism at the early seedling stage but later showed normal growth and development resembling wild type. In addition, knockout of *ObDMR1* compromised basil downy mildew susceptibility. Collectively, our data in this chapter demonstrates the success of using CRISPR/Cas9-mediated gene editing to generate complete gene knockout basil mutants, the ease in obtaining transgene-free mutant plants in the successive generation, the development of basil downy mildew resistant plants, and the role of *ObDMR1* in basil downy mildew disease development. These results contribute to the acceleration of basil gene functional analysis, molecular breeding, and development of resistant varieties for commercial use.

Keywords: *Peronospora belbahrii*, basil downy mildew, Genoveser, HIGS, RNAi, lectin, susceptibility gene, ObDMR1, CRISPR/Cas9.

LIST OF ABBREVIATIONS

BDM	Basil downy mildew
bp	Base pair
cDNA	Complementary DNA synthesized from mRNA
CRISPR	Clustered regularly interspaced short palindromic repeat
CRNs	Crinklers
cv.	Cultivar
DAMPs	Damage-associated molecular patterns
dpi	days post inoculation
dsRNA	double-stranded RNA
EER	Glu-Glu-Arg
ER	Endoplasmic reticulum
ETI	Effector-triggered immunity
gDNA	genomic DNA
hr	hour
HIGS	Host-induced gene silencing
InDels	Insertions/deletions
L-type	Legume-type
LxLFLAK	Leu-Xaa-Leu-Phe-Leu-Ala-Lys
Lec	Lectin
LecRLK	Lectin receptor-like kinase
LecRLP	Lectin receptor-like protein
LecP	Lectin -like protein
min	minutes
NAA	1- napthaleneacetic acid
NB-LRR	Nucleotide-binding leucine-rich-repeat
NOD	Nucleotide-binding oligomerization domain
OD_{600}	Optical density measured at $\lambda = 600nm$
ORF	Open reading frame
PAMPs	Pathogen-associated molecular patterns

PCR	Polymerase chain reaction
PRRs	Pattern recognition receptors
PTI	PAMP-triggered immunity
qPCR	Quantitative polymerase chain reaction
R	Resistance
RLPs	Receptor-like proteins
RNAi	RNA interference
rpm	Revolutions per minute
RT	Room temperature
RT-qPCR	Reverse transcription- quantitative polymerase chain reaction
RxLR	Arg-Xaa-Leu-Arg
S	Susceptibility
s	seconds
siRNA	small interfering RNA
TDZ	thidiazuron
T0	First-generation
T1	Second-generation
T2	Third-generation
WT	Wild type

TABLE OF CONTENTS

Contents   **Page**

CHAPTER 1

Plant-pathogen molecular interactions: A brief perspective

CHAPTER 2

Ectopic expression of *Ocimum basilicum* L-type lectin gene *Oblectin 1* in a susceptible cultivar imparts partial resistance to *Peronospora belbahrii*

CHAPTER 3

Functional analysis of *Peronospora belbahrii* candidate pathogenicity-related genes *PbEC1* and *PbORCER1* utilizing host-induced gene silencing

CHAPTER 4

Targeted mutagenesis of basil candidate susceptibility gene *ObDMR1* using CRISPR/Cas9

CHAPTER 5

LIST OF TABLES

LIST OF FIGURES

CHAPTER 1

Plant-pathogen molecular interactions: A brief perspective

Abstract

Plant diseases caused by pathogens pose a significant threat to crop production, impacting the agriculture sector globally. Recent developments in molecular biology and biotechnology have expanded the fundamental knowledge of plant-pathogen interactions by a major fold. High-throughput functional screening methods have helped the scientific community to quickly identify gene function, broadening the application for enhanced disease resistance in plants. Identifying the pathogen determinants involved in pathogenesis and virulence is as prominent as screening of resistance or defense factors in host plants. Many aspects discerning the molecular basis of host resistance and pathogen virulence are underway to provide complete structured information to deploy effective, robust, and durable crop management strategies. This chapter is a short description highlighting the important segments of the current research focus to study the plant-pathogen molecular dynamics.

Keywords: biotechnology, plant-pathogen, molecular interactions, pathogenesis, resistance.

1.1.   Introduction

Plants are the primary producers on earth, vital to the survival of an ecosystem influencing everything from food chains to climate changes. Yet, very little is known about the traits that allow plants to survive in varying conditions or adapt to their respective niche. The plant kingdom has evolved a myriad of strategies to deal with biotic as well as abiotic challenges. Still, the interactions between plant and microbial pathogens display one of the most complex phenomena in biology. Rapidly emerging and evolving phytopathogens pose a significant threat to food security worldwide, where multiple microbial communities harboring the plant hamper its survival collectively. Plant diseases involve diverse symptoms and potentially unlimited exchange of pathogen molecules in cellular components of the plant, determining the fate of host-pathogen compatibility. Agricultural diseases caused by microorganisms can have devastating economic, social and/or ecological consequences on a worldwide scale. Therefore immediate action is required to direct future research to understand the

multidimensional nature of plant-pathogen interactions. Plant pathologists since the early 1900s have been using powerful tools to rigorously identify and evaluate molecules to explain the cause of plant diseases. However, recent discoveries have shown that pathogenicity/virulence factors belong to a complex pathogen genome that invades the host cells with an overwhelming scale of molecular invasion. The interactions between plant-pathogen become furthermore diverse because microorganisms can combine different lifestyles-saprophytic, pathogenic, or symbiotic with undefined boundaries evolving quickly with time. In nature, it has been seen that plants can mount a successful defense against a considerable number of pathogens and are generally resistant to most pathogens where symbiotic and neutral associations dominate, and parasitism is considered as an exception (Zeilinger et al., 2016). To fully comprehend the complex interplay of signals between the host plant and pathogen, it is crucial to decode the function of pathogen and plant signals as well as their respective receptors. All the contributing factors involved in successful infection or resistance offer gripping areas of study to understand the full capability of pathogen and host. It is quite striking that even a single mutational shift in either genes of pathogen or its interacting host receptor has the potential to alter the interactions between plant-pathogen from resistant to susceptible and vice-versa (Giraldo & Valent, 2013). Plants overall health and productivity rely heavily on microbial communication in a given environmental condition conceptualizing the disease triangle model. Conventional agriculture significantly depends on chemicals for warding-off phytopathogens that, unfortunately, cause ecological and health issues. Therefore, breeding seems to be the most acceptable option to select varieties that are resistant to a particular disease. Still, this approach faces several challenges, often leading to nonviable-seed producing varieties. Therefore, modification of the plant defense system against microbial pathogens represents a durable approach for improving disease resistance in economically important crops.

1.2.   Molecular interactions described by the zig-zag model

A plant operates a multifaceted defense signaling mechanism to block pathogen invasion, which predominantly depends upon the invading pathogen and its mode of infection. Thus, it is necessary to understand the plant defense strategy in response to the specific pathogen to gather proper knowledge of pathogenesis and resistance mechanisms. The molecular interactions occurring between a plant-pathogen at the time of contact is exclusively described by Jones and Dangl (Jones & Dangl, 2006). At the cell surface, plants carry specific pattern recognition receptors (PRRs) that recognize pathogen–derived molecules,

called PAMPs (pathogen-associated molecular patterns). This type of recognition activates the first layer of defense response by plant, designated as PAMP-triggered immunity (PTI) (van Schie & Takken, 2014). To suppress PTI, the pathogens rely on their effector repertoires that change host response promoting the compatibility. Effectors secreted from the pathogen are broadly classified into two categories: (1) Extracellular effectors/apoplastic effectors- that mainly resides at the interface between pathogen and its host and functions outside the host cell to alter the host-cell structure. (2) Cytoplasmic effectors- that translocate into the host cells where they interfere with the defense responses of the host. Two important groups of cytoplasmic effectors of plant pathogens include the 'RxLR-effectors' consisting of a signal peptide, a conserved motif Arg-Xaa-Leu-Arg often followed by an EER (Glu-Glu-Arg) and a C-terminal effector domain. The other class of effectors encompasses the 'crinklers' (CRNs) exhibiting a highly conserved N-terminus containing a signal peptide and a Leu-Xaa-Leu-Phe-Leu-Ala-Lys (LxLFLAK) motif followed by a conserved DWL-domain (Wawra et al., 2012, Stassen & Van den Ackerveken, 2011). To counteract the action of effectors, the plants evolved to detect the effectors via host resistance (R) genes. R-gene-mediated immunity termed as ETI (effector-triggered immunity) that encodes intracellular nucleotide-binding leucine-rich-repeat (NB-LRR) proteins, including nucleotide-binding oligomerization domain-like receptors (NOD-like receptors) and receptor-like proteins (RLPs). R proteins act as immune sensors that directly or indirectly perceive effectors triggering distinct molecular mechanisms for resistance (van Schie & Takken, 2014, Tahir et al., 2019). Defense pathways overlap at several levels and are tightly regulated with continuous crosstalk between host and pathogen to determine the fate of overall interactions. The level of disease damage plant experiences varies depending on the outcome of such interactions and the corresponding host responses. Along with molecular interactions, pathogens also require physical connection with their host plant to deliver their repertoires. This model explains the entire complex system that has direct and indirect effects on both plant- and pathogen-directed processes and highlights the importance of studying pathogen to unravel pathogenesis mechanisms as well as analyzing host susceptibility and resistance genes. Since effectors target multiple locations within the cell, studying their location and activity in the host could decipher the mechanisms by which they remodel host defense machinery. Several reports suggest the periodic movement of molecules between plant and its invading pathogen described as 'cross-kingdom' transmission, a strategy that can be exploited to understand the dynamics between plant-pathogen at a deeper molecular level. Advanced biotechnology studies are beginning to unravel the links between the host plant and pathogen interactions at molecular-cellular and

ecological-evolutionary disciplines to realize the full potential of pathosystem genetics and come up with appropriate integrated management strategies.

1.3. Future directions for studying host-pathogen dynamics for the development of disease-resistant plants

The current agriculture system needs refinement to provide sufficient food to the world's growing population, which is projected to spike to at least 9.8 billion by 2050 (Dong & Ronald, 2019). Traditional breeding allows crop improvement but involves a tedious process to select the desired trait from a large population comprising lengthy and labor-intensive steps. Over time precise molecular approaches have emerged including genomics, proteomics, metabolomics, transcriptomics, plant tissue culture and genetic engineering, to broaden the knowledge of host-pathogen dynamics. Genetic engineering refers to the direct alteration of an organism's genetic make-up using biotechnological tools, offering several advantages over conventional breeding to enhance resistance against plant pathogens. It allows the introduction of foreign genes, removal, modification, and manipulation of specific genes-of-interest with minimal or no damage to the rest of the crop genome. As a result, desirable traits in any crop species are easy to achieve in less time over generations. Another advantage of using this powerful tool is the introgression of genetic characteristics from different species and the introduction of new genes into vegetative propagated plants through plant transformation. Accumulated knowledge regarding the molecular mechanisms underlying plant-pathogen interactions and advancements in biotechnology has offered new opportunities for assigning gene roles and engineering resistance in plants against pathogens. Currently, the primary areas of research and application of plant genetic engineering for understanding the basis of plant-pathogen interactions include identification and characterization of plant resistance genes, susceptible plant genes, pathogen-derived resistance factors, and pathogenesis-related genes/gene products described in brief in the following sections.

1.3.1. Identifying pathogen recognition receptors

The ability of a plant to recognize particular patterns of the pathogen (PAMPs) is a common strategy to distinguish between 'self' and 'non-self' molecules (Jones & Dangl, 2006). Such patterns are conserved across species offering broad-spectrum resistance response against varying pathogens. However, not all plants have developed this ability to provide immunity for the invading pathogen. Therefore, screening plant genes (PRRs) using molecular tools

that offer broad-spectrum recognition to varying pathogens is crucial to apprehend the plant immune mechanism (Schwessinger et al., 2015). PAMP detection by PRRs elicits physiological modulations in plant cells triggering a cascade of response essential for the plant to overcome the invasion. Deciphering the fate of activated PRRs is crucial in determining the concept of plant immunity. Functional evaluation and expression profiles of the diverse genes constituting PRR complexes at the cell or organ level are not widely known and require intensive research. Studies involving the comprehensive integration of genetic approaches are needed to understand the development and activation of PRR complexes along with their following links in downstream signaling networks for innate immunity.

1.3.2. Mining resistance genes

Resistance (R) genes enable a plant to overcome effector molecules of the pathogen to prevent susceptibility of the host to infection. R genes continuously evolve to counteract and detect the new emerging effectors (Jones & Dangl, 2006). Identification of a multitude of R genes relating to several pathogens throughout the plant kingdom has been thoroughgoing. Engineering specific resistance provides temporary relief since new effectors emerge in response to the specified R-genes (Kim et al., 2016). Therefore, identification and introgression of R genes that confer robust and durable resistance will open new avenues for selecting breeding lines and understanding signal transduction triggering defense responses (Kim et al., 2016). Advanced molecular approaches are required to recognize the genes from plants outside of a crop's breeding source to ensure sustainability by mining through a vast genetic pool of R genes. Already well-known molecules involved in defense signaling, regulation, or other processes are being exploited to boost basal defense in plants by overexpressing them under the control of a strong constitutively expressing promoter. This strategy takes advantage of using a plant's natural immune system and doesn't involve the introduction of new metabolic pathways allowing the development of enhanced resistant plants. Recent molecular approaches have accelerated the identification of promoters and super-promoters to advance the overexpression studies to study the basal mechanisms of defense.

1.3.3. Modifying plant susceptibility genes

Certain pathogen carries the ability to exploit host genes or gene product/s to colonize, invade, infect and extract nutrients from its compatible host partner; such genes termed as plant susceptibility (S) genes. In many cases, naturally occurring *S* genes have identified in

plant genome without knowing the nature of the corresponding dominant gene. In many other instances, random mutagenesis has produced disease-resistant offspring with mutant *s* genes. Reverse genetic tools have provided *S* gene mutant screens that have demonstrated strategies by which pathogen infection is compromised, some due to imbalanced amino-acid/hormone signaling (Mukhtar et al., 2011). Genetic studies have hypothesized that *S* gene mutant plants offer more durable resistance because of their central role in facilitating the infection and serving as (indirect) negative regulators of plant immunity (Humphry et al., 2011). It has been proposed that in case of host *S* gene null mutants, pathogens will have to evolve new functions to overcome this loss of susceptibility if the S factor serves to be a relevant requirement for the pathogen. Such evolution of a new biological function can be considered to be slow or even impossible, based on the complexity (Wessling et al., 2014). Thus, it is easier for a pathogen to lose or modify a single *R*-gene effector partner to tackle ETI than to overcome the loss of a host susceptibility gene. Modifying or editing susceptibility genes to restrict virulence of the pathogen, holds great potential in crop protection by identifying necessary genes responsible for the infection. It is also important to evaluate the aftermath of modifying susceptibility genes by studying them in detail through molecular approaches before setting them in the field. Versatile genome editing approaches for studying S gene function is rapidly increasing to understand fundamental mechanisms of infection and resistance as these susceptibility factors can be used as bait to either find antagonists that are involved in resistance or downstream transduction (Engelhardt et al., 2018). Besides this, traditional breeding strategies are being improved by exploring susceptibility elements in desired cultivars. For the optimal exploitation of S genes, research with the latest mutagenesis and gene editing approaches should focus on further unraveling the molecular mechanisms and to increase the breeding capacities.

1.3.4. Screening and modification of pathogen genes

Molecular techniques are being utilized to knock down pathogen genes to determine the genes essential for pathogen survival and virulence. Pathogen-derived resistance has been long observed in transgenic plants expressing genes derived from pathogens, often display immunity to the plant (Dong & Ronald, 2019). More studies are undergoing to identify pathogen genes with diverse features and functions to understand the fundamental behavior of the pathogens under different stimuli that can be applied to fill the gaps in understanding the mechanisms between plant and pathogen interactions.

1.4.   Conclusion

Recent developments in the biotechnology sector have opened a new era for scientists working to develop disease-free plants, increase crop yields, and minimize the usage of chemicals to understand the fundamental mechanisms of complex plant-pathogen relations. The pursuit of a molecular basis for plant-pathogen interaction is expected to provide key information that will enable us to realize the necessary steps for food security and sustainable agriculture. For plant scientists, the challenge is to speed up the understanding of the molecular and epidemiological basis of plant diseases and develop practical solutions for preventing, reducing, or managing plant diseases facing modern agriculture today and in the future. Advances in molecular biology, plant pathology and biotechnology have made significant development to overcome such challenges. The emerging databases generated by genomics provide a unique opportunity for the design of more versatile, high-throughput, sensitive, and specific molecular assays to address the major limitations of the current technologies. There is a great need for future research to fully understand the complex nature of plant-pathogen interactions and produce disease-resistant crop plants that are resilient to biotic stresses.

1.5. References

Dong OX, Ronald PC, 2019. Genetic engineering for disease resistance in plants: Recent progress and future perspectives. *Plant Physiol* **180**, 26-38.

Engelhardt S, Stam R, Huckelhoven R, 2018. Good Riddance? Breaking disease susceptibility in the era of new breeding technologies. *Agronomy Journal* **8**, 114.

Giraldo MC, Valent B, 2013. Filamentous plant pathogen effectors in action. *Nat Rev Microbiol* **11**, 800-14.

Humphry M, Reinstadler A, Ivanov S, Bisseling T, Panstruga R, 2011. Durable broad-spectrum powdery mildew resistance in pea er1 plants is conferred by natural loss-of-function mutations in PsMLO1. *Mol Plant Pathol* **12**, 866-78.

Jones JD, Dangl JL, 2006. The plant immune system. *Nature* **444**, 323-9.

Kim SH, Qi D, Ashfield T, Helm M, Innes RW, 2016. Using decoys to expand the recognition specificity of a plant disease resistance protein. *Science* **351**, 684-7.

Mukhtar MS, Carvunis AR, Dreze M*, et al.*, 2011. Independently evolved virulence effectors converge onto hubs in a plant immune system network. *Science* **333**, 596-601.

Schwessinger B, Bahar O, Thomas N*, et al.*, 2015. Transgenic expression of the dicotyledonous pattern recognition receptor EFR in rice leads to ligand-dependent activation of defense responses. *PLoS Pathog* **11**, e1004809.

Stassen JH, Van Den Ackerveken G, 2011. How do oomycete effectors interfere with plant life? *Curr Opin Plant Biol* **14**, 407-14.

Tahir J, Rashid M, Afzal AJ, 2019. Post-translational modifications in effectors and plant proteins involved in host-pathogen conflicts. *Plant Pathology* **68**, 628-44.

Van Schie CC, Takken FL, 2014. Susceptibility genes 101: how to be a good host. *Annu Rev Phytopathol* **52**, 551-81.

Wawra S, Belmonte R, Lobach L, Saraiva M, Willems A, Van West P, 2012. Secretion, delivery and function of oomycete effector proteins. *Curr Opin Microbiol* **15**, 685-91.

Wessling R, Epple P, Altmann S*, et al.*, 2014. Convergent targeting of a common host protein-network by pathogen effectors from three kingdoms of life. *Cell Host Microbe* **16**, 364-75.

Zeilinger S, Gupta VK, Dahms TE*, et al.*, 2016. Friends or foes? Emerging insights from fungal interactions with plants. *FEMS Microbiol Rev* **40**, 182-207.

CHAPTER 2

Ectopic expression of *Ocimum basilicum* L-type lectin gene *Oblectin 1* in a susceptible cultivar imparts partial resistance to *Peronospora belbahrii*

Abstract

Plant lectins are carbohydrate-binding proteins, many of which have been shown to play essential roles in plant immunity. Basil downy mildew (BDM) caused by the obligate biotrophic oomycete *Peronospora belbahrii* is among the most devastating basil disease leading to a significant production loss globally. Due to the lack of efficient control strategies and the highly evolving nature of the pathogen, understanding the resistance mechanism of basil is urgently required to promote breeding. Transcriptional profiling of a resistant and a susceptible basil cultivar during infection revealed strong induction of a gene, which encodes for a protein with N-terminal signal peptide and a C-terminal L-type lectin domain; designated *Oblectin 1,* present only in the disease-resistant cultivar. Quantitative reverse transcription PCR (RT-qPCR) confirmed its high levels of expression in the resistant cultivar during the early infection time course, but undetected in the susceptible cultivar, suggesting a plausible role of *Oblectin 1* in mediating resistance. To genetically identify its role and generate disease-resistant plants, *Oblectin 1* was ectopically expressed in the susceptible cultivar Genoveser using *Agrobacterium*-mediated stable transformation. High transformation efficiency was achieved in generating multiple transgenic lines with varying transgene expression levels. An approach coupling a kanamycin resistance assay with quantitative PCR was adopted to attain homozygous transgenic lines in the successive second and third generations. Infection assays showed that homozygous transgenic lines conferred partial resistance to *P. belbahrii*, indicated by reduced pathogen proliferation determined by qPCR. This result implicates that the L-type lectin gene *Oblectin 1* in basil serves as one of the key players in providing resistance against BDM.

Keywords: lectin, *Peronospora belbahrii*, *Oblectin 1*, BDM, transformation, L-type lectin

2.1. Introduction

Plants are subject to constant attacks by a broad range of pathogens, including oomycetes, bacteria, fungi, viruses, and nematodes. Global food security is highly threatened by the ever-increasing loss of crops due to plant diseases in the face of the rising human population in the

21st century. The key to tackle this issue is to accelerate the fundamental understanding of plant-pathogen interactions by studying pathogenesis and resistance mechanisms in-depth to reinforce crop management strategies.

Pathogen entry into host cells involves a critical step and takes place through natural openings such as stomata, hydathodes, lateral roots, accidental wounds, or specialized structures like haustoria; or through the action of lytic enzymes (Lannoo et al., 2014). Filamentous plant pathogens (fungi and oomycetes) rupture plant cell walls by releasing enzymes to dismantle polysaccharides, proteins, and lignin-based polymers (Chaliha et al., 2018, Zhao et al., 2013). The resultant fragmented products termed as damage-associated molecular patterns (DAMPs), which accumulates in the apoplastic fluids or extracellular spaces, serving to be the first molecular interaction between plant and pathogen interface, exposing the pathogen to plant membranes. The apoplastic interface also represents the zone where plants come in direct contact with microbes to distinguish between symbionts and pathogens, based on their molecular-pattern signatures, termed as pathogen-associated molecular patterns (PAMPs) (Chaliha et al., 2018). PAMPs also play an essential role in the fitness/survival of the pathogen and includes a broad range of molecules such as carbohydrates, lipids, proteins, peptides, lipooligosaccharides of gram-negative bacteria, bacterial flagellin, glucans, glycoproteins from oomycetes, glycolipids, chitin from fungal cell wall, etc. (Zhang & Zhou, 2010, Chaliha et al., 2018). PAMPs-triggered immunity (PTI) plays a pioneer role in providing non-host resistance as well as basal resistance to non-adapted or adapted pathogens (Saijo et al., 2018, Boutrot & Zipfel, 2017). As a counter-strategy, the pathogens secrete an arsenal of virulence effectors to overpower PTI to establish a successful infection. However, the host recognizes one or more effectors via intracellular nucleotide-binding (NB) leucine-rich repeat (LRR) domain receptors to activate robust ETI (Saijo et al., 2018). Overall the pathogens experience a complex orchestrated two-tiered plant immune system comprised of pathogen-associated molecular patterns (PAMPs)-triggered immunity (PTI) and effector–triggered immunity (ETI) (Dangl & Jones, 2001, Chisholm et al., 2006, Jones & Dangl, 2006). Differences in the activation of these regulatory networks have direct consequences on resistance/susceptibility to the invading pathogen. PTI confers broad resistance towards pathogens, while ETI is race-specific as effectors are highly polymorphic. PTI and ETI are always under strong negative selection pressure, provoking the genes involved to rapidly evolve, resulting in a molecular arms race between pathogen and host determining the fate of interaction (van Schie & Takken, 2014).

Lectin-like (Lec)-proteins embodies a diverse set of plant protein/molecules, highly variable in structure and occurring insoluble as well as membrane-associated form (De Schutter & Van Damme, 2015). Lectins are carbohydrate-binding proteins ubiquitously present in all kingdoms of life, having the capability to selectively recognize and bind reversibly to specific glycosylated macromolecules such as glycolipids, proteoglycans, polysaccharides and free sugars, but display no enzymatic activity towards the recognized sugar (Bellande et al., 2017). Calcium/magnesium or any other metal ion binding sites of lectins are known to mediate direct interactions with sugar molecules (Bellande et al., 2017). The strong affinity between lectins and their carbohydrate-binding partners is often achieved through multivalent interactions in the form of oligomerization (di- or tetramerizations) of two or more lectin domains (Boraston et al., 2004). Lectin groups are classified under highly diverse protein families based on their sugar specificity, displaying considerable structural diversity based on their folds and carbohydrate-binding site architectures (De Schutter & Van Damme, 2015). Based on amino acid sequences, structures, and properties of the lectin domain(s), lectins are classified into several types including, C-type lectins that require calcium ions for carbohydrate-binding, G-type lectins that fall under *Galanthus nivalis* agglutinin-related proteins and L-type lectins abundantly found in legume seeds. On the basis of domain organization, lectin proteins fall under three predominant categories: (i) LecRLK (Lectin receptor-like kinase), constituting signal peptide, lectin domain, transmembrane domain and intracellular kinase domain; (ii) LecRLP (Lectin receptor-like protein, sharing similar properties as LecRLKs except the lack of the kinase domain; and (iii) LecP, soluble protein with only signal peptide and lectin domain (Bellande et al., 2017). In addition to the classification based on structural domains, lectins are also grouped based on expression patterns: (i) constitutively-expressing lectins, present at high concentration, (ii) inducible plant-lectins, present at a low basal level (De Schutter & Van Damme, 2015). The constitutively-expressing lectins are secretory proteins routed either to the vacuole for deposition in seeds and specialized vegetative storage tissue acting as storage proteins or to the vacuole, extracellular space and the plasma membrane suggesting a role in plant defense (Bellande et al., 2017, Lannoo & Van Damme, 2014, De Schutter & Van Damme, 2015). Inducible plant lectins are low abundant proteins responding to biotic and abiotic stresses by upregulating their expression, located throughout the plant cell in cytoplasm and nucleus, proposing to play an important role in plant-stress physiology (Lannoo & Van Damme, 2010, De Schutter & Van Damme, 2015). Most of the known plant lectins carry one or more lectin domains coupled with other unrelated domains such as aerolysin, AIG1, chitinase, dirigent,

F-box, Kelch, kinase, LRR, NB-ARC, PAG, or TIR domains (Lannoo & Van Damme, 2014).

Carbohydrate moieties of the pathogen (PAMPs) or plant (DAMPs) origin are critical determinants of host-pathogen interactions (Lannoo et al., 2014). The characteristic of plant lectins to bind carbohydrate ligands allows these modulatory proteins to play roles in various cellular processes such as plant immunity, symbiosis, and plant development, both intra- and extra-cellularly (Lannoo & Van Damme, 2014, Bellande et al., 2017, Van Holle & Van Damme, 2018). Carbohydrate-binding lectin proteins are reported to recognize the characteristic epitopes of plant pathogens or damage-associated patterns, using protein-protein interactions or/and protein-glycan interactions to initiate immune responses at the host-pathogen interface (Lannoo et al., 2014). Many lectins are found to be involved in plant defenses against pathogens (Lannoo & Van Damme, 2014). For example, overexpression of salicylic acid (SA)-induced legume lectin-like protein 1 (SAI-LLP/LecP-I.7) in Arabidopsis was reported to induce defense against *Pseudomonas syringae*, supporting the finding that plant LecPs contribute in plant immunity (Wang & Bouwmeester, 2017). Some LecRLKs and LecRLPs are known to serve as PRRs to recognize PAMPs initiating PTI (Lannoo & Van Damme, 2014). The role of LecRKs in plant immunity was exemplified by lectin domain-containing Arabidopsis L-type *LecRK-I.9, whose* mutants showed susceptibility to the bacterium *Pseudomonas syringae* and two oomycetes *Phytophthora brassicae* and *Phytophthora capsici*; on the other hand, the overexpression of *LecRK-I.9* enhanced resistance against these three pathogens (Wang et al., 2016c). Consistent with this, a recent study showed that the ectopic expression of Arabidopsis *LecRK-I.9* and *LecRK-IX.1,* which is another L-type LecRK*,* in *Nicotiana benthamiana* conferred resistance to *Phytophthora* (Wang et al., 2018). Such studies show that proteins carrying the L-type lectin domain play a key role in mediating defense responses against the invading pathogen. However, the understanding of L-type lectin function from various plant species is still limited. Up till now, no L-type lectin genes have been characterized for their function in plant immunity in *Ocimum* species.

Global production of basil, a popular herb widely used in food, therapeutics, and cosmetic industries, is threatened by an obligate biotrophic oomycete *Peronospora belbahrii*, causing basil downy mildew (BDM) (Wyenandt et al., 2010, da Costa et al., 2015). *Ocimum basilicum*, commonly known as sweet basil, holds high economic importance, is highly susceptible to *P. belbahrii* (Wyenandt et al., 2015). Current control strategies for BDM rely

on a handful of fungicides with low efficacy and the risk of evolving fungicide-resistant strains (Cohen et al., 2017, Wyenandt et al., 2015). Besides, a broad application of chemicals poses a high threat to human health and the environment, adding to the extra production cost. Oomycetes (kingdom Stramenopila) are notorious phytopathogens with a high evolutionary potential to overcome host-resistance, fungicide-resistance, and capability to jump to a new host (Stassen & Van den Ackerveken, 2011). No identified *Ocimum* species among sweet basil offers resistance or tolerance against BDM, which has compelled scientists to expand genetic resistance in sweet basil (Cohen et al., 2017). Traditional breeding involving interspecific hybridization has been a challenge in developing resistant sweet basil cultivars due to sexual incompatibility, hybrid F1 sterility, and difficulty in segregating undesirable traits (Ben-Naim et al., 2018, Cohen et al., 2017). Therefore, extensive research is required to study the role of resistance components to expand the knowledge about plant-oomycete interactions.

A better understanding of immune defense response mechanisms of *P. belbahrii* is essential to explore resistance gene pool for breeding and to deploy durable disease-control cultivars of sweet basil. This finding led us to investigate the function of a candidate *Oblectin 1* gene, identified in a resistant cultivar with high expression during the early infection stage. Here, we report the cloning of this L-type LecP, *Oblectin 1,* obtained from resistant basil and its ectopic expression in a susceptible cv. Genoveser by generating transgenic plants. Transgenic basil lines ectopically expressing *Oblectin 1* were generated using *Agrobacterium*-mediated stable transformation. Compared with the non-transformed wild-type plants, homozygous third-generation transgenic plants displayed enhanced resistance towards BDM pathogen growth and proliferation at the early infection stage, suggesting that *Oblectin 1* functions as a defense-related factor.

2.2.   Materials and Methods

2.2.1. Plant materials and growth conditions

Basil cultivars Genoveser, BA107 and Dolly seeds were provided by Enza Zaden and were grown in 3.5'' square pots (McCONKEY) filled with soil mix (SunGro Horticulture Sunshine Mix #4) and cultivated in controlled growth chamber under following conditions: 25 °C, 50% relative humidity, a 12/12 hrs day/night photoperiod intensity of 125 μmolm^{-2}s^{-1} provided by cool white fluorescent bulbs. The same growth conditions were applied to regenerated

transgenic T0 (first-generation) basil plants as well as T1 (second-generation) and T2 (third-generation) basil plants. Well developed T0 and T1 basil plants were grown in the greenhouse in 11 cm diameter round pots (McCONKEY) with 16 hrs light/8 hrs of the dark period at 25-27 °C. Selfing bags were mounted at the beginning of flowering to control cross-pollination. Genoveser cultivar was used for *Agrobacterium*-mediated transformation. Plant food fertilizer was provided to growing plants once a week as per the company's instructions.

2.2.2. mRNA-seq analysis and gene annotation

To dissect the molecular basis specifying host resistance and pathogen virulence of basil-*P. belbahrii* interactions, multiplexing mRNA-seq analysis, was performed with samples from *P. belbahrii* sporangia, and leaves of both susceptible (Dolly) and resistant (BA107) basil cultivars (cv.) during the infection time course. Samples were collected for *P. belbahrii* sporangia, susceptible cultivar Dolly (non-infected, infected at 1-day post-inoculation (dpi), 2dpi), and resistant cultivar BA107 (non-infected, infected at 1dpi and 2dpi). Total RNA was isolated using the QIAGEN RNeasy Plant Mini Kit and treated with DNA-free kit (Ambion) to remove any contaminating genomic DNA. Libraries for Illumina sequencing were prepared using TruSeq RNA Sample Prep Kit v2. Multiplexing PE-100 mRNA sequencing was performed in one lane with the Hiseq2500 system. Reads were aligned against transcripts of the Indian sweet basil (Rastogi et al., 2014) and analyzed using DESeq (Anders & Huber, 2010). Basil transcripts up-regulated at least fivefold during infection compared with non-infected plants were annotated using Blast2GO (Conesa et al., 2005) against the Arabidopsis database. Selected genes of interest were also subjected to NCBI Conserved domain search (Marchler-Bauer et al., 2017) and InterProScan (Jones et al., 2014) to predict gene functions. The presence of a secretion signal peptide was predicted using SignalP 5.0 (Almagro Armenteros et al., 2019).

2.2.3. Vector construction

The plant binary vector pE1776 (Lee et al., 2007) was modified to incorporate a double-HA tag for expressing C-terminal fusion proteins. The modified plasmid was designated as pE1776-2HA (M. Tian unpublished). The DNA fragment encoding the open reading frame (ORF) of BA107 *Oblectin 1* with the stop codon removed was cloned to pE1776-2HA through XhoI and SpeI restriction sites. The DNA fragment was amplified from cDNA generated from BA107 infected leaf tissue at 1dpi. The primers BA107lectin1-FXhoI (5'-

GCG<u>CTCGAG</u>ATGAACAAATTCCTCAAAACCCT-3') and BA107lectin1-RSpeI (5'-GCG<u>ACTAGT</u>CTCATCAGTCCTTAAACTACCCGA-3') were used for the amplification. The introduced restriction sites are underlined, followed by gene-specific sequences. Sanger sequencing of the resultant plasmids was performed to confirm the sequence of the insert. The resultant pE1776-2HA-Oblectin1 was transformed into *Agrobacterium tumefacians* EHA105 using electroporation (Mersereau et al., 1990).

2.2.4. Stable transformation

Sweet basil cv. Genoveser was transformed with *Agrobacterium tumefacians* EHA105 harboring plasmid pE1776-2HA-Oblectin1 using the method described previously with slight modifications (Deschamps & Simon, 2002, Phippen & Simon, 2000). Agrobacteria strain carrying the desired plasmid, stored at -80 °C, were streaked on LB plate supplemented with 50 μg/ml Kanamycin, 5 μg/ml Chloramphenicol and 15 μg/ml Rifampicin and grown for two days at 28 °C. On the day of basil transformation, bacterial cells were scraped from the overnight plate and suspended in *Agrobacterium* inoculation media (IN) [MS + 3% sucrose + 16.8 μM TDZ (thidiazuron), pH 5.7, supplemented with 200 μM acetosyringone] to OD_{600} = 0.6. This suspension was incubated at room temperature (RT) in the dark with gentle shaking at 70 rpm for 2 hrs. Meanwhile, the first pair of true leaves from 3-week-old Genoveser plants was plucked and surface sterilized in 12% (v/v) Clorox solution for 5 min. Two explants were excised from regions close to the leaf base along the midrib of each leaf using cork borer number 2. After the completion of *Agrobacterium* suspension incubation, the explants were immersed in this suspension for 30 min at RT. Explants were then taken out, and the excess suspension was removed by pressing the explants gently between two layers of sterile filter paper. These explants were co-cultivated with *Agrobacteria* on callus and shoot induction (SI) media (MS + 0.8% agar + 3% sucrose + 16.8 μM TDZ, pH 5.7) supplemented with 200 μM acetosyringone, with the abaxial side facing the media, for three days in the dark at 25 °C. For induction and selection of transgenic calli and shoots, explants were transferred to SI media supplemented with 200 μg/ml Timentin and 30 μg/ml Kanamycin), and grown for 4-6 weeks in dark at 25 °C with sub-culturing every two weeks onto fresh media. Once the shoots developed on calli, they were transferred to Root Induction (RI) media [MS + 0.8% agar + 3% sucrose + 0.054 μM NAA (1- napthaleneacetic acid), pH 5.7] supplemented with 200 μg/ml Timentin and 30 μg/ml Kanamycin, and grown for 1 week in the dark at 25 °C, and later under a 12-hrs photoperiod cycle for 4-8 weeks with regular

sub-culturing performed every two weeks. Plantlets with properly defined root and shoot systems were removed from media jars, washed thoroughly with water to remove the media, and then planted in moistened soil (SunGro Horticulture Sunshine Mix #4). The plants were grown under 100% relative humidity for 3 to 4 days in a tray covered with a plastic dome in a growth chamber set at 25 °C with a 12-hrs photoperiod. Humidity was gradually reduced over the next 2 to 3 days, and then the plants were transferred to the greenhouse to harvest seeds. As soon as the flowering stalks emerged, selfing bags were mounted on the stalks to collect seeds. The seeds were harvested manually and stored at RT with proper aeration.

2.2.5. Genetic confirmation of transgene integration by PCR

Approximately 50 mg leaf tissue from newly regenerated transgenic basil lines were excised and put in cryo-vial tubes with a stainless metallic bead (5 mm). Crude gDNA from the leaf tissues was extracted by crushing the sample using 400 μl of DNA Extraction buffer [200mM Tris-HCl (pH 7.5), 250mM NaCl, 25mM EDTA and 0.5% SDS] in a Beat beater (FastPrep-24 by MP Biomedicals) at 4.0 m/s speed for 20 s. The following DNA isolation steps were performed as per (Shao & Tian, 2018) wherein the entire homogenized solution was centrifuged at 13000 rpm for 10 min. The resulting supernatant (300 μl) was mixed with an equal volume of 100% isopropanol and incubated at RT for 10 min. The supernatant was discarded after 10 min centrifugation at full speed. The pellets were washed with 1 ml of chilled 70% ethanol and centrifuged at full speed for 1 min. The supernatant was completely removed, and the pellets were air-dried at RT for 1 hr. The pellet was finally resuspended in 100 μl AE buffer (QIAGEN DNeasy Plant Mini Kit) and stored at 4 °C overnight. The gDNA was quantified using Nanodrop 2000 spectrophotometer (Thermo Scientific). 1 μl of this crude gDNA was used as a PCR template using primers BA107Oblectin1-F: 5'-TTCAACGGAAGTCGACCAAC-3' and R-HA-Tag-R: 5'-AGCGTAATCTGGAACATCGTATGGGTA-3' for amplifying the inserted *Oblectin 1* fragment within the vector cassette using Phusion High-fidelity DNA polymerase (M0530S-New Englands Biolab). PCR conditions started with an initial denaturation of 30 s at 98 °C, followed by 35 cycles of 98 °C for 15 s at for denaturation, 15 s at 67 °C for annealing (as calculated using Tm calculator from NEB Tm calculator) and 60 s at 72 °C for elongation with final extension at 72 °C for 7 min. PCR products were visualized on a 1% agarose gel by electrophoresis under 120 V for 35 min.

2.2.6. Gene expression analysis of *Oblectin 1* during infection and in T0 transgenic sweet basil lines

For gene expression of *Oblectin 1* during infection, 4-week-old Dolly and BA107 plant were spray inoculated with *P. belbahrii* sporangial suspension (2×10^4 sporangia/ml). Infected whole leaves were collected immediately after inoculation, and 1- and 2-days post-inoculation (dpi). Samples were ground in liquid nitrogen using mortar and pestle for RNA isolation. For the expression of *Oblectin 1* in the first generation (T0) transgenic sweet basil lines, leaf discs were collected in 1.5 ml micro-centrifuge tubes, rapidly frozen in liquid nitrogen, and ground using blue pestle (Axygen Scientific Inc). Total RNA was isolated using QIAGEN RNeasy Plant Mini Kit as per the instruction manual. All the RNA samples were treated with DNA-free kit (Ambion) to remove any contaminating genomic DNA. Synthesis of the first strand of cDNA from 1μg RNA was performed using the Invitrogen SuperScript II Reverse Transcription Kit according to kit's instructions. Specific primers for RT-qPCR were designed to yield a product size of 100-120bp were BA107Oblectin1-RTF: 5'-TTCAACGGAAGTCGACCAAC-3' & BA107Oblectin1-RTR: 5'-ATTACACCGCCGCTATCATC-3'; Ob-β-tubulin-F: 5'-GCTTGCTGTCAATCTCATTCC-3' & Ob-β-tubulin-R: 5'-TCTGGAACAGTGAGTGCTCTG-3'. Constitutively expressed *Ocimum basilicum β-tubulin* was used as an internal control to normalize the expression of the *Oblectin 1* gene. RT-qPCR reactions were set up using SsoAdvanced Universal SYBR green supermix (Bio-Rad), following the manufacturer's instructions. A 20 μl PCR reaction was set up as follows: 1X SYBR Green supermix, 0.25 μM specific primers, 100 ng cDNA. The program was run in BioRad C1000 Touch Thermal Cycler machine following the initial heating at 95 °C for 30 s, then 40 thermal cycles of denaturation at 95 °C for 10 s, annealing and elongation at 60 °C for 60 s. The final melting was performed by heating to 95 °C, cooling down to 65 °C and rising back to 95 °C at 0.1 °Cs^{-1}. For gene expression of *Oblectin 1* during infection, the data were analyzed using constitutively expressed *Ocimum basilicum β-tubulin* gene as an internal control and compared with the gene expression at 0 dpi by calculation of the fold change ($2^{-\Delta\Delta Ct}$) (Livak & Schmittgen, 2001a). For the expression level of *Oblectin 1* in T0 plants, the relative expression was calculated as $2^{-\Delta Ct}$ using the *β-tubulin* gene as an internal control.

2.2.7. Kanamycin resistance assay followed by qPCR for determination of transgene zygosity

Seeds of self-pollinated plants along with WT were germinated at the same time for transgene segregation analysis of second-generation (T1) and third-generation (T2) sweet basil plants derived from selected T0 transgenic sweet basil lines. A 25 µl drop of 40 µg/ml kanamycin solution was dropped in the center of the first pair of true leaves of 18 days-old basil plants (WT, T1 & T2). The plants were provided with 100% humidity for a day by sealing the trays with dome and placed under light racks at 25 °C with 12 hrs light period. After 10 days, the results were observed by counting the number of plants that turned yellow or remained green in color at the areas treated with kanamycin. Further 10 T1 transgenic basil plants that remained green upon kanamycin drop assay along with WT were used for qPCR analysis following (German et al., 2003) method to detect their transgene zygosity. WT and T1 basil plants that turned yellow upon the treatment were used as control samples. Genomic DNA was isolated from 100 mg of leaf tissues, which were flash-frozen in liquid nitrogen and ground to a fine powder using blue pestle (Axygen Scientific Inc), following QIAGEN DNeasy Plant Mini Kit instructions. 10 ng gDNA was used to set up a 20 µl qPCR reaction containing 1X SYBR Green mix, 0.25 µM specific primers (Oblectin1-qPCR-F: 5'-TTTCGCGGGTATTCTGTTTC-3' & Oblectin1-qPCR-R: 5'-TTTTGACTAGCGAGGCTTGG-3' to amplify *Oblectin 1,* or Ob-β-tubulin-F and Ob-β-tubulin-R to amplify the reference gene *Ocimum basilicum β-tubulin,* used as an internal control). qPCR program was run in Bio-Rad C1000 Touch Thermal Cycler machine with similar conditions as described in section 2.2.7. The amplification was quantified by calculating as $2^{-\Delta Ct}$ (Livak & Schmittgen, 2001b).

2.2.8. Pathogen inoculation and disease quantification

Peronospora belbahrii was isolated from basil plants found in City Mill, Oahu, Hawaii. The infected plants were placed in humid conditions overnight and the sporangia were collected from detached leaves by swirling in deionized water. The propagation and inoculation of *P. belbahrii* on basil were followed as per (Shao & Tian, 2018) procedure. 4-week old basil plants (WT and selected T2 transgenic plants) were inoculated by pipetting four drops of 10 µl sporangial suspension (2×10^4 sporangia/ml) on the first pair of true leaves. Samples from one set of plants were harvested at 4-days post-inoculation (dpi) for pathogen biomass quantification using qPCR. Another set of plants was kept for observation of symptoms. For

pathogen quantification, 3 inoculated leaves from three infected plants were collected as one sample serving as one biological replicate. A total of three biological replicates were analyzed for each line. As soon as the leaves were plucked, they were wrapped in aluminum foil, frozen in liquid nitrogen, and stored at -80 °C until further use. Once sporulation was observed on WT plants, which indicated a successful infection assay, the samples were subjected to gDNA isolation followed by qPCR to quantify pathogen biomass as described previously (Shao & Tian, 2018).

2.3.   Results

2.3.1. Identification of *Oblectin 1* as a candidate gene involved in basil resistance against *Peronospora belbahrii*

To screen potential basil genes involved in resistance against *P. belbahrii*, an initial analysis was conducted using multiplexing mRNA-seq data on infected leaf samples of a resistant cultivar (cv.) BA107 and susceptible cv. Dolly during the infection time course. A gene encoding a putative L-type lectin from BA107, designated as *Oblectin 1*, found to be induced at both 1-day post-inoculation (dpi) and 2-dpi compared with the non-infected control. When using Oblectin 1 as a query to perform the BLASTN search against Dolly transcriptome, no hits were found, implying the absence of a close homolog in Dolly. To validate these results, the expression pattern of *Oblectin 1* was determined by RT-qPCR. The results of qRT-PCR were consistent with the mRNA-seq analysis. The expression of *Oblectin 1* was induced by 65 and 22 fold at 1- and 2-dpi compared with the control for the resistant cv. BA107, but undetected in the susceptible cv. Dolly (Figure 2.1.). *Oblectin 1* was highly induced during infection in a resistant cultivar but not present in a susceptible one, suggesting its role in resistance against *P. belbahrii*.

Oblectin 1 encodes a protein of 271 amino acids. NCBI Conserved Domain search revealed a sizeable conserved domain (Accession: cd06899) of 227 amino acids (29-256) that are commonly present in proteins belonging to lectin_L-type superfamily (cl14058), including legume lectins, lectin-like receptor kinases, arcelin, concanavalinA, and alpha-amylase inhibitor. The conserved features of this functional domain were mapped to the amino acid sequences of Oblectin 1, including a metal-binding site at E^{151}, D^{153} and H^{165}, an N-linked glycosylation site at D^{139}, a homodimer interaction site composed of seven residues (T^{29}, S^{30}, I^{32}, T^{41}, H^{81}, I^{84} and K^{230}), a tetradimer interaction site with 14 residues (T^{29}, S^{30}, I^{32}, T^{41}, H^{81},

I^{84}, N^{177}, R^{193}, S^{204}, H^{214}, F^{215}, Q^{216}, G^{218} and K^{230}) of 17 commonly found in such domain. Signal peptide prediction using SingalP-5.0 identified a putative signal peptide with a likelihood of 0.9953, and the cleavage site between S^{24} and Q^{25} with a probability of 0.7805, suggesting Oblectin 1 encodes a secreted protein. The signal peptide and conserved domain shared by lectin L-type superfamily were also identified using the InterProScan tool. Altogether, these analyses suggested that Oblectin 1 encodes a secreted L-type lectin, represented by a schematic diagram (Figure 2.2.).

2.3.2. Generation of transgenic plants ectopically expressing *Oblectin 1*

To test whether *Oblectin 1* can confer resistance to *P. belbahrii* in a susceptible cultivar, we generated transgenic basil lines ectopically expressing *Oblectin 1* in susceptible cv. Genoveser. *Agrobacterium tumefacians* EHA105 carrying the binary vector pE1776-2HA-Oblectin1 to express *Oblectin 1* fused with a double-HA tag at the C-terminus was used for stable transformation of three-week-old Genoveser explants. After infection with *Agrobacterium* suspension, the explants were co-cultivated with Agrobacteria on callus and shoot induction (SI) media plates supplemented with acetosyringone (Figure 2.3a) for 3 days in the dark. Calli appeared two weeks after transferring and culturing the explants on kanamycin-containing SI media, and shoot buds emerged from calli with regular sub-culturing on fresh media (Figure 2.3b). Shoots with prominent stalks were placed on root induction media (RI) for shoot elongation and root development (Figure 2.3c). Well-developed roots were observed in the regenerated plants after growing on RI media for four weeks, with two weeks under the dark and another two weeks under light conditions (Figure 2.3d). The fully regenerated plants (Figure 2.3e) were acclimatized into the soil after they attained a certain height and allowed to grow in a controlled environment (Figure 2.4f). Fully developed regenerated plants were further transferred in a greenhouse to produce second-generation (T1) seeds. Six independent transformation experiments were carried out, with varied transformation efficiency ranging from 17-76% (Table 2.1.). In total, 110 plantlets with well-defined shoots and roots were regenerated (Table 2.1.). The entire experiment cycle from infection of the explants with *Agrobacteria* to regenerated plantlets with well-defined shoots and roots took approximately three months. 42 regenerated plants were successfully acclimatized into the soil.

2.3.3. Expression levels of *Oblectin 1* in T0 transgenic sweet basil lines

We randomly selected 18 T0 basil plants out of 42 that were acclimatized into the soil to

determine the integration of the transgene into the *O. basilicum* Genoveser genome by PCR using primers (Figure 2.4a) to amplify an 830-bp fragment containing partial *Oblectin 1* and the double-HA coding sequence. All 18 regenerated plants were tested positive for the presence of transgene, suggesting successful integration through stable transformation (Figure 2.4b). These were named and labeled as T0 basil lines #1-18. To examine the expression levels of *Oblectin 1* in independent T0 transgenic basil plants, 16 T0 transgenic basil lines (#1-#16) along with WT were pursued for RT-qPCR analysis. Varying levels of expression were detected in 50% of the T0 basil lines. The highest transcript level was observed for line #6 displaying a relative expression of 8.5, followed by #4, #3, #7 and #8 with a relative expression between 3-4 (Figure 2.4c). Either low or no expression of *Oblectin 1* was detected for the remaining tested T0 basil lines. T0 basil lines #3, #4, #6, #7 and #8 were chosen for further analysis to test the role of *Oblectin 1* in plant resistance to *P. belbahrii*. These selected basil lines were self-hybridized to harvest T1 sweet basil seeds.

2.3.4. Selection of T1 transgenic sweet basil plants ectopically expressing *Oblectin 1*

To identify potential homozygous transgenic basil plants in T1 segregating populations, T1 basil plants of five selected T0 basil lines #3, #4, #6, #7 and #8 were subjected to kanamycin resistance assay to determine the presence of transgene, followed by qPCR to determine transgene copy number (zygosity). Since transfer DNA (T-DNA) contains the *NPTII* selectable marker gene (Figure 2.4a) that confers resistance to kanamycin, we used this characteristic to develop a simple method to identify T1 basil plants either heterozygous or homozygous for the transgene. The kanamycin-treated leaves from the homozygous as well heterozygous plants were expected to remain green due to their kanamycin resistance, in contrast to the yellowing (whitening) phenotype shown in plants null of the transgene. Kanamycin resistance assay was performed on 18-day-old T1 and WT Genoveser plants. 10 days later, all WT basil plants turned yellow (later white) at the point of contact with kanamycin drop, whereas a certain percentage of T1 basil plants showed discoloration while others maintained normal green leaves (Figure 2.5.). The counts of T1 basil plants that turned yellow or remained green upon kanamycin drop are listed in Table 2.2. This accounting was done to estimate the segregation ratio. As sweet basil is allotetraploid, we expected to observe a 3:1 ratio of green plants to discolored plants. However, we did not observe this pattern clearly, maybe because the total number of plants tested for each line was not large enough, the expression of kanamycin resistance was not high, or the genetics of the allotetraploid sweet basil did not strictly behave like a diploid organism. In any case, this

assay allowed us to identify the transgenic plants without labor-intensive molecular testing. Line #4 was excluded from further analysis as the T1 populations contained a low percentage of green plants (Table 2.2.). 10 T1 green plants with one yellow plant derived from each independent T0 basil lines together with the corresponding T0 plant were further subjected to qPCR to identify the potential homozygous transgenic plants. In the qPCR assay, the amplification of the *Oblectin 1* fragment was normalized using *β-tubulin* as the reference gene, and calculated as $2^{-\Delta Ct}$ values (Table 2.3.). Although we expected to get the results belonging to three categories: plants that scored around double the amplification value with respect to T0, plants that showed the same value as T0, and plants that had no amplification similar to WT, we did not obtain the clear-cut results. In this case, we selected 3-4 T1 plants with the highest amplification for each T0 line for propagation to get T2 seeds. These included #3-2, #3-5, #3-7 and #3-10; #6-1, #6-3, #6-5 and #6-7; #7-1, #7-3, #7-7 and #7-10; #8-5, #8-7 and #8-9. The chosen T1 basil lines were self-crossed to produce third-generation (T2) seeds.

2.3.5. Selection of T2 homozygous -transgenic sweet basil lines for pathogen assay

T2 basil plants from fifteen self-pollinated T1 transgenic basil lines (#3-2, #3-5, #3-7 and #3-10; #6-1, #6-3, #6-5 and #6-7; #7-1, #7-3, #7-7, #7-10; #8-5, #8-7 and #8-9) were subjected to kanamycin resistance assay to determine the homozygosity. Kanamycin resistance of T2 basil plants was evaluated by counting the number of plants that turned yellow or remained green, as shown in Table 2.4. Except for #3-2 and #3-5, T2 basil plants derived from other T1 basil lines all remained green, suggesting that these T1 basil lines and the derived T2 basil plants are homozygous. Four homozygous T2 basil lines #3-7, #6-7, #7-3, and #8-9 were selected for infection assay to evaluate the role of the *Oblectin 1* gene in resistance against *P. belbahrii*. In a previous study, it was reported that the overexpression of *AtLecRK-I.9* in Arabidopsis led to more compact leaf rosettes with smaller and slightly wrinkled leaves (Bouwmeester et al., 2011). In parallel with this, T2 transgenic basil lines (#3-7, #6-7, #7-3 and #8-9) were analyzed for any visible growth or developmental alterations. Seeds of these selected T2 basil lines together with WT were planted at the same time by sowing two seeds in each square pot. The growth of seedlings was later monitored for any morphological alterations starting from 1-week-old plantlets until six weeks. 4-week-old plantlets were photographed, showing similar phenotypes as WT. All transgenic selected homozygous T2 basil plants exhibited normal development such as germination time, leaf morphology,

branching, and plant height similar to untransformed WT (Figure 2.6.).

2.3.6. Homozygous T2 sweet basil lines inhibit pathogen proliferation during an early infection time course

Oblectin 1 showed induced expression at 1- and 2-dpi during infection in a resistant cv. BA107, suggesting its possible role in mediating resistance against *P. belbahrii*. In order to investigate the function of *Oblectin 1* in susceptible cv. Genoveser, accumulation and proliferation of pathogen in homozygous T2 basil lines (#3-7, #6-7, #7-3 and #8-9) ectopically expressing *Oblectin 1* was assessed using qPCR following pathogen infection. 4-week old plants were inoculated with 2 x 10^4 sporangia ml^{-1} and samples were collected 4-days post-inoculation (4-dpi) to run qPCR. A significant reduction in pathogen biomass was observed for all tested lines (Figure 2.7.) compared to WT. The relative pathogen biomass at 4 dpi in #6-7, #3-7, #7-3 and # 8-9 was 0.02, 0.11, 0.16 and 0.63 respectively, in comparison to 1.09 in WT (Figure 2.7.). Symptom development was assessed by monitoring chlorosis and tissue collapse after 15 dpi, which were visible in all inoculated plants, including T2 transgenic basil lines, but developed later in T2 transgenic basil lines compared to WT. Altogether, these results suggested that ectopically expressing *Oblectin 1* in a susceptible cultivar enhanced resistance to *P. belbahrii*; however, the resistance was not able to provide complete protection from this pathogen under the infection conditions we applied.

2.4. Discussion

Plants are exposed to a challenging environment all the time, resisting the abiotic and biotic stressors. Therefore, plants have developed an intricate network to harmonize responses to multiple stimuli by modulating various genes that participate in signal transduction, recognition, and transcriptional regulation (Ma et al., 2018). L-type or legume-like lectin proteins are known to likely perform roles in maintaining cell wall integrity by sensing cell wall/membrane alterations under multiple stresses (Wu et al., 2014). Little has been known about the molecular mechanisms underlying LecRLK/LecRLP/LecPs-dependent defense responses, despite the handful reports deciphering the function and signaling pathways of LecRLKs (Balague et al., 2017). The mRNA-seq analysis identified *Oblectin 1* gene to be differentially expressed between disease resistant (BA107) and susceptible (Dolly) cultivar (cv.). This result was validated using qRT-PCR that displayed induced expression of *Oblectin 1* in BA107 at 1- and 2-dpi, whereas no expression was seen in Dolly (Figure 2.1.). The amino acid sequence of Oblectin 1 revealed the presence of a signal peptide along with an L-

type lectin domain carrying N-glycosylation site and metal-ion binding sites. The open reading frame of BA107 *Oblectin 1*, was introduced into susceptible cv. Genoveser plants through *Agrobacterium*-mediated transformation after successful cloning in binary vector pE1776-HA-tag (Figure 2.4a). Multiple T0 transgenic basil plants overexpressing *Oblectin 1* were obtained as a result of a successful and efficient transformation system developed for basil. Different levels of expression of *Oblectin 1* were identified for independent T0 transgenic lines, while a few lines did not show any expression (Figure 2.4c). Variation in expression could be attributed to the fact that stable transformation using *Agrobacterium* leads to the integration of the transgene at random sites affecting the expression of the transgene (Hwang et al., 2017). T0 basil plants with relatively high expression of *Oblectin 1* were selected for the propagation of T1 seeds. A simple screening method, kanamycin resistance assay followed by qPCR, was adopted to select the basil plants carrying the homozygous transgene in the segregating T1 population. As sweet basil is allotetraploid, T1 plants are expected to follow a segregation trend as per the Mendelian ratio of 3:1 in kanamycin resistance characteristic, distinguishing the plants carrying transgene versus transgene-null plants. Further qPCR assay enables us to discriminate homozygous from heterozygous transgenic plants using the parental T0 plants to calibrate the transgene copy number, with the copy number of the homozygotes expected to be the double of heterozygotes or the parental T0 plant. Differentiation between homozygous and heterozygous transgenic plants in the segregating population is essential to identify the role of the targeted gene using genetically uniformed plants. Our data displayed variations in segregating kanamycin resistance ratios as well as qPCR values, which could be due to various reasons including small percentage of plants used for each tested line, low expression of kanamycin resistance due to position effect of transgene, or the genetics of allotetraploid sweet basil that did not strictly follow a diploid fashion. There are other factors too that influence transgene expression and inheritance, including transgene itself, the host genome and the interaction between them (Tizaoui & Kchouk, 2012). Nevertheless, kanamycin resistance assay coupled with qPCR allowed us to quickly and easily identify homozygotes without the labor-intensive methods. T2 sweet basil lines uniformly displaying no discoloration upon kanamycin treatment were presumed to be homozygous and selected for further inoculation assay. Homozygous T2 basil lines #3-7, #6-7, #7-3 and #8-9, supported reduced pathogen growth on leaves infected with *P. belbahrii* at 4-days post-inoculation (Figure 2.7.). Our results suggest that *Oblectin 1* gene functions as a resistance component to reduce pathogen biomass at an early stage of infection, making the plants more tolerant to the

disease. More experiments of pathogen infection assay are needed to confirm this finding. Additionally, morphology assessment of homozygous transgenic T2 basil lines #3-7, #6-7, #7-3 and #8-9 displayed no aberrant developmental defects due to transgene integration and/or expression.

Although literature has shown that lectin domain-containing proteins play roles in plant defense, functional studies of this gene family in basil have not been carried out previously. Currently, breeding for resistance has primarily focused on exploiting the introgression of resistance (*R*) genes that mediate ETI upon recognition of compatible effectors, but oomycetes can quickly evolve to modify the effectors to circumvent *R* gene recognition making such approach non-durable (Wang et al., 2016c). As a number of L-type lectins serve as PRR to initiate PTI, therefore they are hypothesized to provide broad-spectrum resistance. Due to the elaborate roles played by L-type lectins in various host plants, they represent ideal candidates to explore plant-pathogen interactions in depth. *Oblectin 1* did not impart full resistance against *Peronospora belbahrii* in this study, but further characterization of more L-type-lectin domain-containing proteins will offer a valuable avenue for studying plant-pathogen molecular interactions to promote breeding for improved downy mildew resistance in basil.

2.5.   References

Almagro Armenteros JJ, Tsirigos KD, Sonderby CK*, et al.*, 2019. SignalP 5.0 improves signal peptide predictions using deep neural networks. *Nat Biotechnol* **37**, 420-3.

Anders S, Huber W, 2010. Differential expression analysis for sequence count data. *Genome Biol* **11**, R106.

Balague C, Gouget A, Bouchez O*, et al.*, 2017. The Arabidopsis thaliana lectin receptor kinase LecRK-I.9 is required for full resistance to Pseudomonas syringae and affects jasmonate signalling. *Mol Plant Pathol* **18**, 937-48.

Bellande K, Bono JJ, Savelli B, Jamet E, Canut H, 2017. Plant lectins and lectin receptor-like kinases: How do they sense the outside? *Int J Mol Sci* **18**.

Ben-Naim Y, Falach L, Cohen Y, 2018. Transfer of downy mildew resistance from wild basil (Ocimum americanum) to sweet basil (O. basilicum). *Phytopathology* **108**, 114-23.

Boraston AB, Bolam DN, Gilbert HJ, Davies GJ, 2004. Carbohydrate-binding modules: fine-tuning polysaccharide recognition. *Biochem J* **382**, 769-81.

Boutrot F, Zipfel C, 2017. Function, discovery, and exploitation of plant pattern recognition receptors for broad-spectrum disease resistance. *Annu Rev Phytopathol* **55**, 257-86.

Bouwmeester K, De Sain M, Weide R*, et al.*, 2011. The lectin receptor kinase LecRK-I.9 is a novel Phytophthora resistance component and a potential host target for a RXLR effector. *PLoS Pathog* **7**, e1001327.

Chaliha C, Rugen MD, Field RA, Kalita E, 2018. Glycans as modulators of plant defense against filamentous pathogens. *Front Plant Sci* **9**, 928.

Chisholm ST, Coaker G, Day B, Staskawicz BJ, 2006. Host-microbe interactions: shaping the evolution of the plant immune response. *Cell* **124**, 803-14.

Cohen Y, Ben Naim Y, Falach L, Rubin AE, 2017. Epidemiology of basil downy mildew. *Phytopathology* **107**, 1149-60.

Cohen Y, Vaknin M, Ben-Naim Y*, et al.*, 2013. First report of the occurence and resistance to mefenoxam of Peronospora belbahrii, causal agent of downy mildew of basil (Ocimum basilicum) in Isreal. *Plant Disease* **97**, 692.

Conesa A, Gotz S, Garcia-Gomez JM, Terol J, Talon M, Robles M, 2005. Blast2GO: a universal tool for annotation, visualization and analysis in functional genomics research. *Bioinformatics* **21**, 3674-6.

Da Costa AS, Arrigoni-Blank MF, De Carvalho Filho JLS*, et al.*, 2015. Chemical diversity in basil germplasm. *The Scientific World Journal*.

Dangl JL, Jones JD, 2001. Plant pathogens and integrated defence responses to infection. *Nature* **411**, 826-33.

De Schutter K, Van Damme EJ, 2015. Protein-carbohydrate interactions as part of plant defense and animal immunity. *Molecules* **20**, 9029-53.

Deschamps C, Simon JE, 2002. Agrobacterium tumefaciens-mediated transformation of Ocimum basilicum and O. citriodorum. *Plant Cell Reports* **21**, 359-64.

German MA, Kandel-Kfir M, Swarzberg D, Matsevitz T, Granot D, 2003. A rapid method for the analysis of zygosity in transgenic plants. *Plant Science* **164**, 183-7.

Hwang HH, Yu M, Lai EM, 2017. Agrobacterium-mediated plant transformation: biology and applications. *Arabidopsis Book* **15**, e0186.

Jones JD, Dangl JL, 2006. The plant immune system. *Nature* **444**, 323-9.

Jones P, Binns D, Chang HY*, et al.*, 2014. InterProScan 5: genome-scale protein function classification. *Bioinformatics* **30**, 1236-40.

Lannoo N, Van Damme EJ, 2010. Nucleocytoplasmic plant lectins. *Biochim Biophys Acta* **1800**, 190-201.

Lannoo N, Van Damme EJ, 2014. Lectin domains at the frontiers of plant defense. *Front Plant Sci* **5**, 397.

Lannoo N, Van Damme EJ, Albenne C, Jamet E, 2014. Plant glycobiology-a diverse world of lectins, glycoproteins, glycolipids and glycans. *Front Plant Sci* **5**, 604.

Lee LY, Kononov ME, Bassuner B, Frame BR, Wang K, Gelvin SB, 2007. Novel plant transformation vectors containing the superpromoter. *Plant Physiol* **145**, 1294-300.

Livak KJ, Schmittgen TD, 2001a. Analysis of relative gene expression data using real-time quantitative PCR and the 2-DELTADELTACT method. *Methods (Orlando)* **25**, 402-8.

Livak KJ, Schmittgen TD, 2001b. Analysis of relative gene expression data using real-time quantitative PCR and the 2(-Delta Delta C(T)) Method. *Methods* **25**, 402-8.

Ma N, Liu C, Li H*, et al.*, 2018. Genome-wide identification of lectin receptor kinases in pear: Functional characterization of the L-type LecRLK gene PbLRK138. *Gene* **661**, 11-21.

Marchler-Bauer A, Bo Y, Han L*, et al.*, 2017. CDD/SPARCLE: functional classification of proteins via subfamily domain architectures. *Nucleic Acids Res* **45**, D200-D3.

Mcgowan J, Fitzpatrick DA, 2017. Genomic, network, and phylogenetic analysis of the oomycete effector arsenal. *mSphere* **2**.

Mersereau M, Pazour GJ, Das A, 1990. Efficient transformation of Agrobacterium tumefaciens by electroporation. *Gene* **90**, 149-51.

Phippen WB, Simon JE, 2000. Anthocyanin inheritance and instability in purple basil (Ocimum basilicum L.). *J Hered* **91**, 289-96.

Rastogi S, Meena S, Bhattacharya A*, et al.*, 2014. De novo sequencing and comparative analysis of holy and sweet basil transcriptomes. *BMC Genomics* **15**, 588.

Saijo Y, Loo EP, Yasuda S, 2018. Pattern recognition receptors and signaling in plant-microbe interactions. *Plant J* **93**, 592-613.

Schmittgen TD, Livak KJ, 2008. Analyzing real-time PCR data by the comparative C(T) method. *Nat Protoc* **3**, 1101-8.

Shao D, Tian M, 2018. A qPCR approach to quantify the growth of basil downy mildew pathogen Peronospora belbarhii during infection. *Current Plant Biology* **15**, 2-7.

Stassen JH, Van Den Ackerveken G, 2011. How do oomycete effectors interfere with plant life? *Curr Opin Plant Biol* **14**, 407-14.

Tizaoui K, Kchouk ME, 2012. Genetic approaches for studying transgene inheritance and genetic recombination in three successive generations of transformed tobacco. *Genet Mol Biol* **35**, 640-9.

Van Holle S, Van Damme EJM, 2018. Signaling through plant lectins: modulation of plant immunity and beyond. *Biochem Soc Trans* **46**, 217-33.

Van Schie CC, Takken FL, 2014. Susceptibility genes 101: how to be a good host. *Annu Rev Phytopathol* **52**, 551-81.

Wang Y, Bouwmeester K, 2017. L-type lectin receptor kinases: New forces in plant immunity. *PLoS Pathog* **13**, e1006433.

Wang Y, Bouwmeester K, Beseh P, Shan W, Govers F, 2014. Phenotypic analyses of Arabidopsis T-DNA insertion lines and expression profiling reveal that multiple L-type lectin receptor kinases are involved in plant immunity. *Mol Plant Microbe Interact* **27**, 1390-402.

Wang Y, Nsibo DL, Juhar HM, Govers F, Bouwmeester K, 2016b. Ectopic expression of Arabidopsis L-type lectin receptor kinase genes LecRK-I.9 and LecRK-IX.1 in Nicotiana benthamiana confers Phytophthora resistance. *Plant Cell Rep* **35**, 845-55.

Wang Z, Cheng J, Fan A*, et al.*, 2018. LecRK-V, an L-type lectin receptor kinase in Haynaldia villosa, plays positive role in resistance to wheat powdery mildew. *Plant Biotechnol J* **16**, 50-62.

Wu T, Wang R, Xu X, *et al.*, 2014. Cucumis sativus L-type lectin receptor kinase (CsLecRK) gene family response to Phytophthora melonis, Phytophthora capsici and water immersion in disease resistant and susceptible cucumber cultivars. *Gene* **549**, 214-22.

Wyenandt CA, Simon JE, Mcgrath MT, Ward DL, 2010. Susceptibility of basil cultivars and breeding lines to downy mildew (*Peronospora belbahrii*). *HortScience* **45**, 1416-9.

Wyenandt CA, Simon JE, Pyne RM*, et al.*, 2015. Basil Downy Mildew (Peronospora belbahrii): Discoveries and Challenges Relative to Its Control. *Phytopathology* **105**, 885-94.

Zhao Z, Liu H, Wang C, Xu JR, 2013. Comparative analysis of fungal genomes reveals different plant cell wall degrading capacity in fungi. *BMC Genomics* **14**, 274.

Zhang J, Zhou JM, 2010. Plant immunity triggered by microbial molecular signatures. *Mol Plant* **3**, 783-93.

Tables

Table 2.1. *Agrobacterium*-mediated transformation efficiency to ectopically express *Oblectin 1* in sweet basil cv. Genoveser.

Expt #	Explants	Shoot regeneration #	Root development #	# Plants Acclimatized (T0)	Transformation efficiency (%)
1	78	120	20	13	25.64
2	63	95	11	6	17.46
3	65	109	19	4	29.23
4	50	90	22	5	44.00
5	25	50	19	9	76.00
6	32	40	19	5	59.37

Table 2.2. Kanamycin resistance assay on segregating transgenic sweet basil T1 population derived from T0 sweet basil lines expressing exogenous *Oblectin 1*.

	No. of plants turned yellow	No. of plants remained green	Total no. of plants
WT	70	0	70
#3 T0	27	27	54
#4 T0	12	40	52
#6 T0	12	41	53
#7 T0	12	59	81
#8 T0	23	47	70

Table 2.3. $2^{-\Delta Ct}$ values obtained through qPCR to determine zygosity of T1 sweet basil plants from segregating T1 population.

T0	#3		#6		#7		#8	
	T1 #	$2^{-\Delta ct}$	T1 #	$2^{-\Delta ct}$	T1 #	$2^{-\Delta ct}$	T1 #	$2^{-\Delta ct}$
	3-1	0.3737	6-1	0.3562	7-1	0.4512	8-1	0.1407
	3-2	0.3852	6-2	0.3472	7-2	0.4328	8-2	0.1847
	3-3	0.0666	6-3	0.3628	7-3	0.5098	8-3	0.1873
	3-4	0.0630	6-4	0.3345	7-4	0.1717	8-4	0.1970
	3-5	0.3756	6-5	0.4765	7-5	0.4365	8-5	0.2866
	3-6	0.1252	6-6	0.3465	7-6	0.3165	8-6	0.2061
	3-7	0.4129	6-7	0.3521	7-7	0.5277	8-7	0.3660
	3-8	0.1087	6-8	0.3142	7-8	0.3780	8-8	0.2003
	3-9	0.1931	6-9	0.3331	7-9	0.3038	8-9	0.3407
	3-10	0.5612	6-10	0.3464	7-10	0.4823	8-10	0.1977
	3-T0	0.044	6-T0	0.2663	7-T0	0.819	8-T0	0.2402
	3-y*	0.0004	6-y*	0.0019	7-y*	2.1994	8-y*	0.0001
	WT	0.0004	WT	0.0012	WT	0.0006	WT	0.00007

y* T1 transgenic sweet basil plant that turned yellow upon kanamycin drop application

Table 2.4. Kanamycin resistance assays on transgenic T2 sweet basil plants of selected T1 transgenic sweet basil lines.

Plant ID	No. of plants remained green	No. of plants turned yellow	Total no. of plants tested
#3-2 T1	2	23	25
#3-5 T1	1	15	16
#3-7 T1	20	0	20
#3-10 T1	18	0	18
#6-1 T1	15	0	15
#6-3 T1	19	0	19
#6-5 T1	17	0	0
#6-7 T1	21	0	0
#7-1 T1	21	0	21
#7-3 T1	27	0	27
#7-7 T1	16	0	16
#7-10 T1	21	0	21
#8-5 T1	30	0	30
#8-7 T1	40	0	40
#8-9 T1	32	0	32
WT	0	98	98

Figures
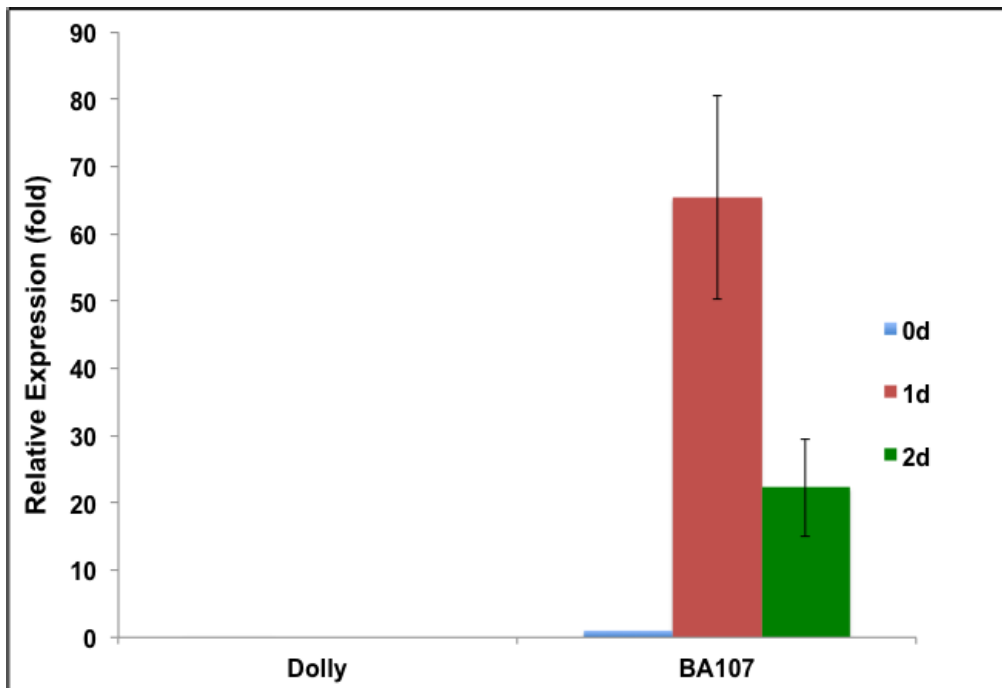
Figure 2.1. *Oblectin 1* **is highly induced in a resistant cultivar during infection by** *Peronospora belbahrii.* Relative expression (fold change) of *Oblectin 1* during infection of Dolly and BA107 at 0,1 and 2 days post inoculation (dpi) determined by qRT-PCR, with amplification of *Ocimum basilicum β-tubulin* as an endogenous control. The expression level at 0 day was set to 1. Error bars represent standard deviations from three technical replicates.
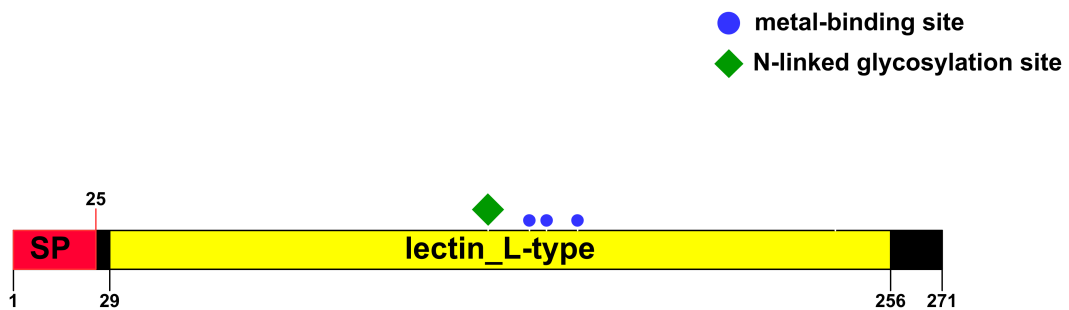
Figure 2.2. Schematic illustration of Oblectin 1 domain structures. Oblectin 1 spanning 271 amino acids contains a signal peptide (SP), and a conserved lectin_L-type domain with metal-binding and N-linked glycosylation sites as shown in the figure.
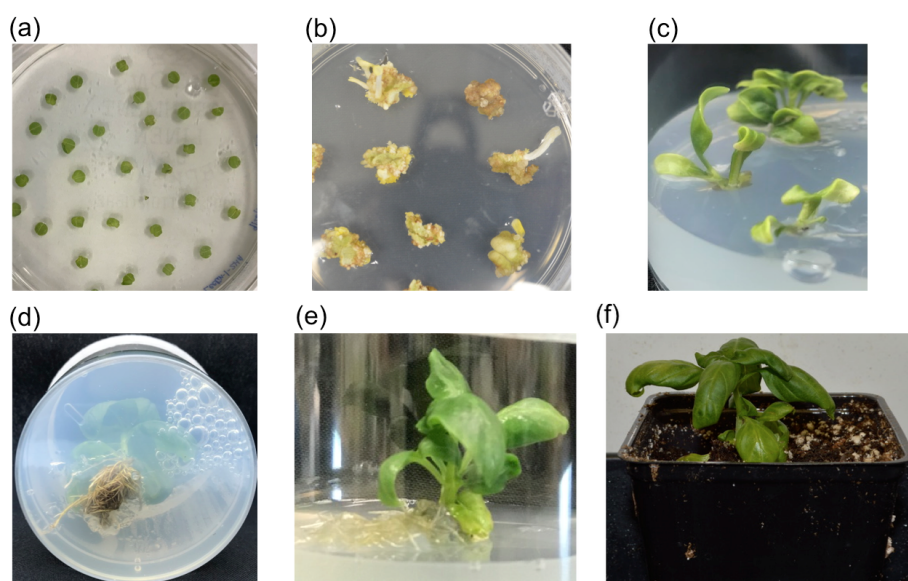
Figure 2.3. Stages of transformation and regeneration of transgenic sweet basil cv. Genoveser plants expressing *Oblectin 1*. (**a**) Co-cultivation of leaf explants with *Agrobacterium* on callus and shoot induction (SI) media in dark for 3 days for induction of calli. (**b**) Callus formation and shoot regeneration on SI media after 2 weeks in dark. **(c)** Individual shoots on root induction (RI) media for shoot elongation and root development. **(d)** Well developed root of individual plant on RI media after 2 weeks under light conditions. **(e)** Well-developed regenrated plantlet on RI media **(f)** Acclimatization of plantlet in soil.
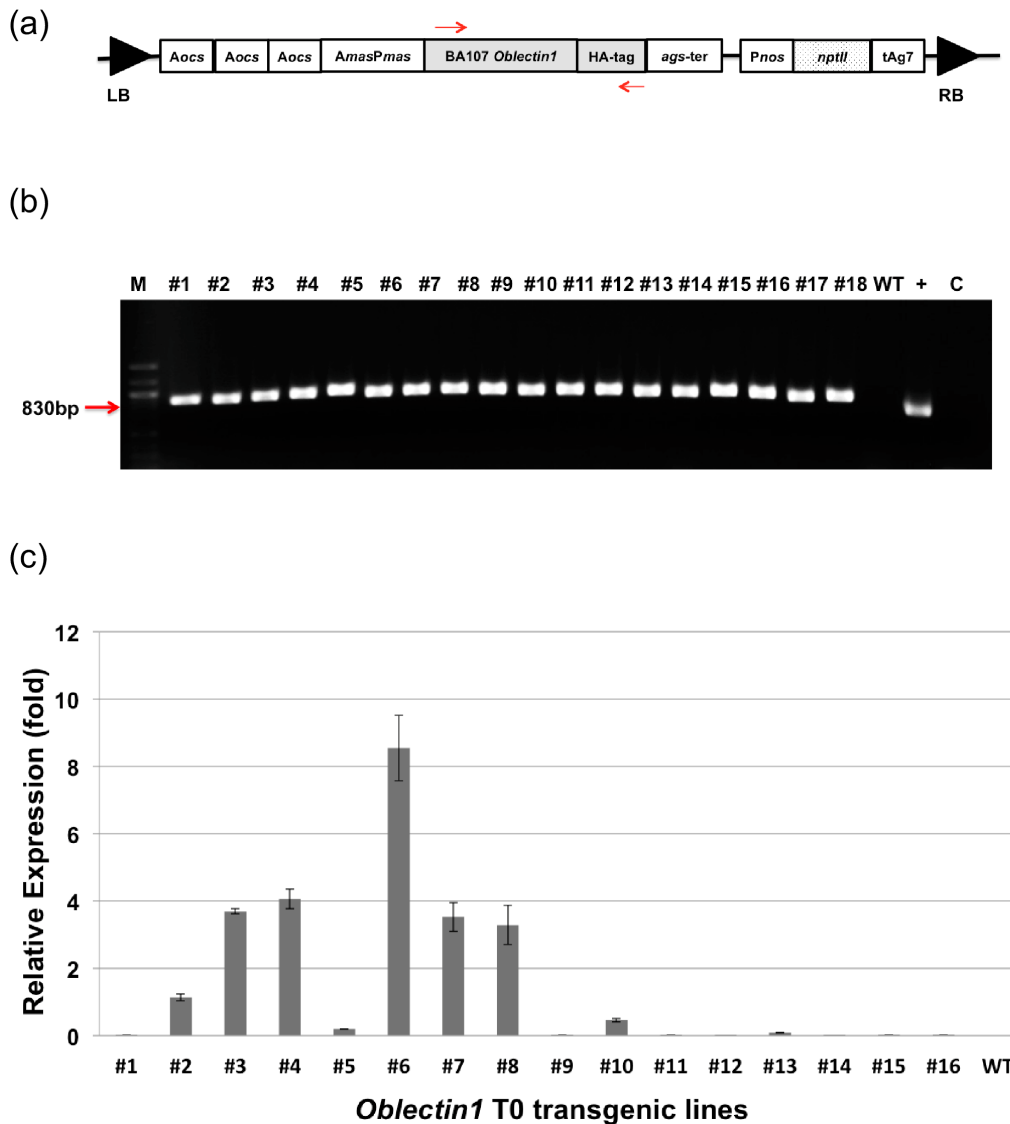
Figure 2.4. Molecular characterization of T0 transgenic _Ocimum basilicum_ lines. (a) Schematic representation of the T-DNA regions of the plasmid pE1776-2HA-Oblectin 1 used for stable transformation to express Oblectin 1 fused with a double-HA tag at the C-terminus. The plasmid was derived using pE1776 (Lee et al., 2007), which carries a super-promoter composed of three tandem repeats of octopine synthase transcriptional activating element (A_ocs_) and mannopine synthsae 2' activating and promoter element (A_mas_P_mas_) for constitutive expression of transgene, polyA adition signal from agropine synthase gene (_ags-_ ter), nopaline synthase promoter (P_nos_), _nptII_ gene conferring resistance to kanamycin and polyA addition signal for T-DNA gene 7 (tAg7). Primers used to amplify the transgene fragment from T0 transgenic lines are indicated by red arrow showing their positions. **(b)** Electrophoresis of PCR products confirming integration of _Oblectin 1_ transgene in T0 transgenic lines (#1-#18). +, positive control with pE1776-2HA-Oblectin1 plasmid as template; WT, Wild-type untransformed basil Genoveser as a negative control; C, no

template control; M is 100 bp DNA ladder. **(c)** Relative expression levels of *Oblectin 1* in T0 transgenic lines and WT, analyzed using qRT-PCR and normalized to *O. basilicum β-tubulin*. The error bars represent ± standard deviations from three technical replicates.

Figure 2.5. Kanamycin resistance assay to identify T1 homozygous transgenic sweet basil plants. 25 μl drops of 40 μg/ml Kanamycin were placed on the center of the first pair of true leaves of 18-days-old T1 transgenic and WT plants. Photograph was taken 10 days after kanamycin application.
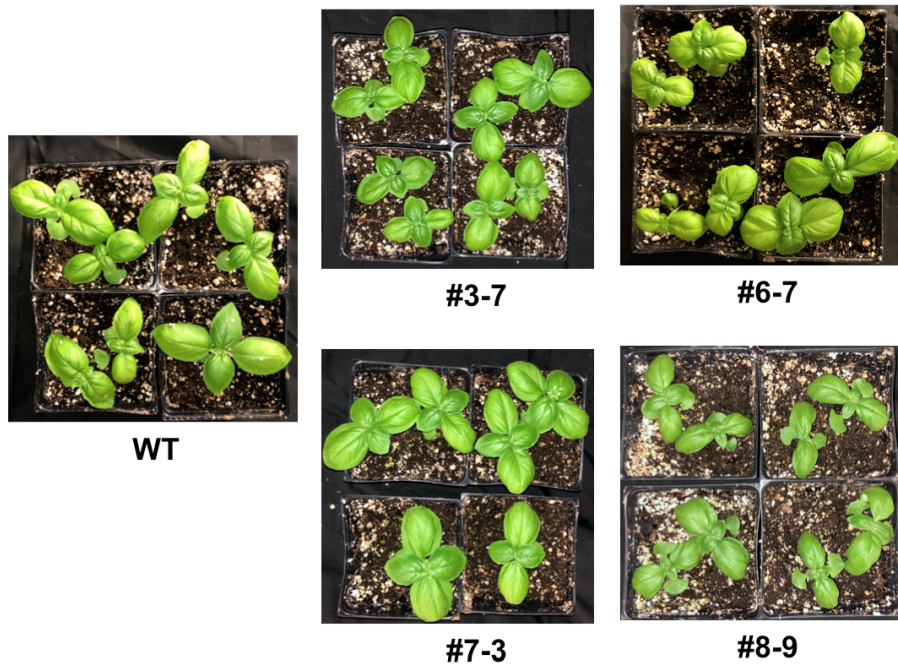
Figure 2.6. Morphology assessment of T2 transgenic sweet basil cv. Genoveser plants.
Photographs of 4-week-old wild type (WT) and T2 plants of the indicated homozygous
transgenic lines.
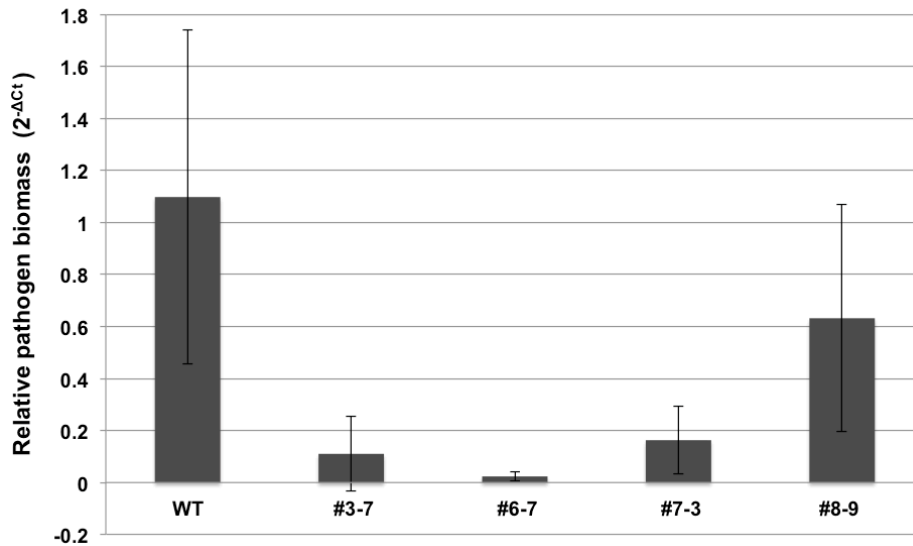
Figure 2.7. Quantification of pathogen biomass on *Oblectin1*-expressing T2 sweet basil lines using qPCR. Samples were collected from the wild type (WT) and T2 plants at 4 days post inoculation (dpi)**.** The growth was quantified as the ratio of the amplification of *P. belbahrii ITS2* to *O. basilicum β-tubulin,* calculated as $2^{-\Delta Ct}$. The error bars represent ± standard deviations of the mean of three biological replicates.

CHAPTER 3

Functional analysis of *Peronospora belbahrii* candidate pathogenicity-related genes *PbEC1* and *PbORCER1* utilizing host-induced gene silencing

Abstract

Basil downy mildew, caused by the obligate biotrophic oomycete *Peronospora belbahrii*, is a major threat to global basil production. Unfortunately, the lack of effective control strategies has made this disease challenging to combat. Despite holding high economic importance, little to no functional evidence for genes involved in the pathogenesis of *P. belbahrii* is currently available because transformation protocols are lacking, leaving a vast majority of effectors functionally uncharacterized. Host-induced gene silencing (HIGS) is an RNA interference (RNAi)-based approach in which small interfering RNAs are produced in the host plants to silence the targeted pathogen transcript, making HIGS a powerful tool to determine the function of pathogen genes and develop disease-resistant varieties. Transcriptomic analysis identified two potential pathogenicity-related factors based on effector- containing features and/or sequence conservation among plant pathogenic oomycetes; *Peronospora belbahrii Effector Candidate 1* (*PbEC1*) and *Peronospora belbahrii Oomycete RxLR-Containing Endoplasmic reticulum Resident 1* (*PbORCER1*) respectively. Expression of intron-containing hairpin RNA (ihpRNA) constructs targeting transcripts of *PbEC1,* or *PbORCER1* was achieved by generating transgenic sweet basil plants. Homozygous transgenic plants in the successive generations were selected by performing a kanamycin resistance assay coupled with a quantitative polymerase chain reaction (qPCR) on the segregating populations. Upon infection with *P. belbahrii*, the expression of *PbORCER1* on homozygous transgenic plants expressing ihpRNA of *PbORCER1* was significantly reduced compared with its expression on the wild type (WT) plants, suggesting successful silencing of *PbORCER1*. Knockdown of *PbORCER1* expression corresponded to the reduced pathogen growth, indicating the role of *PbORCER1* in pathogen proliferation. The pathogen growth on transgenic plants expressing ihpRNA of *PbEC1* was also significantly reduced compared to WT. However, the silencing of *PbEC1* transcripts was not observed likely because its expression was very highly induced during infection, which masked the detection of silencing. Collectively, our data suggest that HIGS is functional in silencing *P. belbahrii* genes, and therefore holds great potential for gene function analyses and controlling basil downy mildew.

3.1. Introduction

In broad essence, all plants have an elaborate multilayered defense mechanism against a wide range of pathogens. Pathogens experience complex two-tiered plant defense mechanisms, including Pattern-triggered immunity (PTI) and Effector-triggered immunity (ETI), based on the ability of the plant to switch-on signal transduction to suppress pathogen growth and invasion. PTI activates upon recognition of highly conserved pathogen-associated molecular patterns (PAMPs). To suppress PTI, pathogens deliver effector proteins, some of which are recognized by plant resistance proteins to activate ETI. Pathogens then mutate or lose these recognized effectors to evade ETI or evolve new effectors to suppress ETI. Therefore plant-pathogen interactions are orchestrated by compelling molecular strategies explicitly defined by the zig-zag model, in which effectors play a central role in determining the outcomes (Dangl & Jones, 2001, Chisholm et al., 2006, Jones & Dangl, 2006).

Hundreds of effectors have been predicted and identified from the genome of many plant fungal and oomycete pathogens. These effectors are generally classified as apoplastic effectors and cytoplasmic effectors. Apoplastic effectors function in the extracellular space, while cytoplasmic effectors translocate inside host cells and function at various subcellular compartments (Kamoun, 2006). Many oomycete genomes encode a superfamily of cytoplasmic effectors designated as RxLR effectors (McGowan & Fitzpatrick, 2017), which are defined by a N-terminal signal peptide and a downstream conserved Arg-any amino acid-Leu-Arg (RxLR) sequence motif and often followed by an dEER (Asp-Glu-Glu-Arg) motif (Tyler et al., 2006, Jiang et al., 2008). The RxLR-dEER motif serves as a translocation signal to mediate host cell entry (Dou et al., 2008, Whisson et al., 2007). The modular feature of RxLR effectors has facilitated their identification from genomic and transcriptomic sequences using bioinformatics approaches. A large number of RxLR effectors have been identified from all *Phytophthora* and downy mildew with genomic or transcriptomic sequences available (Haas et al., 2009, Jiang et al., 2008, Baxter et al., 2010, Tian et al., 2011, Yin et al., 2015, Stassen et al., 2012, McGowan & Fitzpatrick, 2017).

Endoplasmic reticulum (ER) holds an integral cell responsibility of protein synthesis and

folding, post-translational processing of proteins, quality control of misfolded proteins, and secretion of extracellular proteins (Kumar et al., 2017). ER mainly accommodates two different groups of proteins, (i) ER-resident proteins aiding in ER-specific functions and (ii) secretory proteins in the process of moving to extracellular space. Many ER-resident proteins contain a signal peptide, and a retention signal, which is typically a tetra-peptide at C-terminus consisting of (K/R/H/Q/S/A) (D/E/N/Q) EL (Goh et al., 2017). ER proteins having KDEL are known to be involved in protein secretion pathways, protein folding and sorting, and involvement in signaling pathways for cell development, proliferation, differentiation, survival, and cell death (Yamamoto et al., 2003). During host infection, many fungal proteins are processed in the ER, critical for disease progression *in planta* (Guillemette et al., 2014). A recent report demonstrated that the targeted disruption of *MoERR1*, an ER retention receptor, retarded the growth of *Magnaporthe oryzae*, significantly reducing the disease (Goh et al., 2017).

RNA silencing also known as RNA interference (RNAi) is an evolutionary conserved eukaryotic gene-expression regulatory mechanism involving a collection of biochemical pathways where numerous small RNA (sRNA) molecules, typically 21-24 nucleotides (nt) long, e.g., miRNA (micro RNA), siRNA (small interfering RNA), tasiRNA (*trans*-acting siRNA), and natsi (natural antisense siRNA), modulate the expression of target genes using complementary base-pairing with mRNAs. Production of sRNAs is achieved through the action of a Dicer-like (DCL) RNA helicase with an RNase III catalytic activity on double-stranded RNA (dsRNA) molecules as precursors either synthesized independently by RNA-dependent RNA polymerase or single-stranded RNAs folded into a secondary hairpin-like form (Kettles et al., 2019). Once sRNAs are produced, they bind to Argonaute (AGO) class endonucleases, forming RNA-induced Silencing Complex (RISC) to target mRNAs, usually negatively regulating target gene expression at the post-transcriptional level (Kettles et al., 2019). RNAi regulates numerous developmental processes and responses against biotic stresses (Kettles et al., 2019). Recent findings have demonstrated cross-kingdom gene silencing occurring at some level of plant-pathogen interactions, particularly defined in the *Arabidopsis thaliana- Botrytis cinerea* pathosystem. *B. cinerea* delivers sRNAs to plant cells to inhibit the accumulation of specific plant-defense related transcripts for facilitating pathogen invasion and virulence (Wang et al., 2016b). Meanwhile, Arabidopsis delivers sRNAs to pathogen cells to silence pathogen genes critical for pathogenicity (Cai et al., 2018). The discovery of sRNAs navigating between plant and pathogen cells to modify gene

expression has led to the development of a novel functional genomics tool and crop protection strategy relying on the RNAi mechanism. Host-induced gene silencing (HIGS) is an RNAi based strategy that involves the expression of hairpin RNAs or dsRNAs corresponding to essential pathogen mRNAs in plants. Uptake of sRNAs generated *in planta* by the pathogen induces silencing of the targeted pathogen transcripts. HIGS has been exploited as a functional genomic tool to silence gene-of-interest as well as to engineer pathogen resistance for various pathogens including *Fusarium graminearum*, *Fusarium culmorum*, *Fusarium verticillioides*, *Sclerotinia sclerotiorum*, *Rhizoctonia solani*, *Phytophthora infestans*, *Blumeria graminis*, *Puccinia striiformis* f. sp. *tritici*, *Puccinia triticina*, *Fusarium oxysporum* f. sp. *cubense*, *Bremia lactucae* (Guo et al., 2019, Nowara et al., 2010, Cheng et al., 2015, Chen et al., 2016, Qi et al., 2018, Song & Thomma, 2018, Sanju et al., 2015). HIGS is particularly a desirable experimental tool for gene-functional analyses of obligate biotrophs since they are recalcitrant to transformation.

The obligate biotrophic oomycete *Peronospora belbahrii* is the causative agent of basil downy mildew (BDM), which poses a major threat to basil production globally affecting basil-utilizing culinary, cosmetic and therapeutics industries by a large margin (Wyenandt et al., 2015). BDM establishes during the wet season with warm temperature leading to the development of chlorotic lesions delineated within veins and profuse sporulation of fuzzy grey spores on the abaxial side of leaves, later leading to complete collapse of the infected leaves (Cohen et al., 2013, Garibaldi et al., 2007). Air-borne spore dissemination causes fast disease spread, leading to tremendous losses as a result of which basil is unmarketable for consumption and extraction of essential oils (Cohen et al., 2013). BDM severely affects sweet basil (*Ocimum basilicum*) among many other species of the genus *Ocimum*. Sweet basil is considered to be tetraploid (2n=4x=48) with allopolyploid formation (Pyne et al., 2018), primarily valued for its peculiar savory properties, and holds high economic demand among growers worldwide (Wyenandt et al., 2015). Control of *P. belbahrii* on sweet basil mainly relies on the use of fungicides; however, only limited fungicides with low efficacy are available and their repeated use poses a high risk of developing fungicide-resistant strains (Wyenandt et al., 2015, Cohen et al., 2017). The most efficient approach to halt the rapid dissemination of BDM is to use disease-resistant cultivars, but no resistant or tolerant cultivar has been discovered for *Ocimum basilicum* yet (Cohen et al., 2017). Traditional breeding involving interspecific hybridization is hindered by sexual incompatibility, hybrid F1 sterility and difficulty in segregating undesirable traits (Ben-Naim et al., 2018, Cohen et al., 2017).

Therefore, it is imperative to use advanced molecular tools like HIGS to generate resistance to BDM.

The pathogenicity mechanisms of *P. belbahrii* are largely unknown. Similar to other plant pathogenic oomycetes, *P. belbarhii* encodes a large number of effector proteins. The identification of these effectors is expected to reveal the pathogenicity mechanisms of *P. belbahrii.* As an obligate biotroph, the most promising functional genomics tool is HIGS. Here we report the identification and characterization of two *P. belbahrii* proteins that likely play a role in pathogenicity, including Effector Candidate 1 (PbEC1) and Oomycete RxLR-Containing Endoplasmic reticulum Resident 1 (PbORCER1). *PbEC1* was identified as a *bona fide* effector of *P. belbahrii* having a functional signal peptide and an RxLR translocation motif and highly induced during infection, suggesting its role in *P. belbahrii* virulence (Shao, 2017). PbORCER1 was initially identified as a putative RxLR effector due to the presence of a signal peptide and an RxLR motif, the typical feature of an oomycete RxLR effector. However, it also contains an endoplasmic reticulum (ER) retention signal at the C-terminus, suggesting that it is an ER-resident protein. ORCER1 homologs in plant pathogenic oomycetes exhibit a remarkable degree of sequence conversation and are single-copy in each genome, suggesting its essential role in pathogen growth, development and/or infection. Both *PbEC1* and *PbORCER1* were pursued to characterize their roles in pathogenicity using the HIGS approach. Transgenic sweet basil plants harboring RNAi constructs of *PbEC1* or *PbORCER1* were generated, and the silencing of these two genes during infection and the affected pathogen growth was assessed. The data provided in this study indicate that the silencing of *PbORCER1* compromises the infectivity of basil downy mildew pathogen *P. belbahrii*. However, the results produced for *PbEC1* were insufficient to characterize its role in pathogenesis. Overall, our findings suggest that HIGS can be effectively carried out to verify the cause-effect relationship between the silencing of *P. belbahrii* genes and the impairment of pathogen growth.

3.2. Materials and Methods

3.2.1. Plant material

Basil seeds (cultivar Genoveser, Dolly, and BA107) provided by Enza Zaden Company were used for this study. Sweet basil cultivar Genoveser, which is susceptible to basil downy mildew pathogen, was used in all experiments as wild type (WT) and for *Agrobacterium*-mediated transformation. All basil plants were cultivated in 3.5'' square pots (McCONKEY)

filled with the soil mix (SunGro Horticulture Sunshine Mix #4) and cultivated in a controlled growth chamber at 25 °C, 50% relative humidity and 12/12 hrs day/night photoperiod. The same growth conditions were applied to regenerated transgenic T0 basil plants as well as T1 and T2 basil plants. Well-developed T0 and T1 basil plants were further grown to full maturity in the greenhouse in 11cm diameter round pots (McCONKEY) with 16 hrs light/8 hrs dark cycle at 25-27 °C. To avoid cross-pollination selfing bags were mounted on flowering stalks as soon as they emerged on the plants.

3.2.2. Identification and analysis of PbORCER1 and its homologs in other plant pathogenic oomycetes

PbORCER1 was initially identified as a candidate RxLR effector from an initial multiplexing mRNA-seq analysis performed on *P. belbahrii*-infected sweet basil leaves during infection time course and *P. belbahrii* sporangia (M. Tian, unpublished). To identify whether PbORCER1 has conserved homologs among other pathogens, BLASTP was performed against all annotated proteins from fungi and oomycetes available in FungiDB (https://fungidb.org/fungidb/). Also, we performed BLASTP and TBLASTN against NCBI non-redundant protein or nucleotide database, TBLASTN against NCBI Expressed sequence tags (est), Transcriptome Shotgun Assembly (TSA), and Sequence Read Archive (SRA) associated with *Plasmopara viticola* and *Pseudoperonospora cubensis* to identify additional homologs. To determine the mode of natural selection process of PbORCER1 homologs, the rates of nonsynonymous nucleotide substitutions per site (d_N) and the rates of synonymous nucleotide substitutions per site (d_S) in all pairwise comparisons were calculated using YN00 program of PAMLX, a graphic user interface for PAML (Phylogenetic Analysis by Maximum Likelihood) 4 software package developed by (Yang, 2007). DNA sequences corresponding to amino acid sequences spanning from 10 amino acids upstream of the RxLR start to the stop codon were used for the analysis.

3.2.3. RNAi vector construction

A 443-bp fragment containing partial 5' UTR (untranslated region) and the sequence coding the N-terminus of *PbEC1* was PCR-amplified from cDNAs generated from basil leaves infected with *P. belbahrii* using the primer set PbEC1-HIGS-F: 5'-**ACCA<u>GGTCTCA</u>GGAG**AGAACTTCAAAAGTCTGTTTGGCC-3' and PbEC1-HIGS-R: 5'-**ACCA<u>GGTCTCA</u>TCGT**TCCGTCTGGAAGGTCGGTGTAGTGT-3'). The same

cDNA was used to amplify a 500-bp fragment of *PbORCER1* encoding the N-terminus of the protein, using the primer set PbORCER1-HIGS-F: 5'-**ACCA**GGTCTCAGGAGGCGCTTACTCCGTCTATAAGCGAGT-3' and PbORCER1-HIGS-R: 5'-**ACCA**GGTCTCATCGTCCCTTTTCGATATGTTTTCGGAGAG-3'). Protective bases- BsaI (underlined)- adaptor is shown in bold. PCR was carried out using Phusion high-fidelity DNA polymerase (New England Biolabs) with an initial denaturation at 98 °C for 2 min followed by 35 cycles of 98 °C for 30 s, 72 °C for 15 s and 72 °C for 75 s and a final extension at 72 °C for 7 min. The PCR products were gel-purified using QiaQuick gel extraction kit (Qiagen) and cloned into a pRNAi-GG plasmid (Yan et al., 2012), respectively. Golden gate cloning method was adopted to generate *PbEC1* and *PbORCER1* intron-containing hairpin RNA (ihpRNA) constructs (or RNAi-HIGS construct) for stable basil transformation. Golden gate cloning reaction was performed using 50 ng purified PCR product, 200 ng pRNAi-GG plasmid, BsaI enzyme (NEB), T4 DNA ligase, and T4 DNA ligase buffer (NEB). The restriction-ligation tube was initially incubated at 37 °C for 2 hrs, followed by incubation at 50 °C (final digestion) for 5 min and a final heat inactivation step at 80 °C for 5 min. The resultant ligated plasmid containing all necessary elements of ihpRNAi cassette (expressing sense and antisense sequences flanking a PDK intron) and NPTII (kanamycin resistance) expression cassettes was transformed into *E. coli* DH5α competent cells via heat-shock method and sent for sequencing using primers (PDK-F: 5'-GTCGAACATGAATAAACAAGGT-3' and PDK-R: 5'-CTTCGTCTTACACATCACTTGTCA) to confirm the recombinant plasmid and orientation of the insert. The confirmed binary vectors, pRNAi-GG-PbEC1 and pRNAi-GG-PbORCER1, were further transformed into *Agrobacterium tumefacians* EHA105 using electroporation (Mersereau et al., 1990).

3.2.4. Generation of transgenic sweet basil lines

The RNAi constructs pRNAi-GG-PbEC1 and pRNAi-GG-PbORCER1 were introduced in susceptible basil cv. Genoveser, respectively, via *Agrobacterium*-mediated transformation following a previously reported method with slight modifications (Deschamps & Simon, 2002, Phippen & Simon, 2000). *Agrobacterium* strain EHA105 carrying the desired plasmid, stored at -80 °C, were streaked on LB plate supplemented with 50 μg/ml Kanamycin, 5 μg/ml Chloramphenicol and 15 μg/ml Rifampicin and grown for two days at 28 °C before the experiment day. Similar steps were followed to regenerate plants using basil explants as

discussed in Chapter 2 (section 2.2.4.) The transformation efficiency was calculated by the ratio of the total number of plants with a fully developed shoot and root system to the total number of starting explants.

$$\text{Transformation efficiency (\%)} = \frac{\text{number of total plants with well-developed shoots and roots}}{\text{number of starting explants}}$$

3.2.5. Genetic screening of (T0) transgenic sweet basil plants

Approximately 50 mg leaf tissue of newly regenerated transgenic basil lines was used to isolate genomic DNA (gDNA) following the crude gDNA extraction method described in Chapter 2 (section 2.2.5.). 1 µl of the isolated crude gDNA was used as a PCR template to amplify approximately 800bp of T-DNA fragment using primers P21-F (5'-ACCATTTACGAACGATAGCC-3') (Yan et al., 2012) & PDK-R with Phusion High-fidelity DNA polymerase (M0530S-New Englands Biolab). PCR conditions started with an initial denaturation of 30 s at 98 °C, followed by 35 cycles of 98 °C for 15 s, 60 °C 15 s for annealing (as calculated using Tm calculator from NEB Tm calculator) and 60 s at 72 °C for elongation with the final extension step at 72 °C for 7 min. PCR products were visualized on a 1% agarose gel by electrophoresis under 120 V for 35 min.

3.2.6. Quantification of transgene expression in T0 transgenic sweet basil plants using RT-qPCR

Total RNA was isolated from leaf tissue of first-generation (T0) transgenic sweet basil lines by grinding the frozen tissue using blue pestle (Axygen Scientific Inc) followed by QIAGEN RNeasy Plant Mini Kit instructions. All the RNA samples were treated with DNA-free kit (Ambion) to remove any contaminating genomic DNA. First-strand cDNA was synthesized with 1µg of RNA using Invitrogen SuperScript II Reverse Transcription Kit. qPCR was performed on BioRad C1000 Touch Thermal Cycler machine using primers (PDK-qPCR-F: 5'-AGAAATTCCAATCTGCTTGT-3'; PDK-qPCR-R: 5'-TGATAGATCTTGCGCTTTGTT-3') that amplify PDK gene and another set of primers (Obtubulin-F2: 5'-GCTTGCTGTCAATCTCATTCC-3' & Obtubulin-R2: 5'-TCTGGAACAGTGAGTGCTCTG-3') that amplify *Ocimum basilicum β-tubulin* gene, used as an internal control to normalize the gene expression. The reaction was performed using 1X SsoAdvanced Universal SYBR Green Supermix (Bio Rad), 0.25 µM specific primers and 100 ng cDNAs, with the program set as follows: initial heating at 95 °C for 30 s, then 40 thermal cycles of denaturation at 95 °C for 10 s, annealing and elongation at 60 °C for 60 s.

The final melting was performed by heating to 95 °C, cooling down to 65 °C and rising back to 95 °C at 0.1 °Cs^{-1}. The relative transcript was assessed by the $2^{-\Delta Ct}$ method with three technical replicates (Schmittgen & Livak, 2008).

3.2.7. Transgene zygosity determination via kanamycin resistance assay followed by qPCR

Seeds of self-pollinated sweet basil plants along with WT were germinated at the same time for progeny analysis of second-generation (T1) and third-generation (T2) selected transgenic lines. 18-days old sweet basil plants (WT, T1 & T2) with emerging first pair of true leaves were subjected to kanamycin resistance assay followed by qPCR using crude gDNA of experimented leaves using the same procedures as discussed in Chapter 2 (section 2.2.7.). 10 ng isolated crude gDNA was used to set up a 20 µl qPCR reaction containing 1X SYBR Green mix, 0.25 µM specific primers (PDK-qPCR-F & PDK-qPCR-R to amplify *PDK* and Obtubulin-F2 & Obtubulin-R2 as an internal control). qPCR program was run in Bio-Rad C1000 Touch Thermal Cycler machine with similar program conditions as described in section 3.2.7. The amplification of the *PDK* gene was quantified by calculating as $2^{-\Delta Ct}$ (Livak & Schmittgen, 2001b).

3.2.8. Pathogen inoculation and disease quantification

Peronospora belbahrii was isolated from basil plants found in City Mill, Oahu, Hawaii. The propagation and maintenance of the pathogen were done similarly, as described in Chapter 2 (section 2.2.8). The T2 transgenic plants, along with WT, as control were inoculated under the same procedures and conditions, as mentioned in Chapter 2 (section 2.2.8). One set of the plants was kept to monitor symptoms, while the other set was used to collect samples at 4-days-post inoculation (dpi) for pathogen biomass quantification using qPCR. Once the spores were visually seen on WT leaves, indicating successful inoculation assay, the samples were subjected to qPCR assay to quantify the pathogen biomass described previously (Shao & Tian, 2018). qPCR assay on inoculated leaves was determined similarly as previously discussed in Chapter 2 (section 2.2.8.).

3.2.9. Determination of gene silencing efficiency of HIGS by qRT-PCR

qRT-PCR was used to evaluate the transcript levels of *PbEC1* or *PbORCER1* during *P. belbahrii* infection of transgenic plants expressing HIGS constructs. The leaf tissues from

both WT and transgenic plants were collected at 4-days post-inoculation. Three inoculated leaves from three infected plants were collected as one sample serving as one biological replicate. A total of three biological replicates were analyzed for each line. As soon as the leaves were plucked, they were wrapped in aluminum foil, frozen in liquid nitrogen, and stored at -80 °C until further use. Once sporulation was observed on WT plants, which indicated a successful infection assay, the samples were subjected to RNA isolation to assess the endogenous expression of *PbEC1* or *PbORCER1*. Total RNA isolation and reverse transcription was performed with the same procedure described in section 3.2.6. qRT-PCR was performed using *PbEC1* primers (PbEC1-qRT-F: 5'- CTAACCGCTGCTCCATTGTC-3' & PbEC1-qRT-R: 5'- CGGTGTCATTGCTTCTTCAC-3') or *PbORCER1* primers (PbORCER1-qRT-F: 5'-GAGGATTGCGGAAGGATACA-3' & PbORCER1-qRT-R: 5'-AGCTCTGCGATTCCTGTTGT-3'), which were designed to amplify the region not contained in pRNAi-GG-PbEC1 or pRNAi-GG-PbORCER1. *P. belbahrii β-tubulin* (*Pbβ-tubulin*) gene was used as the internal reference for normalization using specific *Pbβ-tubulin* primers (Pbtubulin-F: 5'-CGGAAACTGGCTGTGAACTT-3' & Pbtubulin-R: 5'-CAAAGCACGGTACTGCTGAG-3'). A 20 μl reaction was set up with 1X SYBR Green supermix (Bio Rad), 0.25 μM specific primers, and 400 ng cDNA adopting reaction/program conditions, as mentioned in 3.2.6. The expression of *PbEC1* and *PbORCER1* in this study were assayed by calculating the ratio of relative transcripts of *PbEC1*/*PbORCER1* relative to

P. belbahrii β-tubulin by analyzing $2^{-\Delta Ct}$ (Livak & Schmittgen, 2001b).

3.3. Results

3.3.1. PbORCER1 shows a remarkable degree of sequence conservation among plant pathogenic oomycetes

PbORCER1 initially identified from *P. belbahrii* transcripts as a putative RxLR effector due to the presence of a signal peptide (SP) and a downstream RxLR motif, the feature of a typical RxLR effector (Figure 3.1). However, it also has an ER-retention signal KDEL, suggest that it is ER resident protein. Besides, it also has a domain with tetratricopeptide repeats (TPR), which is present in many other ER-resident proteins (Graham et al., 2019). TPR is a structural motif identified in a wide variety of proteins found to be involved in mediating protein-protein interactions, suggesting that PbORCER1 functions by interacting with other proteins.

To identify whether PbORCER1 has conserved homologs among other pathogens (fungi and oomycetes), BLASTP against all protein models in FungiDB was performed. A significant single hit with an e-value $< 6 \times e^{49}$ was present in all plant- and animal-pathogenic oomycetes with genome sequences available in FungiDB, whereas no hit with an e-value $< 1 \times e^{-6}$ was detected in filamentous fungi, indicating that this protein is highly conserved and specific to a large number of oomycetes. Therefore, it was named as Oomycete RxLR-Containing Endoplasmic reticulum Resident 1 (ORCER1). Further BLASTP and TBLASTN against NCBI non-redundant protein or nucleotide database was performed along with TBLASTN against NCBI Expressed sequence tags (est), Transcriptome Shotgun Assembly (TSA) and Sequence Read Archive (SRA) to identify additional homologs of *P. belbahrii* ORCER1 (PbORCER1). The amino acid sequences of ORCER1 homologs exhibit a remarkably high degree of sequence conservation. Except in *Pythium* spp., whose ORCER1 homologs share 50-65% identity with homologs from other oomycetes, ORCER1 from other species share identity ranging from 71%-96% across the whole protein length (Table 3.1.).

In the course of pathogen evolution and speciation, nucleotide mutations are random and yet the selection pressure has maintained a high level of conservation among ORCER1 homologs. For ORCER1 in all pairwise comparisons, synonymous (d_S) nucleotide substitution is much greater than nonsynonymous (d_N) substitutions, indicating that they are under purifying selection (Figure 3.1b). This result suggests that the roles of ORCER1 in oomycete infection and survival are crucial that only nucleotide mutations that preserved the amino acid sequences have survived the selection during pathogen evolution. Therefore, *PbORCER1* represents an ideal candidate for silencing using the HIGS approach to determine the effectiveness of this tool in silencing *P. belbahrii* genes and allow us to identify the role of *PbORCER1* in pathogenesis.

3.3.2. Generation of transgenic sweet basil plants expressing intron-containing hairpin RNAs of *PbEC1* and *PbORCER1*

To test if HIGS can be used to generate downy mildew-resistant sweet basil plants, we transformed a susceptible cultivar Genoveser with the intron-containing hairpin RNA (ihpRNA)-expressing construct pRNAi-GG-PbEC1 or PRNAi-GG-PbORCER1 that targets *PbEC1* or *PbORCER1* respectively. These constructs express ihpRNAs consisting of a PDK intron flanked by the sense and antisense strands of *PbEC1*/*PbORCER1* gene fragments under the control of the double CaMV 35S promoter and NOS terminator, and also carries a

kanamycin resistance gene (*NPTII*) (Figure 3.3a) Leaf discs were prepared from the first pair of true leaves from 3-week-old Genoveser plants and used as explants. These explants were then infected with *A. tumefaciens* EHA105 strains harboring either pRNAi-GG-PbEC1 or pRNAi-GG-PbORCER1, and co-cultivated with the Agrobacteria on callus and shoot induction (SI) media plates supplemented with acetosyringone (Figure 3.2a) for three days in the dark. The explants were later transferred to SI media containing kanamycin to induce the formation of transgenic calli and shoots. Callus development was observed two weeks after culturing the explants on kanamycin-containing SI media from which tiny shoot buds emerged (Figure 3.2b). Shoots with emerging stalks were later transferred to root induction media (RI) (Figure 3.2c) for further development of branching shoots and root formation (Figure 3.2d). Fully developed shoots with proper root systems were observed in the regenerated plants after growing on RI media for four weeks (Figure 3.2d). The plantlets were then acclimatized into the soil and grown in a controlled growth chamber (Figure 3.2e) for 3 weeks, and later transferred to the greenhouse (Figure 3.2f) to produce T1 seeds. Six independent transformation experiments were performed for each construct yielding a transformation efficiency ranging from 17-47% for the HIGS construct to silence *PbEC1* (Table 3.2.) and 17-45% transformation efficiency for the *PbORCER1* ihpRNA construct (Table 3.2.). The high transformation efficiency contributed to the success of developing transgenic sweet basil plants in a short duration of time with multiple lines of first-generation (T0) plants. A total of 39 and 40 T0 sweet basil plants transformed with *PbEC1* ihpRNA construct and *PbORCER1* ihpRNA construct respectively, were acclimatized in soil.

3.3.3. Integration and expression of ihpRNA cassette in independent T0 sweet basil plants

17 kanamycin-resistant sweet basil lines (labeled from #1- #17) transformed with the *PbEC1* ihpRNA construct were randomly selected to confirm the integration of transgene via PCR using specific primers located in the double 35S promoter and PDK intron (Figure 3.3a). Successful amplification of the *PbEC1* sense strand cassette was observed in all of them (Figure 3.3b). Similarly, 20 randomly selected regenerated T0 sweet plants (labeled from #1-#20) transformed with the *PbORCER1* ihpRNA construct were tested positive for amplifying *PbORCER1* sense-strand cassette (Figure 3.3b). All tested lines displayed a band with an estimated size of about 800-bp, indicating successful integration of the transgene.

To quantify the relative expression levels of ihpRNAs, qRT-PCR was performed on randomly selected 14 (#1-#14) and 17 (#2-#18) T0 transgenic sweet basil lines carrying

RNAi construct for *PbEC1* and *PbORCER1* respectively, using primers that amplify a fragment within the PDK intron. For T0 plants transformed with RNAi-construct of *PbEC1*, varying levels of expression was observed in 70% of T0 lines, among which #13 displayed the highest relative expression of 0.39 followed by #9, #10, #5 and #11 with relative expression ranging between 0.22-0.04 (Figure 3.4a). The remaining tested T0 lines either showed very low or no transcript levels. Of these 14 tested T0 lines, the transgenic lines #5, #9, #10 and #13 showing relatively higher expression of *PDK* were selected for further study. Similarly, for the 17 transgenic lines (#2 to #18) carrying *PbORCER1* RNAi construct, different levels of relative expression were found in 70% of the lines while the remaining did not show any significant expression. #5 showed the highest relative expression of 0.24, with others falling in a range of ≤ 0.1 (Figure 3.4b). The transgenic lines selected for further studies to evaluate HIGS of *PbORCER1* were #4, #5, #6, #11 and #17. All T0 sweet basil lines selected for further analysis were subjected to self-hybridization to harvest T1 seeds.

3.3.4. Selection of T1 transgenic sweet basil lines expressing ihpRNA cassette

To identify the potential homozygous transgenic plants in the T1 segregating population, the kanamycin resistance assay followed by qPCR was performed. T1 sweet basil plants of selected T0 lines (*PbORCER1*-RNAi T0 lines #4, #5, #6, #11 and #17 and *PbEC1*-RNAi T0 lines #5, #9, #10 and #13) were first assayed for kanamycin resistance. Kanamycin drop on T1 segregating population is expected to show discoloring (yellowing) phenotype for transgene-null plants whereas no discoloration is expected for plants either hetero- or homozygous for the transgene. The phenotypic observation was monitored ten days after dropping kanamycin on young 18-day-old T1 and WT plants. The results indicated strong discoloration (yellowing/whitening) on all WT plants and a few T1 basil plants. In contrast, the majority of the remaining T1 plants maintained green at the point of kanamycin drop. A full account of T1 basil plants turning yellow or remaining green are listed in Table 3.3. for *PbEC1* ihpRNAi-expressing T1 plants and *PbORCER1* ihpRNAi-expressing plants, respectively. This accounting was done to estimate the segregation ratio. Since sweet basil was reported to be allotetraploid, it is expected to observe a phenotypic ratio of 3:1 in the segregating population. However, this pattern of segregation was not evident from our results, which could be attributed to various reasons, including a small percentage of plants used for each tested line, low expression of kanamycin resistance, or due to allotetraploid nature of sweet basil. Nevertheless, this assay assisted in identifying transgenic plants without labor-intensive molecular testing. Following kanamycin-resistant assay, qPCR was

performed to select homozygous T1 sweet basil plants delineating them from heterozygotes. 10 T1 green basil plants with one yellow plant derived from each independent T0 basil lines together with the corresponding T0 plant were subjected to qPCR. The amplification of the PDK fragment was normalized using *O. basilicum β-tubulin* as the reference gene and calculated as $2^{-\Delta Ct}$ values (Table 3.4. and Table 3.5.). Although we expected to get the results belonging to three categories: plants that scored around double the amplification value with respect to T0, plants that showed the same value as T0, and plants that had no amplification similar to WT, we did not obtain the clear-cut results. We selected T1 basil plants from each independent T0 line displaying maximum amplification value at second-generation propagation. #11 T1 (Table 3.5.) was excluded from further analysis as it did not generate any ct values, which could be attributed to the fact that this line might not carry the transgene cassette or due to other experimental failures. For #6 and #17, only nine and five T1 plants were tested, respectively. There was a huge variation involved in the #17 T1 basil line (Table 3.5.) when compared to the T0 plant, which can be an experimental error. The T1 basil plants selected further for T2 propagation expressing *PbORCER1* RNAi-cassette were #4-2, #4-3, #4-9 and #4-10; #5-1, #5-2, #5-5, #5-7 and #5-8; #6-2, #6-3, #6-6, #6-7; no line was selected for #17 since it involved a lot of variation in values. Similarly the T1 basil plants having RNAi-expressing cassette of *PbEC1*, selected for T2 propagation were #5-3, #5-4, #5-5 and #5-8; #9-1, #9-2, #9-3 and #9-9; #10-1, #10-2, #10-3 and #10-7; #13-2, #13-3, #13-5 and #13-6.

3.3.5. Selection of T2 homozygous-transgenic basil lines expressing ihpRNA cassette for pathogen inoculation assay

T2 basil plants from sixteen (carrying *PbEC1*-RNAi cassette) and twelve (carrying *PbORCER1*-RNAi cassette) T1 basil lines were further subjected to kanamycin resistance assay to confirm the integrity of homozygous status. Assessment of the assay was done by counting the number of plants that turned yellow or remained green at kanamycin drop point (Figure 3.5,Table 3.6, Table 3.7.). Except for T1 basil line #10, #13 and #5-3, #5-4 (Table 3.6.), all T2 plants remained green, indicating homozygosity inheritance. Similarly, except #6-2, all T2 lines derived from independent T1 lines expressing the ihpRNA cassette of *PbORCER1* had no effect of kanamycin. Homozygous T2 lines (#5-5, #9-1) and #13-2 (Table 3.6.) and homozygous T2 lines (#4-3, #5-7, and #6-7 from Table 3.7.) were selected for pathogen infection assays to test if HIGS silenced pathogen genes *PbEC1* and

PbORCER1 respectively and the resulted impact on disease severity.

All six transgenic T2 basil lines selected for disease assays were observed for any morphological phenotype showing abnormality in growth and development. Seeds of homozygous T2 sweet basil plants together with WT were germinated at the same time to inspect growth and development alterations starting from 1-week-old plants until six weeks. Twenty-five seeds were sown in individual round pots for WT and each selected T2 sweet basil line. 3-weeks-old basil plants were photographed, showing similar phenotypes as WT basil plants. All plants displayed normal growth, such as germination time, leaf morphology, branching, and plant height (Figure 3.6a and 3.6b).

3.3.6. Inconsistent silencing of *PbEC1* and reduced pathogen growth mediated by *in planta* expressed ihpRNA of *PbEC1*

To investigate whether expressing *PbEC1*-ihpRNA in susceptible basil cultivar could silence *PbEC1* and inhibit the growth of *P. belbahrii*, 4-weeks-old T2 basil plants along with WT were inoculated. qRT-PCR analysis was performed on infected samples collected 4-days post-inoculation (dpi) to determine if the silencing signals from transgenic plants were able to silence *PbEC1*. The results suggested that the transcript abundance of *PbEC1* was reduced by 49% in line #13-2 compared to WT, whereas *PbEC1* expression in homozygous T2 lines #5-5 and #9-1 was not significantly affected with similar relative expression of approximately 220 as WT (Figure 3.7a). To determine the disease severity, quantification of pathogen growth by qPCR was done on leaf samples collected on infected T2 and WT basil plants at 4-dpi. Different levels of reduction in pathogen biomass were observed for #5-5, #9-1, #13-2 compared with WT with relative amplification values of 10, 21, 26, respectively, compared with 40 of WT (Figure 3.7b). Even though the reduction of the pathogen was observed in all inoculated transgenic lines, the silencing of *PbEC1* transcripts was not consistently observed likely because its expression was very highly induced during infection, which masked the detection of silencing.

3.3.7. Knockdown of *PbORCER1* suppresses pathogen proliferation

To demonstrate the silencing of *PbORCER1* by HIGS, the expression level of *PbORCER1* was assayed in inoculated T2 sweet basil lines (#4-3, #5-7, and #6-7) along with WT at 4-days post-inoculation (dpi) using qRT-PCR by normalizing the transcript levels with *P. belbahrii β-tubulin*. *PbORCER1* transcript levels significantly decreased by 59%, 53% and

55% in homozygous lines #4-3, #5-7 and #6-7, respectively, when compared to WT control (Figure 3.8a), suggesting that HIGS was effective in silencing *PbORCER1*. To determine whether the silencing of *PbORCER1* affected the pathogen growth, quantification of *P. belbahrii* biomass in inoculated plants was assayed using qPCR at 4-dpi by normalizing the amplification of *PbITS2* with *O. basilicum β-tubulin*. Pathogen accumulation significantly decreased in #4-3, #5-7 and #6-7 T2 transgenic lines yielding a relative amplification of 7, 27 and 17, respectively, compared to 44 present in WT (Figure 3.8b). The reduced pathogen biomass in the transgenic lines was consistent with HIGS-mediated silencing, indicating the role of *PbORCER1* in pathogenesis.

3.4. Discussion

Recent advances in genome/transcriptome sequencing have revealed a plethora of effectors and candidate effectors from a wide range of plant pathogens responsible for virulence. However, the majority of effectors and pathogenicity-related genes remain uncharacterized. Gene silencing in pathogens by interfering RNAs derived from engineered plant genomes termed as HIGS or host-mediated RNAi. HIGS has emerged as a powerful tool for generating transgenic plants to control plant diseases and study the function of candidate pathogenicity genes. Lack of an efficient and reproducible transformation method for obligate biotrophic pathogens hampers the genetic validation of candidate genes using the pathogens directly, but adopting HIGS can alleviate this difficulty. Candidate pathogenicity-related gene discovery in the basil downy mildew pathogen *P. belbahrii* employing a bioinformatic survey to mine genes that have effector motifs and are specifically upregulated during infection; and also for genes that share high sequence conservation among its homologs in a range of species.

This study represents an attempt to characterize two candidate pathogenicity-related genes via HIGS to examine the possible role of cross-kingdom siRNAs/dsRNAs transfer and gene silencing during interactions of *P. belbahrii* with sweet basil. PbEC1, a candidate RxLR effector, possesses a functional cleavable signal peptide (SP) and an RxLR motif, with upregulated expression during infection, suggesting its potential role in pathogenicity (Shao, 2017). PbORCER1 initially annotated as a candidate RxLR effector due to the presence of a signal peptide and a downstream RxLR motif, was later found likely to be an ER-resident protein due to the presence of a TPR domain and ER retention signal 'KDEL' at C-terminus. Nevertheless, ORCER1 homologs in plant pathogenic oomycetes are single-copy, showing a

remarkable degree of sequence conservation, and identified to be under purifying selection, suggesting that it is an essential gene for pathogen growth, development and/or infection, and therefore an ideal target for using HIGS to generate disease resistance. To assess whether HIGS of *P. belbahrii* genes is operational in stable transgenic basil plants, we exploited an intron-containing hairpin RNA construct to produce dsRNAs corresponding to either *PbEC1* or *PbORCER1* in basil plants. A coding fragment of the *PbEC1* or *PbORCE1* gene (approximately ~500 bp) was cloned into the Golden Gateway vector pRNAi-GG to obtain the respective RNAi construct. Subsequently, these constructs were stably integrated into downy mildew-susceptible cv. Genoveser to express hairpin dsRNA molecules corresponding to *PbEC1* or *PbORCER1*, respectively, using *Agrobacterium*-mediated transformation.

Plant transformation using Agrobacteria for a given transgene may yield independent transgenic plants with different phenotypes and expression levels due to somaclonal variations, as well as the positional effect resulting from random integration of the transgene. Therefore, the expression levels of PDK, as an indication of the expression of ihpRNAs of *PbEC1* or *PbORCE1*, varied among independent T0 transgenic sweet basil plants (Figure 3.4a and 3.4b). T0 sweet basil lines showing relatively higher transcript levels were selected for further propagation to second-generation (T1) analysis. T0 regenerated basil plants are usually heterozygous for the transgene. In order to seek for homozygote plants in the T1 segregation population, a zygosity determination analysis was carried out using kanamycin resistance assay coupled with qPCR. Kanamycin resistance assay was performed to distinguish transgenic plants from null-transgene ones by taking advantage of the *NPTII* selectable marker gene of T-DNA, whereas qPCR was used to determine the transgene copy number of the transgenic plants selected based on kanamycin resistance assay. Discrepancies in the expected Mendelian phenotypic (3:1) ratio for the segregation of kanamycin resistance in T1 plants were met. A low number of plants used in this study is insufficient to conclude the accurate segregation ratios. Apart from the positional effect of transgene affecting the expression of the *NPTII* gene, allotetraploidy of sweet basil may also add extra complexity that affects the ratio. In qPCR assay, although we expected to see the amplification of transgene in some T1 transgenic plants to be double of that from other T1 plants and the parental T0 plant, no clear-cut results were observed. The allotetraploidy of sweet basil and different DNA isolation methods used for the T0 and T1 plants may partially explain the discrepancy. Nevertheless, these assays allowed us to quickly select the potential

homozygotes at the T1 generation, most of which were confirmed using T2 populations via kanamycin resistance assay. This saved much work from propagating a large number of T1 plants for seeds when cross-pollination is a concern.

In this study, we found that the ihpRNA of *PbEC1* in homozygous T2 lines were not able to silence *PbEC1* in two out of three lines (Figure 3.7a). However, pathogen biomass was reduced in all tested T2 lines (Figure 3.7b), likely because its expression was very highly induced during infection, which masked the detection of silencing. Since no correlation was found between *PbEC1* transcript levels and pathogen biomass, we were unable to conclude the role of *PbEC1* in pathogenesis. Additional experiments, such as determining the level of *PbEC1* expression at different infection time courses, are needed to resolve the discrepancy. *P. belbahrii* abundance was considerably reduced in transgenic homozygous basil lines expressing ihpRNA of *PbORCER1,* which corresponded to the silencing of *PbORCER1*, suggesting that *PbORCER1* acts as a pathogenicity determinant factor. Thus it can be presumed that the expression of *PbORCER1*-ihpRNA in transgenic basil led to the obstruction of pathogen *PbORCER1* gene expression during the interaction with the host plant. This data suggest that plant-derived dsRNAs or siRNAs, if taken up by *P. belbahrii,* could induce RNAi of pathogen transcripts. Therefore, HIGS-mediated silencing is operational in transgenic basil against BDM pathogen. While we conclude that in our study, the ihpRNA expressed in the transgenic plants caused silencing of *PbORCER1*, resulting in reduced pathogen biomass, the presence of interfering RNAs (dsRNA and/or siRNA) corresponding to *PbORCER1* needs to be confirmed by methods such as northern blotting.

Overall, the silencing of targeted pathogen genes was able to reduce pathogen proliferation at an early stage of infection (4-days post-inoculation), insufficient to confer complete resistance to basil downy mildew. One of the reasons could be attributed to the dependence of *P. belbahrii* on a repertoire of proteins collectively to invade and infect the host, rather than one single gene. Targeting two or more genes in the same HIGS construct is feasible and promising to improve the resistance. Lack of detectable effect of HIGS could also be attributed to the technical limitation of the HIGS method, such as insufficient production of siRNAs with the currently available vectors.

Many other reasons contribute to the overall efficiency of HIGS, first and foremost, being the target gene selected. HIGS efficiency differs for different target genes with distinct functions. Size, sequence specificity and position of the sequence corresponding to the dsRNA are

additional considerations for efficient HIGS strategy (Guo et al., 2019). For example, a study that synthesized several siRNAs for different sites of the same target mRNA demonstrated striking differences in silencing efficiency (Senthil-Kumar & Mysore, 2011).

This study was carried out to assess the potential of RNAi-technology based HIGS approach to identify the roles of candidate effector genes in pathogenesis. Given the ease of design and applicability to a wide range of pathogens, the use of target-specific silencing using HIGS offers unprecedented potential as a new plant protection strategy and reverse genetic tool for improved understanding of a pathosystem. The results from this study suggest that HIGS is operational during sweet basil-*P. belbahrii* interactions, and therefore offers a promising tool for functional genomics studies of *P. belbahrii* and generation of basil downy mildew disease resistance.

3.5. References

Baxter L, Tripathy S, Ishaque N, *et al.*, 2010. Signatures of adaptation to obligate biotrophy in the Hyaloperonospora arabidopsidis genome. *Science* **330**, 1549-51.

Ben-Naim Y, Falach L, Cohen Y, 2018. Transfer of downy mildew resistance from wild basil (Ocimum americanum) to sweet basil (O. basilicum). *Phytopathology* **108**, 114-23.

Cai Q, Qiao L, Wang M, *et al.*, 2018. Plants send small RNAs in extracellular vesicles to fungal pathogen to silence virulence genes. *Science* **360**, 1126–9.

Chen W, Kastner C, Nowara D, *et al.*, 2016. Host-induced silencing of Fusarium culmorum genes protects wheat from infection. *J Exp Bot* **67**, 4979-91.

Cheng W, Song XS, Li HP, *et al.*, 2015. Host-induced gene silencing of an essential chitin synthase gene confers durable resistance to Fusarium head blight and seedling blight in wheat. *Plant Biotechnol J* **13**, 1335-45.

Chisholm ST, Coaker G, Day B, Staskawicz BJ, 2006. Host-microbe interactions: shaping the evolution of the plant immune response. *Cell* **124**, 803-14.

Cohen Y, Ben Naim Y, Falach L, Rubin AE, 2017. Epidemiology of basil downy mildew. *Phytopathology* **107**, 1149-60.

Cohen Y, Vaknin M, Ben-Naim Y, *et al.*, 2013. First report of the occurence and resistance to mefenoxam of Peronospora belbahrii, causal agent of downy mildew of basil (Ocimum basilicum) in Isreal. *Plant Disease* **97**, 692.

Conesa A, Gotz S, Garcia-Gomez JM, Terol J, Talon M, Robles M, 2005. Blast2GO: a universal tool for annotation, visualization and analysis in functional genomics research. *Bioinformatics* **21**, 3674-6.

Dangl JL, Jones JD, 2001. Plant pathogens and integrated defence responses to infection. *Nature* **411**, 826-33.

Deschamps C, Simon JE, 2002. Agrobacterium tumefaciens-mediated transformation of Ocimum basilicum and O. citriodorum. *Plant Cell Reports* **21**, 359-64.

Dou D, Kale SD, Wang X, *et al.*, 2008. RXLR-mediated entry of Phytophthora sojae effector Avr1b into soybean cells does not require pathogen-encoded machinery. *Plant Cell* **20**, 1930-47.

Garibaldi A, Bertetti D, Gullino ML, 2007. Effect of leaf wetness duration and temperature on infection of downy mildew of basil. *Journal of Plant Diseases and Protection* **114**, 6-8.

German MA, Kandel-Kfir M, Swarzberg D, Matsevitz T, Granot D, 2003. A rapid method for the analysis of zygosity in transgenic plants. *Plant Science* **164**, 183-7.

Goh J, Jeon J, Lee YH, 2017. ER retention receptor, MoERR1 is required for fungal development and pathogenicity in the rice blast fungus, Magnaporthe oryzae. *Sci Rep* **7**, 1259.

Graham JB, Canniff NP, Hebert DN, 2019. TPR-containing proteins control protein organization and homeostasis for the endoplasmic reticulum. *Crit Rev Biochem Mol Biol* **54**, 103-18.

Guillemette T, Calmes B, Simoneau P, 2014. Impact of the UPR on the virulence of the plant fungal pathogen A. brassicicola. *Virulence* **5**, 357-64.

Guo XY, Li Y, Fan J*, et al.*, 2019. Host-induced gene silencing of MoAP1 confers broad-spectrum resistance to Magnaporthe oryzae. *Front Plant Sci* **10**, 433.

Haas BJ, Kamoun S, Zody MC*, et al.*, 2009. Genome sequence and analysis of the Irish potato famine pathogen Phytophthora infestans. *Nature* **461**, 393-8.

Hwang HH, Yu M, Lai EM, 2017. Agrobacterium-mediated plant transformation: biology and applications. *Arabidopsis Book* **15**, e0186.

Jiang RH, Tripathy S, Govers F, Tyler BM, 2008. RXLR effector reservoir in two Phytophthora species is dominated by a single rapidly evolving superfamily with more than 700 members. *Proc Natl Acad Sci U S A* **105**, 4874-9.

Jones JD, Dangl JL, 2006. The plant immune system. *Nature* **444**, 323-9.

Kamoun S, 2006. A catalogue of the effector secretome of plant pathogenic oomycetes. *Annu Rev Phytopathol*.

Kettles GJ, Hofinger BJ, Hu P*, et al.*, 2019. sRNA profiling combined with gene function analysis reveals a lack of evidence for cross-kingdom RNAi in the wheat - Zymoseptoria tritici pathosystem. *Front Plant Sci* **10**, 892.

Kumar R, Kumari B, Kumar M, 2017. Prediction of endoplasmic reticulum resident proteins using fragmented amino acid composition and support vector machine. *PeerJ* **5**, e3561.

Livak KJ, Schmittgen TD, 2001b. Analysis of relative gene expression data using real-time quantitative PCR and the 2(-Delta Delta C(T)) Method. *Methods* **25**, 402-8.

Mcgowan J, Fitzpatrick DA, 2017. Genomic, network, and phylogenetic analysis of the oomycete effector arsenal. *mSphere* **2**.

Mersereau M, Pazour GJ, Das A, 1990. Efficient transformation of Agrobacterium tumefaciens by electroporation. *Gene* **90**, 149-51.

Nowara D, Gay A, Lacomme C*, et al.*, 2010. HIGS: host-induced gene silencing in the obligate biotrophic fungal pathogen Blumeria graminis. *Plant Cell* **22**, 3130-41.

Phippen WB, Simon JE, 2000. Anthocyanin inheritance and instability in purple basil (Ocimum basilicum L.). *J Hered* **91**, 289-96.

Pyne RM, Honig JA, Vaiciunas J, Wyenandt CA, Simon JE, 2018. Population structure, genetic diversity and downy mildew resistance among Ocimum species germplasm. *BMC Plant Biol* **18**, 69.

Qi T, Zhu X, Tan C*, et al.*, 2018. Host-induced gene silencing of an important pathogenicity factor PsCPK1 in Puccinia striiformis f. sp. tritici enhances resistance of wheat to stripe rust. *Plant Biotechnol J* **16**, 797-807.

Sanju S, Siddappa S, Thakur A*, et al.*, 2015. Host-mediated gene silencing of a single effector gene from the potato pathogen Phytophthora infestans imparts partial resistance to late blight disease. *Funct Integr Genomics* **15**, 697-706.

Schmittgen TD, Livak KJ, 2008. Analyzing real-time PCR data by the comparative C(T) method. *Nat Protoc* **3**, 1101-8.

Senthil-Kumar M, Mysore KS, 2011. Caveat of RNAi in plants: the off-target effect. *Methods Mol Biol* **744**, 13-25.

Shao D, 2017. Functional characterization of putative effector genes of basil downy mildew pathogen Peronospora belbahrii. *Tropical Plant Pathology, University of Hawaii at Manoa* Master Thesis.

Shao D, Tian M, 2018. A qPCR approach to quantify the growth of basil downy mildew pathogen Peronospora belbarhii during infection. *Current Plant Biology* **15**, 2-7.

Song Y, Thomma B, 2018. Host-induced gene silencing compromises Verticillium wilt in tomato and Arabidopsis. *Mol Plant Pathol* **19**, 77-89.

Stassen JH, Seidl MF, Vergeer PW*, et al.*, 2012. Effector identification in the lettuce downy mildew Bremia lactucae by massively parallel transcriptome sequencing. *Mol Plant Pathol* **13**, 719-31.

Tian M, Win J, Savory E*, et al.*, 2011. 454 Genome sequencing of Pseudoperonospora cubensis reveals effector proteins with a QXLR translocation motif. *Mol Plant Microbe Interact* **24**, 543-53.

Tyler BM, Tripathy S, Zhang X*, et al.*, 2006. Phytophthora genome sequences uncover evolutionary origins and mechanisms of pathogenesis. *Science* **313**, 1261-6.

Wang M, Weiberg A, Lin FM, Thomma BP, Huang HD, Jin H, 2016b. Bidirectional cross-kingdom RNAi and fungal uptake of external RNAs confer plant protection. *Nat Plants* **2**, 16151.

Whisson SC, Boevink PC, Moleleki L*, et al.*, 2007. A translocation signal for delivery of oomycete effector proteins into host plant cells. *Nature* **450**, 115-8.

Wyenandt CA, Simon JE, Pyne RM*, et al.*, 2015. Basil downy mildew (Peronospora belbahrii): discoveries and challenges relative to its control. *Phytopathology* **105**, 885-94.

Yamamoto K, Hamada H, Shinkai H, Kohno Y, Koseki H, Aoe T, 2003. The KDEL receptor modulates the endoplasmic reticulum stress response through mitogen-activated protein kinase signaling cascades. *J Biol Chem* **278**, 34525-32.

Yan P, Shen W, Gao X, Li X, Zhou P, Duan J, 2012. High-throughput construction of intron-containing hairpin RNA vectors for RNAi in plants. *PLoS One* **7**, e38186.

Yang Z, 2007. PAML 4: phylogenetic analysis by maximum likelihood. *Mol Biol Evol* **24**, 1586-91.

Yin L, Li X, Xiang J*, et al.*, 2015. Characterization of the secretome of Plasmopara viticola by de novo transcriptome analysis. *Physiological and Molecular Plant Pathology* **91**, 1-10.

Tables

Table 3.1. Amino acid sequence identity of ORCER1 homologs among eleven oomycete species.

	Pe. bel	Hy. ara	Pl. vit	Br. lac	Ph. pal	Ph. inf	Ph. ram	Ph. par	Ph. cin	Ph. cap	Ph. soj
Pe. bel											
Hy. ara	70										
Pl. vit	69	71									
Br. lac	68	68	72								
Ph. pal	76	78	76	75							
Ph. inf	74	76	77	75	88						
Ph. ram	77	74	73	73	86	83					
Ph. par	75	76	78	75	91	92	84				
Ph. cin	77	80	76	72	91	88	86	89			
Ph. cap	75	77	76	72	87	85	82	86	87		
Ph. soj	77	80	80	71	91	96	85	89	95	88	

The numbers (below the diagonal line) represent the percentage identity for ORCER1.

Peronospora belbahrii (*Pe. bel*), *Hyaloperonospora arabidopsidis* (*Hy. ara*), *Plasmopara viticola* (*Pl. vit*), *Bremia lactucae* (*Br. lac*), *Phytophthora palmivora* (*Ph. pal*), *Phytophthora infestans* (*Ph. inf*), *Phytophthora ramorum* (*Ph. ram*), *Phytophthora parasitica* (*Ph. par*), *Phytophthora cinnamomi* (*Ph. cin*), *Phytophthora capsici* (*Ph. cap*) and *Phytophthora sojae* (*Ph. soj*)

Table 3.2. *Agrobacterium*-mediated transformation efficiency to integrate RNAi-HIGS construct of *PbEC1* and *PbORCER1* in sweet basil.

Expt #	Explants		Shoot regeneration		Root development		Plants Acclimatized (T0)		Transformation efficiency (%)	
	E*	O*	E*	O*	E*	O*	E*	O*	E*	O*
1	85	70	110	97	15	12	7	10	17.64	17.14
2	30	45	59	62	12	8	7	9	40.00	17.77
3	45	45	95	87	21	20	10	6	46.66	44.44
4	63	50	90	90	25	18	6	7	39.68	36.00
5	44	33	40	42	21	11	4	5	47.72	33.33
6	40	42	32	35	15	12	5	3	37.5	28.57

E*: plants transformed with pRNAi-GG-PbEC1 construct

O*: plants transformed with pRNAi-GG-PbORCER1 construct

Table 3.3. Kanamycin resistance assays of T1 segregating populations derived from T0 sweet basil lines expressing RNAi-construct for *PbEC1* and *PbORCER1* respectively.

		No. of plants turned yellow	No. of plants remained green	Total no. of plants
PbEC1	**WT**	30	0	30
	#5 T0	7	53	60
	#9 T0	13	64	77
	#10 T0	18	41	59
	#13 T0	2	65	67
PbORCER1	**WT**	40	0	40
	#4 T0	26	69	95
	#5 T0	28	61	89
	#6 T0	42	24	66
	#11 T0	10	23	33
	#17 T0	42	2	44

Table 3.4. $2^{-\Delta Ct}$ values obtained through qPCR to determine zygosity of T1 sweet basil plants derived from T0 basil lines expressing RNAi-construct for *PbEC1*.

T0	#5		#9		#10		#13	
	T1 #	$2^{-\Delta ct}$	T1 #	$2^{-\Delta ct}$	T1 #	$2^{-\Delta ct}$	T1 #	$2^{-\Delta ct}$
	5-1	0.3300	9-1	0.4918	10-1	1.9544	13-1	0.3393
	5-2	0.5062	9-2	0.4712	10-2	2.0817	13-2	0.4887
	5-3	1.0608	9-3	0.5108	10-3	2.0009	13-3	0.4880
	5-4	0.8187	9-4	0.2801	10-4	0.8835	13-4	0.1178
	5-5	0.7544	9-5	0.2523	10-5	1.7769	13-5	0.4931
	5-6	0.2026	9-6	0.2445	10-6	1.0119	13-6	0.8413
	5-7	0.2927	9-7	0.2597	10-7	2.0047	13-7	0.2832
	5-8	0.8578	9-8	0.2624	10-8	0.7512	13-8	0.4774
	5-9	0.4548	9-9	0.5122	10-9	2.1209	13-9	0.3120
	5-10	0.4086	9-10	0.5567	10-10	1.0048	13-10	0.3276
	5-T0	0.4158	9-T0	0.3455	10-T0	0.7162	13-T0	0.4113
	5-y*	0.0002	9-y*	0.0006	10-y*	0.0006	13-y*	0.0003
	WT	0.0002	WT	0.0001	WT	0.0001	WT	0.0001

y*: T1 transgenic sweet basil plant that turned yellow upon kanamycin drop application

Table 3.5. $2^{-\Delta Ct}$ values obtained through qPCR to determine zygosity of T1 sweet basil plants derived from T0 basil lines expressing RNAi-construct for *PbORCER1*.

T0	#4		#5		#6		#17	
	T1 #	$2^{-\Delta ct}$	T1 #	$2^{-\Delta ct}$	T1 #	$2^{-\Delta ct}$	T1 #	$2^{-\Delta ct}$
	4-1	0.2940	5-1	0.9945	6-1	0.2730	17-1	0.1407
	4-2	0.5437	5-2	0.9876	6-2	0.9609	17-2	0.1847
	4-3	0.5787	5-3	0.4711	6-3	0.6400	17-3	0.1873
	4-4	0.2716	5-4	0.4187	6-4	0.6058	17-4	0.1970
	4-5	0.2495	5-5	0.8899	6-5	0.6363	17-5	0.2866
	4-6	0.2692	5-6	0.4235	6-6	0.6618		
	4-7	0.3122	5-7	0.9154	6-7	0.6853		
	4-8	0.2820	5-8	0.9993	6-8	0.2900		
	4-9	0.5514	5-9	0.4289	6-9	0.6158		
	4-10	0.5731	5-10	0.4455				
	4-T0	0.2884	5-T0	0.3450	6-T0	1.5949	17-T0	1.8914
	4-y*	0.0003	5-y*	0.0005	6-y*	0.0001	17-y*	9.0713
	WT	0.0004	WT	0.0004	WT	0.0001	WT	0.0002

y*: T1 transgenic sweet basil plant that turned yellow upon kanamycin drop application

Table 3.6. Kanamycin resistance assays on T2 sweet basil plants of selected T1 basil lines expressing RNAi-construct for *PbEC1*.

Plant ID	No. of plants remained green	No. of plants turned yellow	Total no. of plants tested
#5-3 T1	8	17	25
#5-4 T1	18	2	20
#5-5 T1	30	0	30
#5-8 T1	20	0	20
#9-1 T1	52	0	52
#9-3 T1	37	0	37
#9-9 T1	31	0	31
#9-10 T1	28	0	28
#10-1 T1	0	24	24
#10-2 T1	5	31	36
#10-3 T1	0	30	30
#10-7 T1	3	14	17
#13-2 T1	28	3	31
#13-3 T1	27	10	37
#13-5 T1	34	6	40
#13-6 T1	41	7	48
WT	0	89	89

Table 3.7. Kanamycin resistance assays on T2 sweet basil plants of selected T1 basil lines expressing RNAi-construct for *PbORCER1*.

Plant ID	No. of plants remained green	No. of plants turned yellow	Total no. of plants tested
#4-2 T1	28	0	28
#4-3 T1	35	0	35
#4-9 T1	15	0	15
#4-10 T1	25	0	25
#5-1 T1	40	0	40
#5-2 T1	40	0	40
#5-5 T1	40	0	40
#5-7 T1	40	0	40
#6-2 T1	10	19	29
#6-3 T1	30	0	30
#6-6 T1	32	0	32
#6-7 T1	35	0	35
WT	0	70	70

Figures

Figure 3.1. Domain features of PbORCER1 and the purifying selection of ORCER1
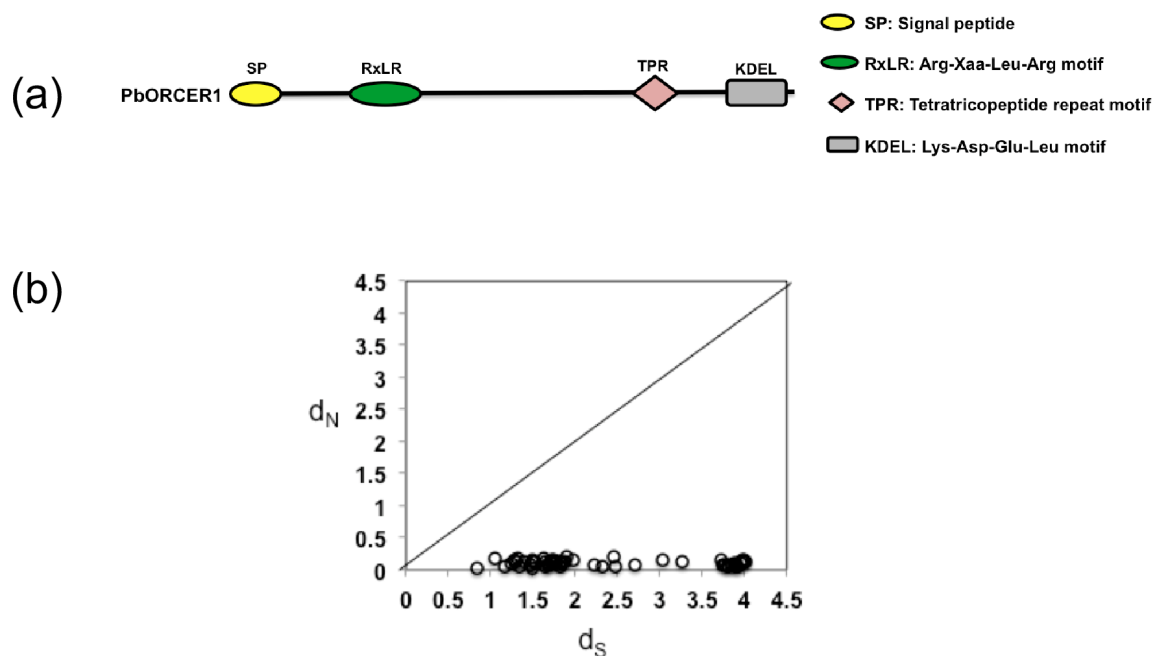
Figure 3.1. Domain features of PbORCER1 and the purifying selection of ORCER1 homologs. (a) Schematic illustration of PbORCER1 containing a signal peptide (SP) and three different motifs: RxLR, TPR and ER retention KDEL. **(b)** Rates of nonsynonymous (d_N) and synonymous (d_S) nucleotide substitutions of pairwise comparisons of ORCER1 homologs. The diagonal line indicates $d_N = d_S$. Circles below the line represent comparison with $\omega = d_N/d_S < 1$.
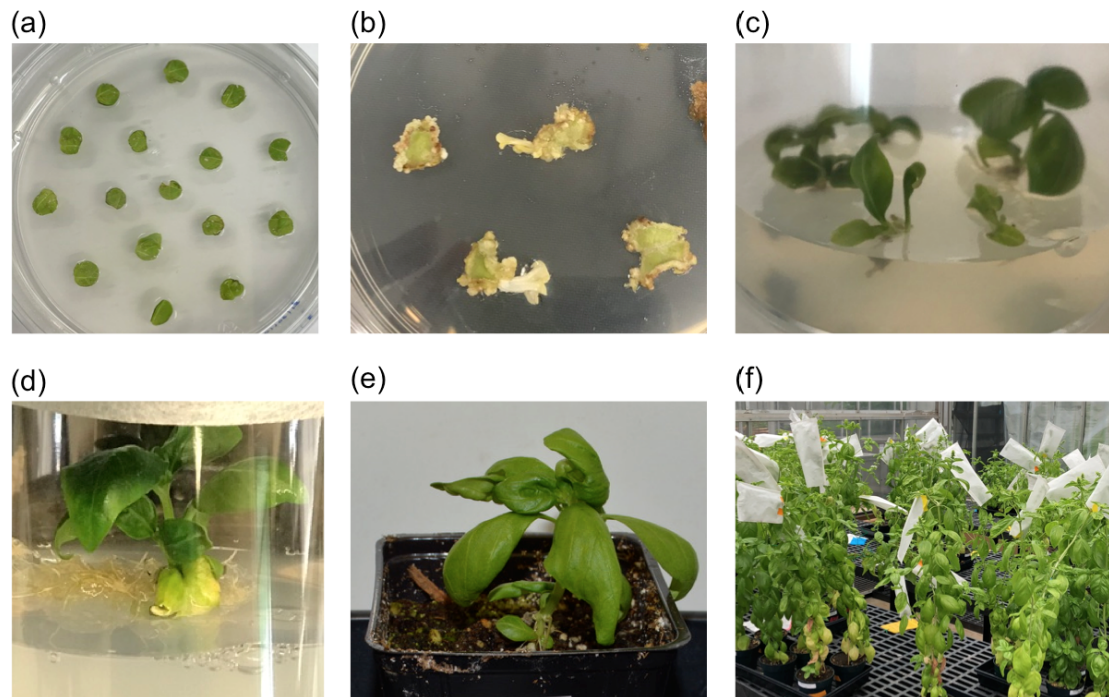
Figure 3.2. Different stages of plant regeneration after *Agrobacterium*-mediated transformation of sweet basil. (**a**) Co-cultivation of leaf explants with *Agrobacteria* on callus and shoot induction (SI) media in dark for 3 days. (**b**) Calli induction with shoot initiation on selective SI media after 2 weeks in dark. (**c**) Differentiated individual shoots on root induction (RI) for shoot elongation and root development. (**d**) Well-developed regenerated plantlet with elongated shoots and defined roots on RI media after 2 weeks under light conditions. (**e**) Ex-vitro acclimatization of regenerated plantlet (**f**) Regenerated plant adapting to greenhouse conditions for generation of seeds with selfing bags mounted on emerging flowering stalks to avoid cross-pollination.
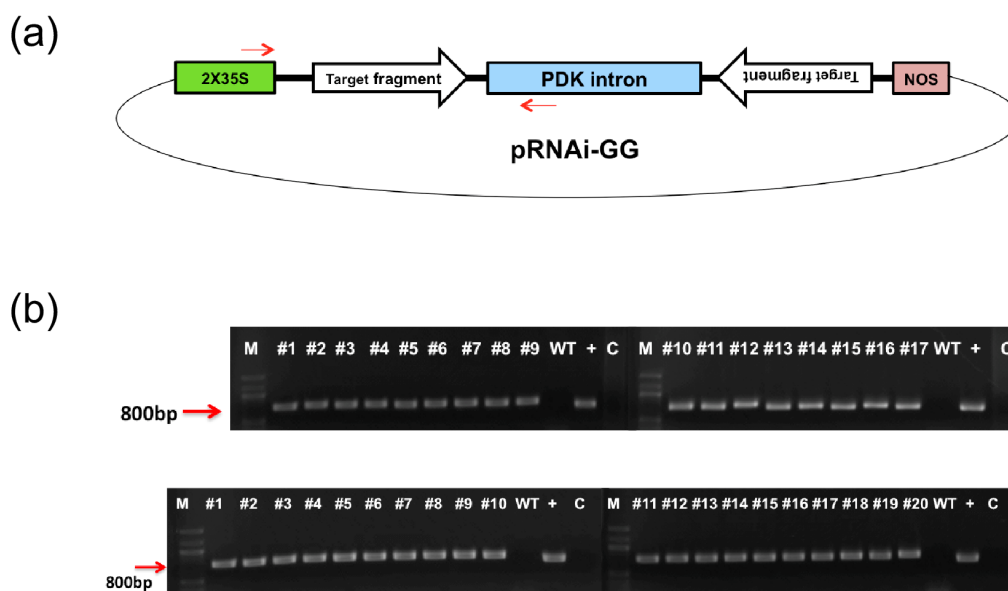
Figure 3.3. Detection of transgene integration of regenerated T0 sweet basil plants. (a) Schematic representation of the silencing construct derived from pRNAi-GG binary vector. The selected region of a target gene was cloned into the vector in sense and antisense orientations flanking a PDK intron (Yan et al., 2012), under the control of the double CaMV 35S promoter and NOS terminator. Red arrows indicate the position of primers used to amplify the transgene fragment from T0 transgenic lines. **(b)** Electrophoresis of PCR products confirming transgene integration in regenerated T0 lines harboring pRNAi-GG-PbEC1 (#1-#17 in upper panel) and pRNAi-GG-PbORCER1 (#2-#20 in lower panel) respectively. +, positive control using pRNAi-GG-PbEC1 (upper panel) and pRNAi-GG-PbORCER1 (lower panel) plasmid as template. WT, wild type Genoveser basil. C, no template control. M is 100bp marker.
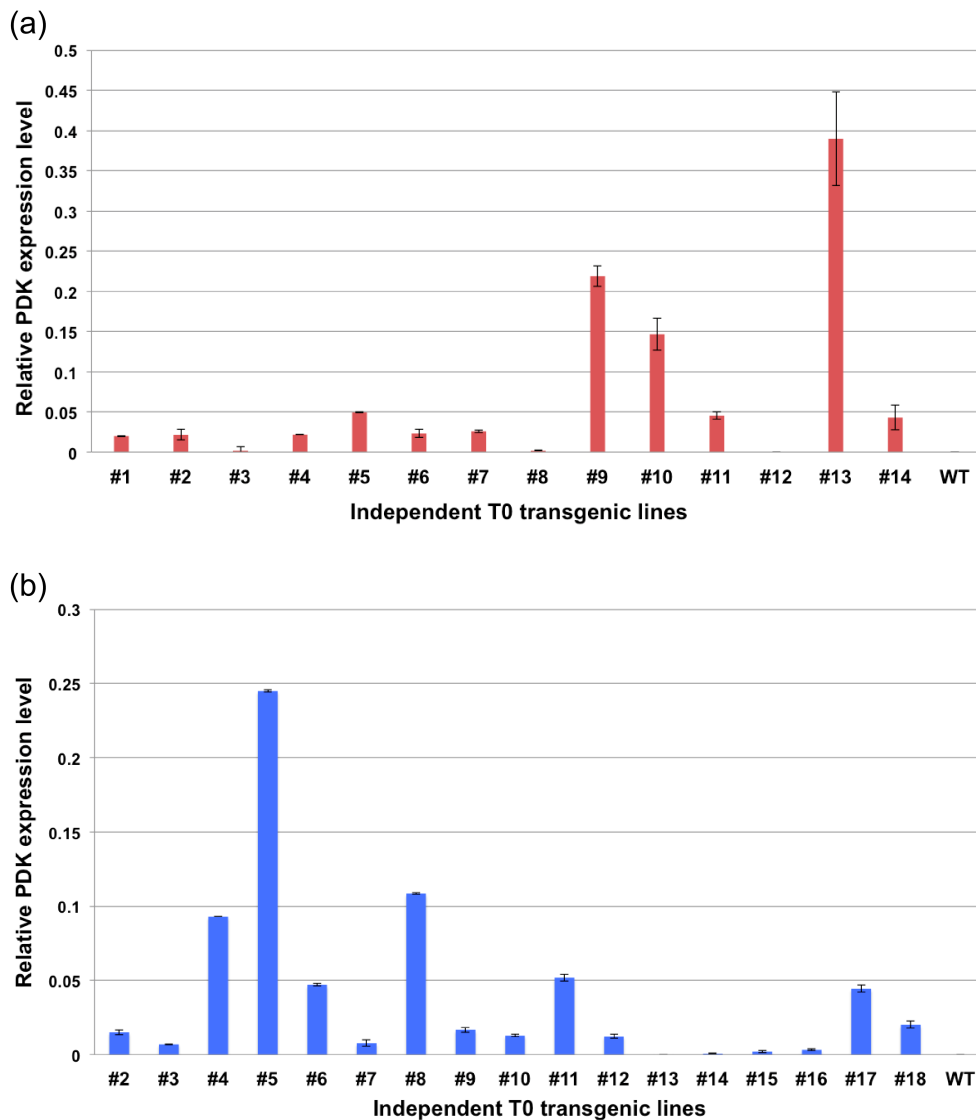
Figure 3.4. Expression levels of ihpRNA among different T0 transgenic sweet basil lines determined by qRT-PCR. (a) Relative expression levels of PDK intron in WT and T0 lines transformed with pRNAi-GG-PbEC1 construct. **(b)** Relative expression levels of PDK intron in WT and T0 lines carrying pRNAi-GG-PbORCER1 construct. The relative expression level is normalized by constitutively expressed *Ocimum basilicum β-tubulin*. The error bars represent ± standard deviations from three technical replicates.

Figure 3.5. Kanamycin resistance assay to select homozygous T2 transgenic sweet basil lines. 25 μl drops of 40 μg/ml kanamycin solution were placed on the center of the first pair of true leaves of 18-days-old T2 transgenic plants carrying *PbORCER1*-RNAi construct and WT plants (represented in red box). Photograph was taken 10 days after kanamycin application.
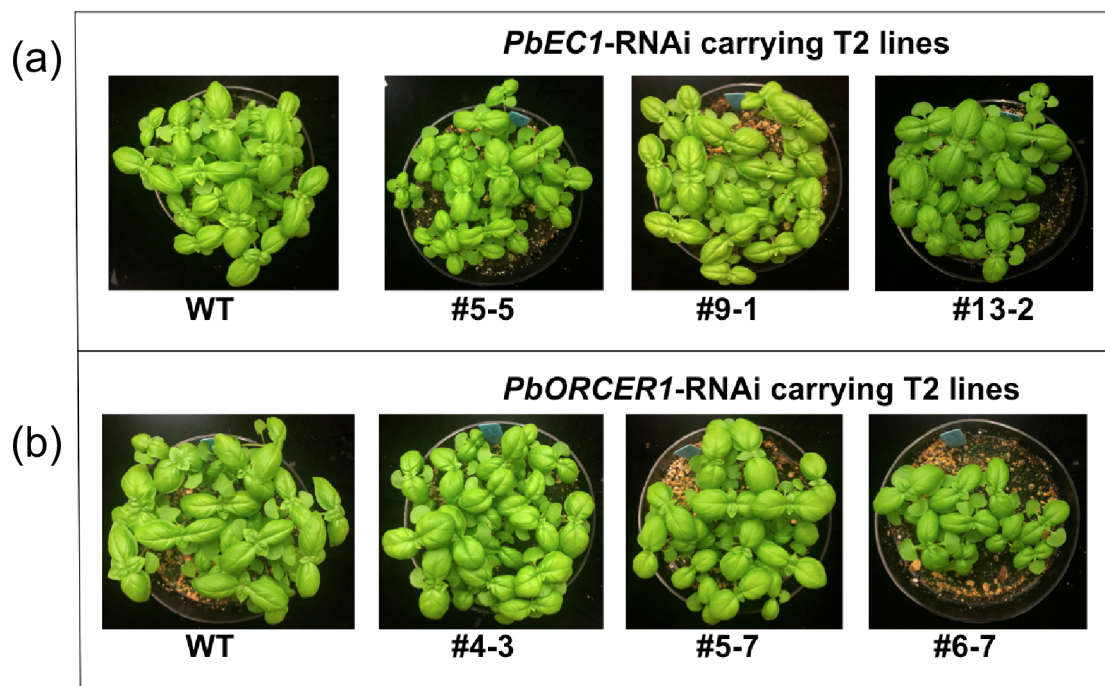
Figure 3.6. Morphological assessment of T2 transgenic sweet basil plants. (a) WT and T2 plants of the indicated homozygous T2 lines (#5-5, #9-1 and #13-2) carrying pRNAi-GG-PbEC1 construct **(b)** WT and T2 plants of the indicated homozygous T2 lines (#4-3, #5-7 and #6-7) carrying pRNAi-GG-PbORCER1 construct. WT, wild type. Three-weeks old plants were used for photographs.
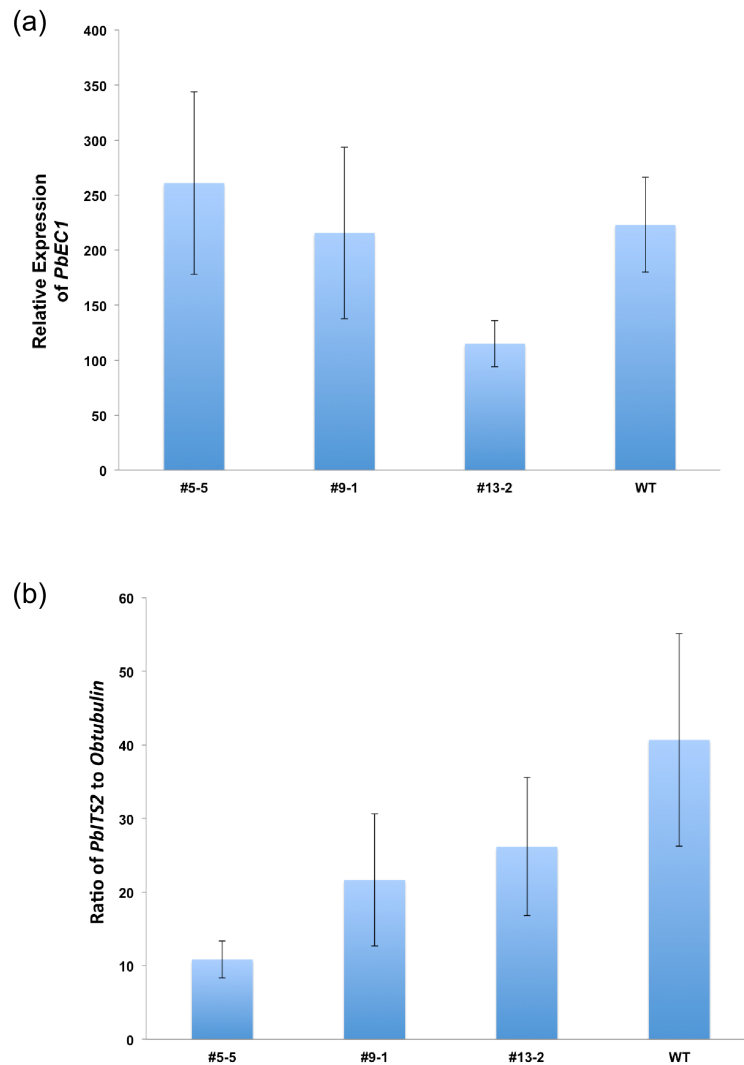
Figure 3.7. Assessment of *PbEC1* expression and *P. belbahrii* growth on T2 homozygous *PbEC1* ihpRNA-expressing basil lines infected with *P. belbahrii*. (a) Relative levels of *PbEC1* transcript abundance in infected WT and homozygous T2 plants at 4 days post inoculation (dpi), determined by RT-qPCR. Values are expressed relative to *P. belbahrii β-tubulin* gene. The error bars represent the standard deviation of the mean of three biological replicates. **(b)** Quantification of pathogen growth at 4dpi using qPCR. The pathogen growth was quantified as the ratio of the amplification of *P. belbahrii ITS2* to *O. basilicum β-tubulin*. Values represent mean ± standard deviation of three biological replicates.
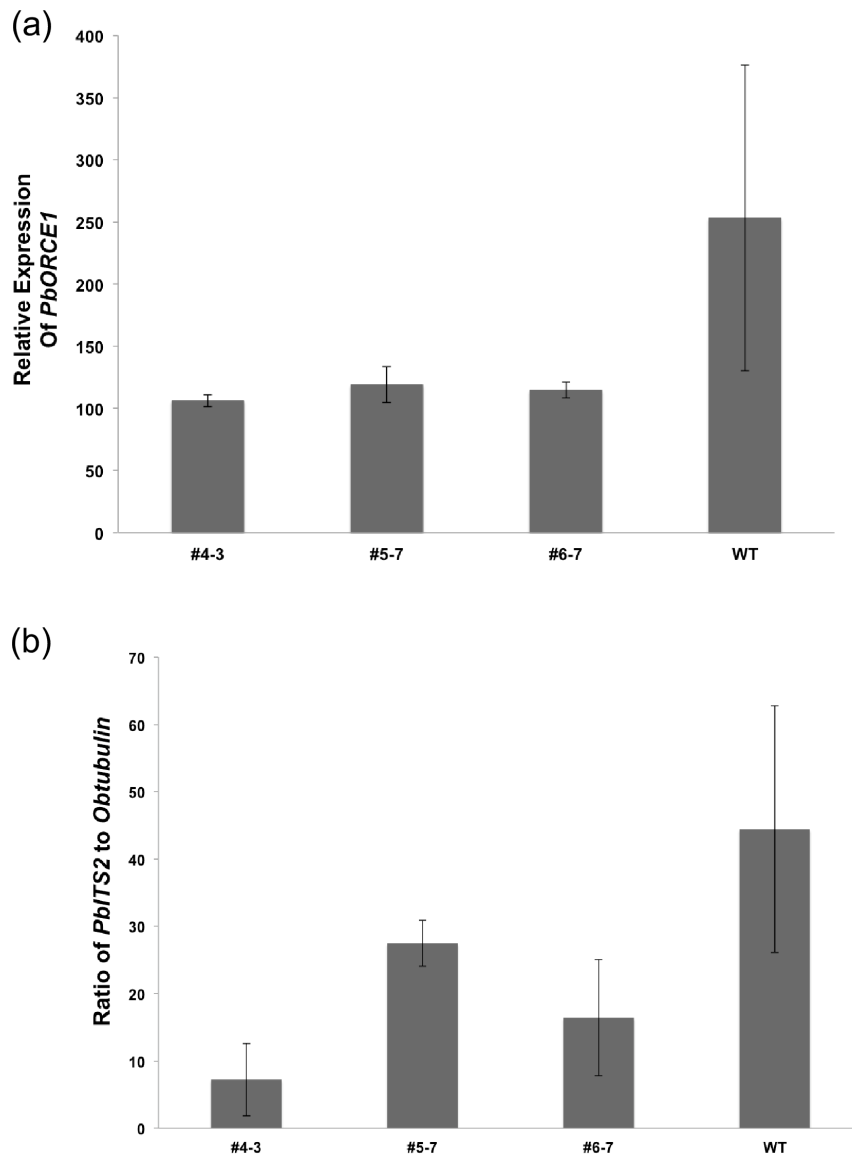
Figure 3.8. Assessment of *PbORCER1* expression and *P. belbahrii* growth on homozygous *PbORCER1* ihpRNA-expressing T2 basil lines infected with *P. belbahrii*. (a) Relative levels of *PbORCER1* transcript abundance in infected WT and homozygous T2 plants at 4 days post inoculation (dpi), determined by RT-qPCR. Values are expressed relative to *P. belbahrii β-tubulin* gene. The error bars represent the standard deviation of the mean of three biological replicates. **(b)** Quantification of pathogen growth at 4dpi using qPCR. The pathogen growth was quantified as the ratio of the amplification of *P. belbahrii ITS2* to *O. basilicum β-tubulin*. Values represent mean ± standard deviation of three biological replicates.

CHAPTER 4

Targeted mutagenesis of basil candidate susceptibility gene *ObDMR1* using CRISPR/Cas9

Abstract

Global production of sweet basil (*Ocimum basilicum*) is in jeopardy due to the obligate biotrophic oomycete pathogen *Peronospora belbahrii*, causing basil downy mildew (BDM). Emerging biotechnology tools promise to broaden disease resistance and accelerate the molecular understanding of *basil- P. belbahrii* interactions. CRISPR/Cas9 gene-editing technology has revolutionized crop breeding and functional genomics. The applicability and efficacy of this robust genomic tool in the allotetraploid sweet basil was tested by editing a potential susceptibility (*S*) gene, *ObDMR1*. *ObDMR1* is the basil homolog of Arabidopsis *DMR1* (*Downy Mildew Resistant 1*) whose mutations conferred nearly complete resistance against Arabidopsis downy mildew pathogen *Hyaloperonospora arabidopsidis*. Two sgRNAs targeting conserved regions of *ObDMR1* coding sequences were designed to mutate at two different sites. A total of 56 transgenic lines were obtained via *Agrobacterium*-mediated stable transformation. Mutational analysis of 54 T0 transgenic lines identified 92% lines carrying indels at target 1 site while a very low indel frequency was detected at target site 2. Deep sequencing of six T0 lines revealed various mutations at target site 1, with a complete knockout of all alleles in one T0 line. T1 homozygous mutant plants with 1-bp frameshift mutations exhibited a dwarf phenotype at young seedling stage, which was indistinguishable from the wild-type (WT) plants in later growth stages. Homozygous transgene-free mutant plants were identified from a T1 segregating population. T2 homozygous mutant plants derived from three independent T0 lines conferred reduced susceptibility to BDM pathogen. This study demonstrates the feasibility of the application of CRISPR/Cas9 in basil functional genomics and breeding BDM resistant varieties.

Keywords: CRISPR/Cas9, gene-editing, *Ocimum basilicum*, *ObDMR1*, transgene-free

4.1.   Introduction

Basil belonging to the genus *Ocimum* in *Lamiaceae* family is a popular herb widely used in culinary, therapeutic, and cosmetic industries (Costa *et al*., 2015; Wyenandt *et al*., 2015).

There are nearly 35-150 species of *Ocimum* distributed across the globe, among which *Ocimum basilicum,* commonly known as sweet basil, is highly demanded, holding a significant economic value (Wyenandt *et al.*, 2015). Different ploidies have been reported across varied species of *Ocimum*, where *O. basilicum* is considered tetraploid (2n = 4x = 48) (Pyne et al., 2018). Karyotyping studies of *O. basilicum* and *O. basilicum* x *O. americanum* F$_1$ hybrids showed preferential chromosome pairing within sub-genomes suggesting allopolyploid formation (Pyne et al., 2018). Global production of sweet basil is severely threatened by an obligate biotrophic oomycete pathogen *Peronospora belbahrii,* which causes basil downy mildew (BDM) (Wyenandt *et al.*, 2010). BDM was first reported in Uganda in 1932 and later in Europe in 2001, and then rapidly spread to almost all regions where sweet basil is cultivated around the world (Cohen et al., 2017). Current control strategies for BDM mainly rely on the use of limited available fungicides, and whose repeated use poses the risk of evolving fungicide-resistant strains (Wyenandt *et al.*, 2015; Cohen et al., 2017). In addition, frequent applications of these chemicals increase production costs and adversely affect human health and the environment. The most robust and cost-effective control strategy to halt the rapid dissemination of BDM is to utilize disease-resistant cultivars, which are currently lacking for sweet basil. Resistance and tolerance have been found in *Ocimum* species differing vastly from sweet basil (Cohen et al., 2017). Traditional breeding involving interspecific hybridization to transfer naturally existing disease resistance genes to sweet basil has been a hassle as it is largely met with sexual incompatibility, hybrid F1 sterility with difficulty in segregating undesirable traits (Ben-Naim et al., 2018; Cohen et al., 2017). One report demonstrating the introgression of resistant gene *Pb1* from wild basil *O. americanum* to *O. basilicum* via interspecific hybridization resulted in sterile F1 plants where tedious backcrossing was applied to obtain viable progenies via embryo rescue (Ben-Naim et al., 2018). Genetic engineering, with the advent of cutting-edge CRISPR/Cas-mediated gene-editing technology, offers a promising platform to broaden resistance resources and accelerate the breeding process.

Adapted from bacterial immune systems, the clustered regularly interspaced short palindromic repeat (CRISPR)/CRISPR-associated protein (Cas) has revolutionized the way scientists perform functional genomics studies and crop breeding as this technology provides an unparalleled tool to precisely edit and modify DNA sequences with high efficiency, high fidelity and easy manipulation (Zhou et al., 2018). The first used CRISPR system for genome editing was CRISPR/Cas9 (Jinek et al., 2012, Jinek et al., 2013), which has been successfully

used in genome editing of many plant species (Haque et al., 2018, Jaganathan et al., 2018). This gene-editing system requires Cas9 and a single guide RNA (sgRNA), which is a fusion of CRISPR RNA (crRNA) containing a 20-nt DNA target sequence upstream of a Cas9 protospacer adjacent motif (PAM, 5'-NGG-3') and trans-activating CRISPR RNA (tracrRNA) (Jinek et al., 2012). The principle behind this technology relies on specific base-pairing of a 20-bp long sequence of sgRNA with the target DNA directing Cas9 endonuclease to cleave the target site 3-nt upstream of the PAM motif (Jiang & Doudna, 2017). The site-directed double-stranded breaks (DSBs) generated by Cas9 activate innate DNA repair by either nonhomologous end-joining (NHEJ) or homology-directed repair (HDR) mechanism. Without a homologous DNA template, the cell repairs the DSB through NHEJ, which is error-prone, causing short insertions or deletions (indels) around the cleavage site (Zhou et al., 2018). When a homologous DNA template is provided, the cell will repair the DSB through HDR, leading to precise mutations or insertions. As this approach can generate homozygous or complete knockout mutants as early as in the first generation of transgenic lines for both diploid and polyploid species (Pan et al., 2016, Wang et al., 2016a, Gumtow et al., 2018), it dramatically speeds up functional genomics studies and shortens the breeding process. Another significant advantage associated with CRISPR/cas9-mediated gene editing is the development of foreign DNA-free crops, which is more acceptable by consumers, as opposed to the conventional way of developing genetically modified (GM) crops. Traditional genetic engineering generates GM crops that embody the transgene within the genome to express new traits. By contrast, the trait generated through CRISPR-meditated gene editing can be segregated from the introduced transgenes; or the desired trait can be achieved via a DNA-free approach for delivery of gene editing reagents. The resultant transgene-free plants can bypass the regulatory restriction standards set by USDA, owing to high public acceptance (Waltz, 2016). Many proof-of-concept studies have used CRISPR for crop nutritional improvement and enhanced resistance to biotic and abiotic stresses (Langner et al., 2018, Borrelli et al., 2018, Jaganathan et al., 2018).

Pathogens exploit plant genes for successful infection and colonization. Plant genes that facilitate pathogen infection are considered as plant susceptibility (S) genes (Schie and Takken 2014). The modification or removal of *S* genes prevents pathogen infection and therefore represents an effective strategy to achieve resistance (Dong & Ronald, 2019, Zaidi et al., 2018). For example, natural loss-of-function mutation and deliberated mutagenesis of *MLO* genes conferred a durable high-level resistance against powdery mildew (PM) (Nie et

al., 2015, Jorgensen, 1992, Wang et al., 2014, Nekrasov et al., 2017). Targeted-mutagenesis of the *S* gene using CRISPR/Cas-mediated technology has recently emerged as a desirable approach to generate broad-spectrum disease resistance (Borrelli et al., 2018, Zaidi et al., 2018). The success of this approach relies on the targeting of a suitable *S* gene. Due to the lack of an effective functional genomics approach in sweet basil, an *S* gene that contributes to susceptibility to basil downy mildew has not been identified. However, a number of *S* genes have been identified in *Arabidopsis* that are required for susceptibility to downy mildew pathogen *Hyaloperonospora arabidopsidis,* one of which is *DMR1* (*Downy Mildew Resistant 1*) (Van Damme et al., 2005, van Damme et al., 2009, Hok et al., 2011, van Damme et al., 2008). *DMR1* encodes a homoserine kinase (HSK) catalyzing the phosphorylation of homoserine (HS). *dmr1* mutants contain high levels of homoserine and are highly resistant to *H. arabidopsidis* (Van Damme et al., 2005, van Damme et al., 2009). DMR1 seems to be conserved in various plant species and its homologs in multiple plant species have shown to be a determining factor for susceptibility to various pathogens. Silencing tomato *DMR1* (*SlDMR1*) enhanced resistance to the powdery mildew pathogen *Oidium neolycopersici* (Huibers et al., 2013). Impairing *DMR1* homolog in potato resulted in a high level of resistance against *Phytophthora infestans,* the oomycete pathogen causing late blight (Sun et al., 2016). In addition, the pepper *DMR1* (*CaDMR1*) was found to be a candidate gene responsible for the major quantitative trait loci (QTL) for resistance to *Phytophthora capsici,* another oomycete pathogen (Rehrig et al., 2014). Therefore, the *DMR1* homolog in sweet basil, *ObDMR1*, represents an ideal candidate *S* gene with a potential role in susceptibility to basil downy mildew.

In the present study, we targeted *ObDMR1* to establish an effective CRISPR/Cas9-mediated gene editing system in sweet basil and generate downy mildew-resistant transgene-free plants. Sweet basil cultivar Genoveser was transformed respectively with two sgRNA/Cas9 binary vectors targeting one or two sites of endogenous *ObDMR1* via *Agrobacterium*-mediated stable transformation. High frequency of small insertion/deletion (indel) mutations and complete knockout of *ObDMR1* were achieved in the first generation (T0) of transgenic plants. Transgene-free homozygous *ObDMR1* mutants were identified in the second generation (T1). *ObDMR1* mutants exhibited dwarf phenotype at the seedling stage, but no aberrant morphological defect for later growth/development stages was observed. Mutation of *ObDMR1* significantly enhanced resistance against infection by *P. belbahrii*. Altogether, this study established an effective gene editing system for sweet basil, with

which *ObDMR1* was genetically determined to be an *S* gene against *P. belbahrii*, and transgene-free sweet basil plants with increased downy mildew resistance were generated.

4.2. Materials and Methods

4.2.1. Plant material and growth conditions

Sweet basil cultivar Genoveser (Enza Zaden) plants used as wild-type (WT) and for *Agrobacterium*-mediated transformation, were grown in a controlled growth chamber set at 25 °C with a photoperiod of 12 hrs. The same conditions were applied to grow newly regenerated transgenic T0, T1 and T2 seedlings. Older T0 and T1 plants were grown in the greenhouse at 25-27 °C with a photoperiod of 16 hrs for seed production. Selfing bags were mounted on flower stalks at the beginning of flowering to avoid cross-pollination.

4.2.2. Identification of the homolog of *Arabidopsis* DMR1 in sweet basil

The homolog of *Arabidopsis* DMR1 in sweet basil (*Ocimum basilicum*), named as *ObDMR1,* was identified by TBLASTX search against non-redundant transcriptomic sequence dataset generated from two sweet basil varieties Red Rubin and Tigullio using Trinity assembly (Torre et al., 2016) using the protein encoding sequence of Arabidopsis *DMR1* (*AtDMR1*) gene (GenBank accession: NM_127281) as a query. A single significant hit was identified and the transcript sequence was retrieved. To amplify *ObDMR1* from sweet basil cv. Genoveser by PCR, we designed a pair of primers (DMR1-Gen-F: 5'-CGTCCCCTATTCTCTCACTATGGC-3'; DMR1-Gen-R: 5'-AAAACCCAGAGACCATGCAAATG-3') targeting 5'-UTR and 3'-UTR of this transcript. Genoveser genomic DNA (gDNA) was extracted from leaf tissue using DNeasy Plant Mini Kit (QIAGEN) according to the user's manual. PCR was performed using Phusion High-Fidelity DNA Polymerase (NEB) with PCR conditions as: initial denaturation at 94 °C for 3 mins; followed by 35 cycles at 94 °C for 15 s, 54 °C for 30 s and 72 °C for 75 s; with a final extension at 72 °C for 7 mins. The resultant PCR product was gel-purified using the QIAquick Gel Extraction Kit (QIAGEN) and subjected to Sanger sequencing using DMR1-Gen-F and DMR1-Gen-R primers. The amino acid sequences of ObDMR1 in Genoveser and AtDMR1 were aligned using BLASTP to assess their homology. The amino acid sequence alignment was also generated using CLUSTALX 2.1 (Larkin et al., 2007) and displayed using BOXSHADE (https://embnet.vital-it.ch/software/BOX_form.html).

4.2.3. Selection of sgRNA target sites for editing *ObDMR1* using CRISPR/Cas9

sgRNA target sites were identified by searching 20-nt sequences immediately upstream of the PAM sequence 5'-NGG-3' within the coding region of Genoveser *ObDMR1* using Eukaryotic Pathogen CRISPR guide RNA design tool (EuPaGDT) (Peng & Tarleton, 2015)(http://grna.ctegd.uga.edu/) with default parameters. The non-redundant transcriptomic assembly of two sweet basil varieties Red Rubin and Tigullio generated using Trinity (Torre et al., 2016) was uploaded as a custom genome to identify potential off-targets. The candidate target sequences with a total score as well as an efficiency score of more than 0.50 were selected and further subjected to secondary structure analyses using the web tool RNAstructure (Reuter & Mathews, 2010) (http://rna.urmc.rochester.edu/RNAstructureWeb/Servers/Predict1/Predict1.html). The target sequences with no more than three hydrogen bonds were chosen for sgRNA synthesis.

4.2.4. Vector construction

The constructs for CRISPR/Cas9-mediated gene editing of *ObDMR1* were generated using plant binary vector pKSE401 as described by Xing et al., 2014 (Xing et al., 2014). For generating the construct expressing one sgRNA (sgRNA1), we used the oligo pair DMR1-target1-F (5'-ATT<u>GTTTCCATTTCCAACATCAC</u>-3') and DMR1-target1-R (5'-AAAC<u>GTGATGTTGGAAATGGAAA</u>-3'). The underlined sequences represent the target site of sgRNA1. The oligos were annealed to produce a double-stranded fragment with 4-nts 5' overhangs at both ends and then ligated into the BsaI-digested pKSE401. The resulting plasmid was named as pKSE401-sgRNA1 (Fig. 2).

For generating the construct expressing two sgRNAs (sgRNA1 and sgRNA2), four oligos (DT1_BsF: 5'-ATATATGGTCTCGATT**<u>GTTTCCATTTCCAACATCAC</u>**GTT-3'; DT1-F0: 5'-T**<u>GATTGTTTCCATTTCCAACATCAC</u>**GTTTTAGAGCTAGAAATAGC-3'; DT2-R0: 5'-AAC<u>TTTGGAATTGCGCCGGCATC</u>AATCTCTTAGTCGACTCTAC-3' and DT2_BsR: 5'-ATTATTGGTCTCTAAAC<u>TTTGGAATTGCGCCGGCATC</u>AA-3') were designed as described by Xing et al. 2014 (Xing et al., 2014). The bold underlined and underlined represent the target sequences of sgRNA1 and sgRNA2, respectively. The DNA fragment containing sgRNA1, U6-26t, U6-29p, and the target sequence of sgRNA2 was amplified using PCR with these four oligos and pCBC-DT1T2 as a template. The PCR reaction was performed using Phusion High-Fidelity DNA Polymerase (NEB) with cycling conditions as: 98 °C for 2 mins followed by 35 cycles at 98 °C for 30 s, 71 °C for 15 s and 72

°C for 90 s; with a final extension at 72 °C for 7 mins. The PCR product was purified using QIAquick PCR Purification Kit (QIAGEN) and then digested by BsaI. The digested PCR product was ligated into the BsaI-digested pKSE401 vector. The resultant plasmid was named as pKSE401-sgRNA1+2 (Fig. 2). Both pKSE401-sgRNA1 and pKSE401-sgRNA1+2 were introduced into *Agrobacterium tumefacians* strain EHA105, respectively, for basil transformation.

4.2.5. Basil transformation

Sweet basil cv. Genoveser was transformed with *A. tumefacians* EHA105 harboring pKSE401-sgRNA1 or pKSE401-sgRNA1+2 based on the method described previously (Deschamps & Simon, 2002; Phippen and Simon 2000) with slight modifications. The Agrobacteria, stored at -80 °C, was streaked on LB plate supplemented with 50 μg/ml kanamycin and 15 μg/ml rifampicin, and grown for two days at 28 °C. A day prior to basil transformation, colonies were spread to a new plate and incubated at 28 °C overnight. On the day of basil transformation, bacterial cells were scraped from the overnight plate and suspended in *Agrobacterium* inoculation media (IN) [MS + 3% sucrose + 16.8 μM TDZ (thidiazuron), pH 5.7, supplemented with 200 μM acetosyringone] to OD_{600} of 0.6. This suspension was incubated at room temperature (RT) in the dark with gentle shaking at 70 rpm for 2 hrs. Meanwhile, the first pair of true leaves from 3-week-old Genoveser plants was plucked and surface sterilized in 12% (v/v) Clorox solution for 5 mins. Two explants were excised from regions close to the leaf base along the midrib of each leaf using cork borer number 2. After the completion of incubation of *Agrobacterium* suspension, the explants were immersed in this suspension for 30 mins at RT. Explants were then taken out, and the excess suspension was removed by pressing the explants gently between two layers of sterile filter paper. These explants were co-cultivated with *Agrobacteria* on callus and shoot induction (SI) media (MS + 0.8% agar + 3% sucrose + 16.8 μM TDZ, pH 5.7) supplemented with 200 μM acetosyringone, with the abaxial side facing the media, for three days in the dark at 25°C. For induction and selection of transgenic calli and shoots, explants were transferred to SI media supplemented with 200 μg/ml Timentin and 30 μg/ml Kanamycin), and grown for 4-6 weeks in the dark at 25 °C with sub-culturing every two weeks onto fresh media. Once the shoots developed on the calli, they were transferred to Root Induction (RI) media [MS + 0.8% agar + 3% sucrose + 0.054 μM NAA (1- napthaleneacetic acid), pH 5.7] supplemented with 200 μg/ml Timentin and 30 μg/ml Kanamycin, and grown for 1 week in

dark at 25 °C, and later under a 12-hr photoperiod cycle for 4-8 weeks with regular sub-culturing performed every two weeks. Plantlets with properly defined root and shoot systems were removed from media jars, washed thoroughly with water to remove the media, and then planted in moistened soil (SunGro Horticulture Sunshine Mix #4). The plants were further grown under 100% relative humidity for 3 to 4 days in a tray covered with a plastic dome in a controlled growth chamber set at 25 °C with a 12-hrs photoperiod. Humidity was gradually reduced over the next 2 to 3 days, and then the plants were transferred to the greenhouse to produce seeds.

4.2.6. Detection of transgene integration and *ObDMR1* mutations in transgenic plants

DNA isolation was performed using approximately 50 mg leaf tissues of regenerated basil plants (T0 and T1), which were smashed with a stainless steel ball (5 mm) in 400 μl of DNA Extraction buffer (200 mM Tris-HCl, pH 7.5, 250 mM NaCl, 25 mM EDTA and 0.5% SDS) using FastPrep-24 (MP Biomedicals) at 4.0m/s for 20 s. The following DNA isolation procedures were performed as described previously (Shao & Tian, 2018). This crude gDNA was used as the template to determine the transgene integration in T0 and T1 plants by PCR. PCR was performed using primers U6-26p-F (5'-TGTCCCAGGATTAGAATGATTAGGC-3') (Xing et al., 2014) & DMR1-target1-R for plants transformed with pKSE401-sgRNA1, and primers U6-26p-F and U6-29p-R (5'-AGCCCTCTTCTTTCGATCCATCAAC-3') (Xing et al., 2014) for plants transformed with pKSE401-sgRNA1+2. To identify the mutations in *ObDMR1*, the primers DMR1-CRISPR-F (5'-CCCGTCTTCTCCTCCGTCAAATC-3') and DMR1-CRISPR-R (5'-AGTTCTGACGGCGACAGAGGACC-3') flanking both sgRNA1 and sgRNA2 target sites were used for PCR to amplify the *ObDMR1* fragment. PCR was performed using Phusion high-fidelity DNA polymerase (NEB). The PCR products were treated with ExoSAP-IT (ThermoFisher Scientific) before subjecting to Sanger sequencing using the above primers. The Synthego ICE v1.1 CRISPR Analysis Tool (https://ice.synthego.com/#/) (Hsiau et al., 2018) was used for chromatogram decoding to assess insertion/deletion (indel) frequency. Sequence trace files from the transgenic lines and WT were uploaded to the server for the analysis.

PCR products from six T0 transgenic lines with the highest indel frequency were purified using the QIAGEN Gel extraction kit and subjected to deep amplicon sequencing for detailed mutation analyses. DNA library preparations, sequencing reactions, and adapter sequence trimming were conducted at GENEWIZ, Inc. (South Plainfield, NJ, USA). DNA library

preparation was performed using the NEBNext Ultra DNA Library Prep kit following the manufacturer's recommendations (Illumina, San Diego, CA, USA). Briefly, end-repaired adapters were ligated after adenylation of the 3'ends followed by enrichment by limited cycle PCR. DNA libraries were validated and quantified before loading. The pooled DNA libraries were loaded on the Illumina instrument according to the manufacturer's instructions. The samples were sequenced using a 2x 250 paired-end (PE) configuration. The Illumina Control Software on the Illumina instrument conducted image analysis and base calling. An approximate of 50,000 amplicon-reads were obtained after trimming for each independent line. Unique sequences with more than 0.5% of total reads were analyzed in detail to determine the types of mutations at the targeted sites of *ObDMR1*.

4.2.7. Morphological phenotyping of T1 homozygous mutant lines

Seeds of T1 homozygous mutant lines along with WT were sown at the same time under the same growth conditions set at 25 °C with a photoperiod of 12 hrs to monitor the germination rate. Growth and development phenotypes were monitored from two weeks until ten weeks. Photographs of a representative 18-day-old plant from each T1 homozygous line and WT were taken.

4.2.8. Disease resistance assays via pathogen biomass quantification using qPCR

Peronospora belbahrii was isolated from basil plants in the nursery of City Mill, Honolulu, Hawaii. Pathogen propagation, maintenance and infection were performed as described previously (Shao & Tian, 2018). 4-week-old basil plants (WT and T2 homozygous mutant plants) were inoculated by dropping four 10 μl drops/leaf of sporangial suspension (2 x 10^4/ml) on the first pair of true leaves. At 4-days post-inoculation (dpi), three inoculated leaves from 3 plants were collected as one sample, which served as one biological replicate. 3 biological replicates were collected for each treatment. As soon as the leaves were plucked, they were wrapped in aluminum foil, frozen in liquid nitrogen and stored at -80°C until genomic DNA (gDNA) isolation. gDNA isolation followed by pathogen biomass quantification was performed as described previously (Shao and Tian 2018). 50 ng of gDNA was used as the template for qPCR in a 20 μl reaction containing 1X SsoAdvanced^{TM} Universal SYBR Green Supermix (Bio-Rad) and 250 nM primers targeting *P. belbahrii ITS2* and *O. basilicum β-tubulin* (Shao and Tian 2018). The pathogen biomass was quantified as the ratio of amplification of *P. belbahrii ITS2* relative to *O. basilicum β-tubulin*, calculated as $2^{-\Delta Ct}$. This experiment was performed thrice.

4.2.9. Disease scoring and spore counting

Peronospora belbahrii was isolated from basil plants in the nursery of City Mill, Honolulu, Hawaii. Pathogen propagation, maintenance, and infection were performed as described previously (Shao & Tian, 2018). Four-week-old WT and T2 homozygous mutant plants were subjected to *P. belbahrii* inoculation by spraying 60 μl of sporangial suspension (1 x 10^4 sporangia/ml) on the first pair of true leaves. At 7-days post-inoculation (dpi), the percentage of leaf areas showing sporulation was recorded for each inoculated leaf. To compare the abundance of sporangia on inoculated leaves of WT and mutant plants, sporangia were collected and counted at 9-dpi. Four inoculated leaves were taken as one sample, which served as one of three biological replicates for each line, and their fresh weight was measured. 15 ml of deionized water was added to each sample to dislodge the spores by vortexing for 1 min at medium speed with a swirling motion. The entire sporangial suspension was transferred to a new tube and the concentration of sporangia was determined using a hemacytometer (Bright-Line, Hausser Scientific Horsham, U.S.A.). The average number of sporangia per gram of leaves was calculated from three biological replicates.

4.3. Results

4.3.1. Identification of the homolog of Arabidopsis *DMR1* in sweet basil

To determine whether a homolog of Arabidopsis DMR1 (AtDMR1, At2g17265) is present in sweet basil, we did a local TLASTX search using the 1113-bp protein coding sequence of AtDMR1 as query against the non-redundant transcriptomic sequence dataset generated from two sweet basil varieties Red Rubin and Tigullio using Trinity assembly (Torre et al., 2016). We identified one significant hit with an E value as 9e-147. All other hits were insignificant with E values higher than 0.11. The single significant hit comp43301_c0_seq2 was a transcript of 1616 bp, with a predicted open reading frame (ORF) of 1137 bp. BLASTP search with its translated amino acid sequence as the query against NCBI non-redundant database found that it was highly similar to homoserine kinase or homoserine kinase-like proteins in various plant species. BLASTP against Araport11 protein sequences in The Arabidopsis Information Resource (Tair) identified AtDMR1 as the best hit. These results suggested that we have identified the homolog of AtDMR1 in sweet basil, designated as ObDMR1.

As we planned to perform CRISPR/Cas9-mediated gene editing of *ObDMR1* in Genoveser, we amplified and sequenced the *ObDMR1* genomic DNA (gDNA) using a pair of primers targeting the 5'-UTR and 3'-UTR of the *ObDMR1* transcript from Red Rubin and Tigullio. Genoveser *ObDMR1* gDNA was predicted to have an open reading frame (ORF) of 1137-bp encoding 361 amino acids. This putative ORF aligned with the ORF of *ObDMR1* transcript from Red Rubin and Tigullio with no gaps (Figure 4.1.), suggesting that there is no intron present from the translation start codon to stop codon. There were a total of 10 single nucleotide polymorphisms (SNPs) with only one leading to the difference in the third amino acid from N-terminus, with alanine (A) in Genoveser and threonine (T) in Red Rubin and Tigullio (Figure 4.1.). The amino acid sequence of ObDMR1 from Genoveser shares a 78.59% identity with AtDMR1 with an E value of 2e-168 (Figure 4.2.). Similar to AtDMR1, a homoserine kinase (HSK) domain belonging to PLN02451 superfamily was identified using the NCBI Conserved Domain Search (Marchler-Bauer et al., 2017).

4.3.2. Selection of sgRNA target sequences and generation of constructs

To test the efficiency of CRISPR/Cas9-mediated gene editing in sweet basil, *ObDMR1* was targeted for mutagenesis. 20-nt long candidate sgRNA target sequences were identified using the online tool EuPaGDT (http://grna.ctegd.uga.edu/) and their RNA secondary structures were analyzed using RNAstructure (http://rna.urmc.rochester.edu/RNAstructureWeb/Servers/Predict1/Predict1.html). As the genome sequence of sweet basil was not available, we used the transcriptomic sequence dataset of two sweet basil varieties Red Rubin and Tigullio (Torre et al., 2016) as the custom genome for off-target analysis. We selected two target sequences for gene editing based on a combined consideration of their locations, total scores, efficiency scores, GC content, absence of off-targets and the number of hydrogen bonds in the predicted RNA structure. Both selected targets lie in regions encoding N-terminal half of the protein. Target 1 is located at 310-329 bp downstream of the translation start site on the sense strand, and Target 2 is located at 362-381 bp downstream of the translation start on the complementary strand (Figure 4.3a). Both have a total score and an efficiency score higher than 0.5, and no off-targets were found (Table 4.2.). The GC content is 40% and 55% for Target 1 and Target 2, respectively. The predicted RNA structures of both targets are relatively less complex with three hydrogen bonds (Table 4.2.).

To perform sweet basil targeted gene-editing using *Agrobacterium*-mediated transformation, we utilized pKSE401, which is a plant binary vector developed for gene editing in dicots (Xing et al., 2014). Two constructs pKSE401-sgRNA1 and pKSE401-sgRNA1+2 were generated that express one sgRNA and two sgRNAs, respectively. pKSE401-sgRNA1 expresses sgRNA1 under the control of Arabidopsis U6-26 promoter and U6-26 terminator (Figure 4.3b). pKSE401-sgRNA1+2 expresses two sgRNAs, with sgRNA1 expression driven by *Arabidopsis* U6-26 promoter and U6-26 terminator, and sgRNA2 under the control of *Arabidopsis* U6-29 promoter and U6-26 terminator (Figure 4.3b). Both constructs express maize-codon optimized Cas9 under the control of the double CaMV 35S promoter, and *NPTII* gene under the control of CaMV 35S promoter for selection of transgenic plants (Figure 4.3b). Both constructs were introduced into *Agrobacterium tumefacians* strain EHA105, respectively, for basil transformation.

4.3.3. Generation of transgenic basil plants expressing gene-editing reagents

To generate transgenic basil plants expressing sgRNA(s) and Cas9, leaf discs prepared from the first pair of true leaves from 3-week-old Genoveser plants were used as explants. These explants were then infected and co-cultivated with *A. tumefaciens* EHA105 strains harboring either pKSE401-sgRNA1 or pKSE401-sgRNA1+2 (Figure 4.4a) on callus and shoot induction (SI) media supplemented with acetosyringone for three days in the dark. Then the explants were transferred to SI media containing kanamycin to induce the formation of transgenic calli and shoots selectively. Calli were seen two weeks after culturing the explants on kanamycin-containing SI media and tiny shoot buds emerged from calli later after subculturing onto fresh media (Figure 4.4b). Shoots with emerging stalks were later placed on root induction media (RI) (Figure 4.4c) for the development of the whole plant (Figure 4.4d). Well-developed shoots and roots were observed in the regenerated plants after growing on RI media for four weeks (Figure 4.4e and 4.4f). The well-developed plants were further acclimatized into the soil and grown in controlled growth chamber (Figure 4.4g) and further transferred in a greenhouse to produce T1 seeds (Figure 4.4h). For transformation with pKSE401-sgRNA1, out of 176 explants, 34 kanamycin-resistant plants were regenerated with an efficiency of 19.3%. For transformation with pKSE401-sgRNA1+2, 48 Kanamycin-resistant plants were regenerated from 238 explants with an efficiency of 20.2%. 24 plants transformed with pKSE401-sgRNA1 and 32 plants transformed with pKSE401-sgRNA1+2 were tested for the integration of the transgene by PCR. All of them were shown to be positive.

4.3.4. Targeted mutagenesis of *ObDMR1* in T0 transgenic plants

To identify the mutations of *ObDMR1* in transgenic plants, a 383-bp fragment spanning both sgRNA target sites was amplified by PCR and subjected to Sanger sequencing. The chromatograms obtained after sequencing were decoded using Synthego ICE v1.1 CRISPR Analysis Tool to assess the indel frequency. Among the 24 T0 plants carrying target 1, we were able to obtain good chromatograms for only 22 lines, which were further subjected to analysis. No mutation was detected in four lines (#13, #15, #2, and #21), while varied percentages of indel mutations were detected in the remaining 18 lines, leading to an 81.8% mutation rate (Figure 4.5a). A similar analysis was run for the 32 T0 transgenic lines transformed with the construct expressing two sgRNAs. A 100% mutation rate was achieved with different percentages of indels detected at the sgRNA1 target site in each individual plant (Figure 4.5b). As sweet basil is tetraploid (Pyne et al., 2018), T0 plants an indel percentage of less than 25% are believed to be the ones having a chimeric mutation. The plants with relatively high indel frequency (≥ 50%) were selected for further downstream experiments. Of the 10 such lines, four died during the acclimatization period while the remaining six, including #9, #11 and #16 carrying target 1; and #7, #24 and #33 carrying both targets, were selected for amplicon deep sequencing.

Amplicon deep sequencing of the 383-bp *ObDMR1* fragments from each of the six lines yielded around 50,000 high-quality reads. A significant percentage of reads contained mutations in the sgRNA1 target site (Figure 4.6.). While mutations were also detected in the sgRNA2 target site for the three lines that carrying two sgRNAs, the percentage of reads with such mutations was lower than 0.5%. The prevalent editions at the sgRNA1 target site included short insertion (+1) and deletions (-1, -2, or -3) as well as a large deletion (-25). 1-bp insertion was the most common mutation type, which appeared in all six lines that were subjected to amplicon sequencing, while 1-3-bp deletions were detected in five lines except #24 (Figure 4.6.). 13% of the amplicon reads in T0 line #24 contained a 25-bp deletion at the target 1 site. A significant percentage of reads contained no mutations (similar as WT) in five lines except for one #33. Line #33 contained four different types of mutations and a negligible amount (0.01%) of wild-type (WT) reads, suggesting that it is a complete knockout mutant (Figure 4.6.). These results indicate that the CRISPR/Cas9-mediated gene editing system in sweet basil is highly efficient, with a capacity to generate complete knockout mutants in the first-generation of transgenic plants.

4.3.5. Obtaining transgene-free homozygous mutants in T1 generation

The three T0 lines (#9, #11 and #16) that contain sgRNA1 were self-fertilized to produce seeds of T1 generation. *ObDMR1* mutations in T1 plants were detected by sequencing the 383-bp *ObDMR1* fragments through Sanger sequencing. The chromatograms obtained from individual T1 plants revealed that the mutations in T0 plants were inherited and segregated. T1 plants showing chromatogram with overlapping peaks same as T0 starting from the Cas9 cleavage site (3-nt upstream of PAM) were considered as heterozygous for the mutation, whereas, T1 plants with a clear insertion of a new nucleotide close to the Cas9 cleavage site were regarded as homozygous mutants (Figure 4.7a). For each T0 line, we tested 10-12 T1 plants for *ObDMR1* mutations. We detected 2-3 T1 homozygous mutants derived from each T0 line. In total, seven T1 homozygous mutant plants were obtained. T1 homozygous mutants derived from T0 lines #9 (#9-2 and #9-9) and #11 (#11-5, #11-7, and #11-8) contained the same mutation with a "T" inserted at the Cas9 cleavage site, while T1 homozygous mutants derived from T0 line #16 (#16-2 and #16-4) contained a "G" insertion (Figure 4.7a and 4.7b). Such mutations resulted in the ObDMR1 open reading frame (ORF) shift and correspondingly altered the amino acid sequences (Figure 4.7a and 4.7b).

To identify transgene-free homozygous mutants, we determined the presence of the transgene in the seven T1 homozygous mutants by amplifying a fragment of sgRNA1 expression cassette delivered by the plasmid pKSE401-sgRNA1. As a template integrity control, the 383-bp *ObDMR1* fragment was successfully amplified from all plants (Figure 4.7c). No amplification of the sgRNA1 expression cassette was observed in T1 line #9-2 and #9-9, while its amplification in other lines was successful (Figure 4.7c), demonstrating that the transgene was segregated out from #9-2 and #9-9. These results indicated the heritability of the *ObDMR1* mutations to next generation independent of the presence of transgene, which lead to transgene-free homozygous mutants.

4.3.6. Dwarf phenotype in T1 homozygous *ObDMR1* mutants at the seedling stage

In order to observe the morphological phenotypic differences under normal growth conditions, T1 homozygous *ObDMR1* mutants, along with WT, were grown in the same controlled growth chambers. Seedlings of *ObDMR1* mutants exhibited varying degrees of stunted growth in comparison to WT (Figure 4.8.). All 18-days-old mutant lines displayed significant dwarfism compared with WT, with #9-2, #9-9, #11-5, #11-7 and #11-8 showing more drastic dwarfism than #16-4 (Figure 4.8.). The notable stunting in plant height was only

observed at the young seedling stage. The difference in height gradually reduced along with age. 45-days or older mutant plants showed similar growth and expansion of leaves as WT.

4.3.7. Knockout of *ObDMR1* in Genoveser reduces susceptibility to *Peronospora belbahrii*

To evaluate whether mutations of *ObDMR1* affect resistance against *Peronospora belbahrii*, T2 plants of T1 homozygous mutant lines #9-9, #11-5 and #16-4 along with WT were subjected to pathogen inoculation. We determined the severity levels of basil downy mildew disease by quantifying the pathogen biomass, recording the percentages of leaf areas covered with sporulation and measuring the abundance of the sporangia on the infected leaves. Pathogen biomass was quantified through a qPCR assay as the relative amplification of *PbITS2* normalized with *O. basilicum β-tubulin*, with samples collected at 4-days after drop inoculation. The pathogen growth was reduced by 28%, 49%, and 80% in mutant lines #9-9, #11-5 and #16-4 respectively, when compared to WT (Figure 4.9a). The percentages of leaf areas covered with sporulation were recorded at 7-days after spray inoculation. Sporulation density was observed in all inoculated leaves of WT, whereas among the inoculated leaves of #9-9, #11-5, and #16-4, sporulation abundance of 44%, 75%, and 44% respectively, was seen. The number of leaves with dense sporulation was significantly higher in WT than the mutant lines (Figure 4.9b). The abundance of sporangia produced upon inoculation was determined at 9-days following spray inoculation. 55%, 31% and 49% reduction in spore production was accounted for in lines #9-9, #11-5 and #16-4 in comparison to WT (Figure 4.9c). Altogether, these results suggest that mutations of *ObDMR1* decrease the susceptibility of sweet basil to *P. belbahrii,* implying that *ObDMR1* represents an essential *S* gene required by *P. belbahrii* for successful infection and proliferation.

4.4.   Discussion

With the rapid advancement in CRISPR/Cas9 gene-editing technology, an upsurge has taken place in fields of functional genomics and breeding for resistance (Wang et al., 2018a). Production of sweet basil is primarily hampered due to the obligate-biotroph pathogen *Peronospora belbahrii* causing basil downy mildew. Introgression of *R*-genes through traditional breeding has failed due to sexual incompatibility and hybrid F1 sterility (Ben-Naim et al., 2018; Cohen et al., 2017). Therefore, a fundamental understanding of basil-

P. belbahrii molecular interactions is currently lacking and requires immediate focus to manage the fast-spreading BDM disease. Although resistance genes have been studied for a long time to provide resistance against specific pathogens, the concept of targeting the susceptibility gene for gene-mutation is relatively new (van Schie & Takken, 2014). *Downy Mildew Resistance 1* (*DMR1*) encodes for homoserine kinase (HSK), required in the amino acid biosynthetic pathway. Sequence homologs of Arabidopsis *DMR1* have already been identified for tomato, potato, and pepper (Huibers et al., 2013, Sun et al., 2016, Rehrig et al., 2014). Impairment in homologs of Arabidopsis *DMR1* in tomato (*SlDMR1*) and potato (*StDMR1*) resulted in enhanced resistance to different pathogens, implying that the functionality of *DMR1* appears retained in different plant species (Sun et al., 2016). Since sweet basil genetic nature is predominantly allotetraploid, it is challenging to conduct forward or reverse genetic studies with conventional approaches (Pyne et al., 2018). CRISPR/Cas9 has proved to be a boon for characterizing genes by targeted mutation in polyploidy plants such as wheat, potato, and switchgrass (Wang et al., 2015a, Zhang et al., 2019, Liu et al., 2018). Therefore, such findings prompted us to validate the function of Arabidopsis *DMR1* homolog in sweet basil (*ObDMR1*) using precise gene-editing technology CRISPR/Cas9.

Previous studies have shown that the efficacy of CRISPR/Cas9 varies depending on certain determining factors, including plant species, gene-of-interest, target-site sequences, promoter driving Cas9, sgRNA sequences, sgRNA promoter and transformation method Cas9 (Wang et al., 2018a, Ma et al., 2016). In our study, a total of 56 T0 lines were regenerated using *Agrobacterium*-mediated stable transformation, 24 targeting site 1; while the other 32 carried the assembly of two sgRNAs, targeting sites 1 and 2 simultaneously. Through SYNTHEGO-ICE analysis, it was generalized that a high mutation rate of 92% was obtained for T0 lines containing mutations at target site 1. Different kinds of indels (insertion/deletions) are incorporated into transgenic lines mediated by CRISPR/Cas9 leading to homozygous, heterozygous, biallelic, multiallelic and chimeric mutations, reported for several plant species like rice, *Arabidopsis thaliana*, maize and grape (Zhang et al., 2014, Wang et al., 2015b, Svitashev et al., 2015, Wang et al., 2018a). Moreover, in our study, the initial screening of all 50 T0 lines displayed heterozygous mutation. However, deep-sequencing of six selected T0 lines #7, #9, #11, #16, #24 and #33 showed a mutation rate of 74%, 47%, 32%, 32.6%, 47% and 99.9%, respectively, at target site 1, suggesting a complete knockout of *ObDMR1* in one transgenic line in the first-generation. This result reflects the

efficiency of the CRISPR/Cas9 system established for sweet basil, having the capacity to generate complete knockout in the first generation itself. Deep sequencing represented very few reads falling below the described cutoff, carrying mutations at target site 2, demonstrating the chances of more chimeric type mutations. The total time frame to carry CRISPR/Cas9 targeted mutation in basil, starting from target design to evaluation of mutations was done in 5 months (Figure 4.10.).

Segregation in the successive generation allowed us to select plants with homozygous insertions at the target 1 site. Transgene-free T1 lines were identified in two out of seven homozygous T1 lines by amplifying sgRNA1 transgene cassette through PCR. Based on the data collected for the mutation in *ObDMR1* among T0 and T1 transgenic plants, it is clear that the mutations of homozygotes are stably inherited regardless of whether T-DNA is present or not. However, heterozygotes retain some wild type alleles that still carry the potential to get mutated. Thus, new mutation types could arise in different tissues at both T0 and T1 generation, as reported earlier (Pan et al., 2016). Transgene-free T1 mutants were identified in this study at T1 generation, lacking the sgRNA transgene fragment, possibly due to the loss of CRISPR/Cas9 cassette during cell division. The continued presence of T-DNA harboring sgRNA and Cas9 cassettes increases the risk of introducing new mutations (Gao et al., 2016).

T1 homozygous lines #9-2, #9-9, #11-5, #11-7, and #11-8 (carrying 'T' insertion) displayed drastic dwarfing phenotypic aberration than #16-4 (carrying 'G' insertion) at the young seedling stage. Such data indicates that only a single nucleotide mutation in *ObDMR1* carries the capacity to cause a change in plant height at the early seedling stage by causing a frameshift mutation with significant effect. It should also be noted that different point mutations at the same site could have different levels of phenotypic effects. For the later phase of development, starting from 6-weeks old plants, all homozygous T1 plants displayed normal growth and expansion of leaf similar to WT. Stunted growth was previously observed in Arabidopsis recessive homozygous *dmr1* mutants (Van Damme et al., 2005, van Damme et al., 2009). This suggests that the complete knockout of *ObDMR1* was successfully achieved using CRISPR/Cas9-mediated gene-editing developed for sweet basil. *ObDMR1* is probably implicated in the regulation of plant height during the seedling stage, similar to its ortholog in Arabidopsis (van Damme et al., 2005). Nevertheless, mutant *ObDMR1* plants

developed normally in later stages, signifying their applicability in breeding practices to develop disease-resistant varieties.

To identify the function of *ObDMR1* in defense against *P. belbahrii*, we compared the pathogen biomass on three homozygous transgenic lines (#9-9, #11-5 and #16-4) with WT at 4-days post-inoculation (dpi). Knocking out *ObDMR1* in Genoveser increased the resistance to *P. belbahrii* by suppressing the pathogen proliferation and suppressing the overall disease incidence as well as severity (Figure 4.8, 4.9a, 4.9b, and 4.9c). This result falls in line with other reports of *DMR1* homologs, which upon impairment in Arabidopsis, tomato and potato resulted in resistance against downy mildew, powdery mildew, and late blight disease, respectively (Huibers et al., 2013, Sun et al., 2016, Van Damme et al., 2005, van Damme et al., 2009).

Off-target effects were theoretically limited or absent due to the rigorous designing of sgRNA based on the available transcriptomic sequences (Torre et al., 2016). Our study generated mostly small mutations (1-2 bp) insertion or deletion in *ObDMR1* targeted site 1, known to be a common feature in other reports as well which is a consequence of CRISPR/Cas9 gene editing (Nishitani et al., 2016, Wang et al., 2018a, Zhou et al., 2018). The validity and efficiency of the entire CRISPR/Cas9 gene-editing tool-kit used in this study depends on two main segments of the vector, one is CaMV 35S-driven zCas9 expression cassette and the other is RNA polymerase III (Pol III)-driven sgRNA expression cassette. A study suggests that the use of zCas9, *Zea mays*-codon optimized Cas9 works considerably better than human-codon optimized Cas9 (Xing et al., 2014). In contrast, the transcriptional activity of Pol III promoter plays a significant role in determining the mutation efficiency by CRISPR/Cas9 (Wang et al., 2018). A report demonstrated that AtU6-26 displays the highest transcriptional activity in model dicot plant Arabidopsis compared to AtU6-1 and AtU6-29 (Li et al., 2007). In our study, both AtU6-26 and AtU6-29 were introduced to drive the expression of sgRNA1 and sgRNA2, respectively. Given the high-efficacy of AtU6-26 promoter, we believe the AtU6-26 promoter qualified to mediate *ObDMR1* targeted-editing in *the O. basilicum* genome at target site 1 site with 92% efficiency found among the 54 tested T0 lines. In contrast, a very low frequency of mutations occurred at target site 2, driven by AtU6-29, which could be one of the reasons of low mutation efficiency. Apart from the expression of Cas9 and sgRNA, CRISPR/Cas9-induced mutations in plants are also affected by the GC content within sgRNA sequence composition and secondary structure of sgRNA

impacting the overall editing efficiency (Ma et al., 2015, Tang et al., 2018). In our study, we used two different sgRNA with varying GC content of 40% and 55%, respectively. It is possible that a lower GC percent in sgRNA works more efficiently for basil gene editing, but this needs to be further verified with more experiments. It has also been reported that the 3'end of sgRNAs, also known as 'seed region,' holds a determining factor in the recognition efficiency of sgRNA to its target (Zhang et al., 2014, Yan et al., 2015), which is another important consideration to cause probable mutations at targeted sites.

Thus, the CRISPR/Cas9 system developed for sweet basil in this study demonstrate to serve as an ideal tool for molecular breeding and developing resistant varieties. Given the high editing efficiency of the CRISPR/Cas9 system developed for sweet basil, it has the potential to construct a genome-wide mutant library in sweet basil, accelerating gene functional analysis.

4.5.   References

Ben-Naim Y, Falach L, Cohen Y, 2018. Transfer of downy mildew resistance from wild basil (Ocimum americanum) to sweet basil (O. basilicum). *Phytopathology* **108**, 114-23.

Borrelli VMG, Brambilla V, Rogowsky P, Marocco A, Lanubile A, 2018. The enhancement of plant disease resistance using CRISPR/Cas9 Technology. *Front Plant Sci* **9**, 1245.

Cohen Y, Ben Naim Y, Falach L, Rubin AE, 2017. Epidemiology of basil downy mildew. *Phytopathology* **107**, 1149-60.

Cohen Y, Vaknin M, Ben-Naim Y*, et al.*, 2013. First report of the occurence and resistance to mefenoxam of Peronospora belbahrii, causal agent of downy mildew of basil (Ocimum basilicum) in Isreal. *Plant Disease* **97**, 692.

Da Costa AS, Arrigoni-Blank MF, De Carvalho Filho JLS*, et al.*, 2015. Chemical diversity in basil germplasm. *The Scientific World Journal*.

Deschamps C, Simon JE, 2002. Agrobacterium tumefaciens-mediated transformation of Ocimum basilicum and O. citriodorum. *Plant Cell Reports* **21**, 359-64.

Dong OX, Ronald PC, 2019. Genetic engineering for disease resistance in plants: Recent progress and future perspectives. *Plant Physiol* **180**, 26-38.

Gao X, Chen J, Dai X, Zhang D, Zhao Y, 2016. An effective strategy for reliably isolating heritable and Cas9-Free Arabidopsis mutants generated by CRISPR/Cas9-mediated genome editing. *Plant Physiol* **171**, 1794-800.

Haque E, Taniguchi H, Hassan MM*, et al.*, 2018. Application of CRISPR/Cas9 genome editing technology for the improvement of crops cultivated in tropical climates: recent progress, prospects, and challenges. *Front Plant Sci* **9**, 617.

Hok S, Danchin EG, Allasia V, Panabieres F, Attard A, Keller H, 2011. An Arabidopsis (malectin-like) leucine-rich repeat receptor-like kinase contributes to downy mildew disease. *Plant Cell Environ* **34**, 1944-57.

Hsiau T, Maures T, Waite K*, et al.*, 2018. Inference of CRISPR edits from sanger trace data. *bioRxiv* doi: https://doi.org/10.1101/251082.

Huibers RP, Loonen AE, Gao D, Van Den Ackerveken G, Visser RG, Bai Y, 2013. Powdery mildew resistance in tomato by impairment of SlPMR4 and SlDMR1. *PLoS One* **8**, e67467.

Jaganathan D, Ramasamy K, Sellamuthu G, Jayabalan S, Venkataraman G, 2018. CRISPR for crop improvement: an update review. *Front Plant Sci* **9**, 985.

Jiang F, Doudna JA, 2017. CRISPR-Cas9 structures and mechanisms. *Annu Rev Biophys* **46**, 505-29.

Jinek M, Chylinski K, Fonfara I, Hauer M, Doudna JA, Charpentier E, 2012. A programmable dual-RNA-guided DNA endonuclease in adaptive bacterial immunity. *Science* **337**, 816-21.

Jinek M, East A, Cheng A, Lin S, Ma E, Doudna J, 2013. RNA-programmed genome editing in human cells. *Elife* **2**, e00471.

Jorgensen JH, 1992. Discovery, characterization and exploitation of Mlo powdery mildew resistance in barley. *Euphytica* **63**, 141-52.

Langner T, Kamoun S, Belhaj K, 2018. CRISPR crops: plant genome editing toward disease resistance. *Annu Rev Phytopathol* **56**, 479-512.

Larkin MA, Blackshields G, Brown NP, *et al.*, 2007. Clustal W and Clustal X version 2.0. *Bioinformatics* **23**, 2947-8.

Ma X, Zhang Q, Zhu Q, *et al.*, 2015. A robust CRISPR/Cas9 system for convenient, high-efficiency multiplex genome editing in monocot and dicot plants. *Mol Plant* **8**, 1274-84.

Ma X, Zhu Q, Chen Y, Liu YG, 2016. CRISPR/Cas9 platforms for genome editing in plants: developments and applications. *Mol Plant* **9**, 961-74.

Marchler-Bauer A, Bo Y, Han L, *et al.*, 2017. CDD/SPARCLE: functional classification of proteins via subfamily domain architectures. *Nucleic Acids Res* **45**, D200-D3.

Nekrasov V, Wang C, Win J, Lanz C, Weigel D, Kamoun S, 2017. Rapid generation of a transgene-free powdery mildew resistant tomato by genome deletion. *Sci Rep* **7**, 482.

Nie J, Wang Y, He H, *et al.*, 2015. Loss-of-function mutations in CsMLO1 confer durable powdery mildew resistance in cucumber (Cucumis sativus L.). *Front Plant Sci* **6**, 1155.

Nishitani C, Hirai N, Komori S, *et al.*, 2016. Efficient genome editing in apple using a CRISPR/Cas9 system. *Sci Rep* **6**, 31481.

Pan C, Ye L, Qin L, *et al.*, 2016. CRISPR/Cas9-mediated efficient and heritable targeted mutagenesis in tomato plants in the first and later generations. *Sci Rep* **6**, 24765.

Peng D, Tarleton R, 2015. EuPaGDT: a web tool tailored to design CRISPR guide RNAs for eukaryotic pathogens. *Microb Genom* **1**, e000033.

Phippen WB, Simon JE, 2000. Anthocyanin inheritance and instability in purple basil (Ocimum basilicum L.). *J Hered* **91**, 289-96.
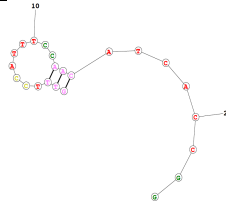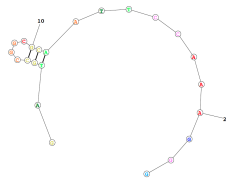
Pyne RM, Honig JA, Vaiciunas J, Wyenandt CA, Simon JE, 2018. Population structure, genetic diversity and downy mildew resistance among Ocimum species germplasm. *BMC Plant Biol* **18**, 69.

Rehrig WZ, Ashrafi H, Hill T, Prince J, Deynze AV, 2014. CaDMR1 cosegregates with QTL Pc5.1 for resistance to Phytophthora capsici in pepper (Capsicum annuum). *The Plant Genome* **7**, 1-12.

Reuter JS, Mathews DH, 2010. RNAstructure: software for RNA secondary structure prediction and analysis. *BMC Bioinformatics* **11**, 129.

Shao D, Tian M, 2018. A qPCR approach to quantify the growth of basil downy mildew pathogen Peronospora belbarhii during infection. *Current Plant Biology* **15**, 2-7.

Sun K, Wolters AM, Vossen JH*, et al.*, 2016. Silencing of six susceptibility genes results in potato late blight resistance. *Transgenic Res* **25**, 731-42.

Svitashev S, Young JK, Schwartz C, Gao H, Falco SC, Cigan AM, 2015. Targeted mutagenesis, precise gene editing, and site-specific gene insertion in maize using Cas9 and guide RNA. *Plant Physiol* **169**, 931-45.

Tang T, Yu X, Yang H*, et al.*, 2018. Development and validation of an effective CRISPR/Cas9 vector for efficiently isolating positive transformants and transgene-free mutants in a wide range of plant species. *Front Plant Sci* **9**, 1533.

Torre S, Tattini M, Brunetti C*, et al.*, 2016. De Novo Assembly and Comparative Transcriptome Analyses of Red and Green Morphs of Sweet Basil Grown in Full Sunlight. *PLoS One* **11**, e0160370.

Van Damme M, Andel A, Huibers RP, Panstruga R, Weisbeek PJ, Van Den Ackerveken G, 2005. Identification of arabidopsis loci required for susceptibility to the downy mildew pathogen Hyaloperonospora parasitica. *Mol Plant Microbe Interact* **18**, 583-92.

Van Damme M, Huibers RP, Elberse J, Van Den Ackerveken G, 2008. Arabidopsis DMR6 encodes a putative 2OG-Fe(II) oxygenase that is defense-associated but required for susceptibility to downy mildew. *Plant J* **54**, 785-93.

Van Damme M, Zeilmaker T, Elberse J, Andel A, De Sain-Van Der Velden M, Van Den Ackerveken G, 2009. Downy mildew resistance in Arabidopsis by mutation of homoserine kinase. *Plant Cell* **21**, 2179-89.

Van Schie CC, Takken FL, 2014. Susceptibility genes 101: how to be a good host. *Annu Rev Phytopathol* **52**, 551-81.

Waltz E, 2016. Gene-edited CRISPR mushroom escapes US regulation. *Nature* **532**, 293.

Wang F, Wang C, Liu P*, et al.*, 2016a. Enhanced rice blast resistance by CRISPR/Cas9-targeted mutagenesis of the ERF transcription factor gene OsERF922. *PLoS One* **11**, e0154027.

Wang S, Zhang S, Wang W, Xiong X, Meng F, Cui X, 2015a. Efficient targeted mutagenesis in potato by the CRISPR/Cas9 system. *Plant Cell Rep* **34**, 1473-6.

Wang X, Tu M, Wang D*, et al.*, 2018a. CRISPR/Cas9-mediated efficient targeted mutagenesis in grape in the first generation. *Plant Biotechnol J* **16**, 844-55.

Wang Y, Cheng X, Shan Q*, et al.*, 2014. Simultaneous editing of three homoeoalleles in hexaploid bread wheat confers heritable resistance to powdery mildew. *Nat Biotechnol* **32**, 947-51.

Wang ZP, Xing HL, Dong L*, et al.*, 2015b. Egg cell-specific promoter-controlled CRISPR/Cas9 efficiently generates homozygous mutants for multiple target genes in Arabidopsis in a single generation. *Genome Biol* **16**, 144.

Wyenandt CA, Simon JE, Mcgrath MT, Ward DL, 2010. Susceptibility of basil cultivars and breeding lines to downy mildew (*Peronospora belbahrii*). *HortScience* **45**, 1416-9.

Wyenandt CA, Simon JE, Pyne RM*, et al.*, 2015. Basil downy mildew (Peronospora belbahrii): discoveries and challenges relative to its control. *Phytopathology* **105**, 885-94.

Xing HL, Dong L, Wang ZP*, et al.*, 2014. A CRISPR/Cas9 toolkit for multiplex genome editing in plants. *BMC Plant Biol* **14**, 327.

Yan M, Zhou SR, Xue HW, 2015. CRISPR Primer Designer: design primers for knockout and chromosome imaging CRISPR-Cas system. *J Integr Plant Biol* **57**, 613-7.

Zaidi SS, Mukhtar MS, Mansoor S, 2018. Genome editing: targeting susceptibility genes for plant disease resistance. *Trends Biotechnol* **36**, 898-906.

Zhang H, Zhang J, Wei P*, et al.*, 2014. The CRISPR/Cas9 system produces specific and homozygous targeted gene editing in rice in one generation. *Plant Biotechnol J* **12**, 797-807.

Zhang Z, Hua L, Gupta A*, et al.*, 2019. Development of an agrobacterium-delivered CRISPR/Cas9 system for wheat genome editing. *Plant Biotechnol J* **17**, 1623-35.

Zhou J, Wang G, Liu Z, 2018. Efficient genome editing of wild strawberry genes, vector development and validation. *Plant Biotechnol J* **16**, 1868-77.

Tables

Table 4.1. Characteristics of the two selected sgRNA target sequences

TARGET	SEQUENCE	PAM	GC%	TOTAL SCORE	EFFICIENCY SCORE	OFF-TARGET	RNA SECONDARY STRUCTURE
1	GTTTCCATTTCCAACATCAC	CGG	40	0.56	0.55	NO	
2	GATGCCGGCGCAATTCCAAA	GGG	55	0.54	0.61	NO	

Figures

```
Genoveser ObDMR1   ATGGCCGCCGTCTGCCTGAAGCTCAACTTCGCCGCCGCCGCCGCCGCCTCCGCCTCCGCAACCACCGTCGCCAACCTATCATCACCAAAGCCCCAAACCC
RR and T ObDMR1    ------A---------------------------------------------------------------------------------------------
ObDMR1               M  A  A  V  C  L  K  L  N  F  A  A  A  A  A  A  S  A  S  A  T  T  V  A  N  L  S  S  P  K  P  Q  T
                           T
```

```
Genoveser ObDMR1   ACTTAAGATTCAACCCATCCGCATCCGCACTATCAACATCCGCTTATTCCAAATCCACTGAGCCTCTACCCGTCTTCTCCTCCGTCAAATCTTTCGCCCC
RR and T ObDMR1    ----------------------------------------------------------------------------------------------------
ObDMR1               H  L  R  F  N  P  S  A  S  A  L  S  T  S  A  Y  S  K  S  T  E  P  L  P  V  F  S  S  V  K  S  F  A
```

```
Genoveser ObDMR1   CGCCACCGTCGCCAACTTGGGCCCTGGCTTCGACTTTCTGGGATGCGCCGTAGACGGAATCGGCGACTACGTCAGCCTCCGAGTCGATCCAGACGTGCAC
RR and T ObDMR1    -----------------------A------------------------T---------------------------------------------------
ObDMR1               P  A  T  V  A  N  L  G  P  G  F  D  F  L  G  C  A  V  D  G  I  G  D  Y  V  S  L  R  V  D  P  D  V  H
```

```
Genoveser ObDMR1   CCCGGCGAAGTTTCCATTTCCAACATCACCGGCGCCGGCTCCAAGCTCAGCAAGAACCCCCTTTGGAATTGCGCCGGCATCGCCGCCATCGCCGTCATGA
RR and T ObDMR1    ------------------------------------------------------------------C---------------------------------
ObDMR1               P  G  E  V  S  I  S  N  I  T  G  A  G  S  K  L  S  K  N  P  L  W  N  C  A  G  I  A  A  I  A  V  M
```

```
Genoveser ObDMR1   AAATGCTCAGCATCCGCTCCGTGGGTCTCTCGCTCTCTCTCGAAAAGGGCCTCCCTCTGGGCAGCGGCCTCGGCTCCAGCGCGGCCAGCGCCGCCGCAGC
RR and T ObDMR1    -----------------------------------------------------------C---------------------------T------------
ObDMR1               K  M  L  S  I  R  S  V  G  L  S  L  S  L  E  K  G  L  P  L  G  S  G  L  G  S  S  A  A  S  A  A  A
```

```
Genoveser ObDMR1   TGCTGTCGCTGTAAACGAGTTGTTCGGGGGGTCCTCTGTCGCCGTCAGAACTCGTGTTCGCCGGTCTGGAGTCTGAGGCGAAGGTCTCCGGCTACCACGCG
RR and T ObDMR1    ---C---------------------------------------------------------------------------------------------------C
ObDMR1               A  A  V  A  V  N  E  L  F  G  G  P  L  S  P  S  E  L  V  F  A  G  L  E  S  E  A  K  V  S  G  Y  H  A
```

```
Genoveser ObDMR1   GACAACGTGGCGCCGTCGATCTTGGGAGGTTTCGTTTTGATACGCAGCTACGACCCTTTGGAACTGATGCAACTAAAGTTTCCCCATGAGAAAAGCTTGT
RR and T ObDMR1    ----------------------------------------------------------------------------------------------------
ObDMR1               D  N  V  A  P  S  I  L  G  G  F  V  L  I  R  S  Y  D  P  L  E  L  M  Q  L  K  F  P  H  E  K  S  L
```

```
Genoveser ObDMR1   ATTTCGTGCTGGTGAATCCGGAATTCGAAGCCCCAACGAAGAAGATGAGAGCGGCGTTGCCGCAGGAAATCACGATGTCGCACCACATATGGAATTCCAG
RR and T ObDMR1    ----------------------------------------------------------------------------------------------------
ObDMR1               Y  F  V  L  V  N  P  E  F  E  A  P  T  K  K  M  R  A  A  L  P  Q  E  I  T  M  S  H  H  I  W  N  S
```

```
Genoveser ObDMR1   CCAAGCTGGGGCTTTGGTTGCGTCTGTTTTGCAAGGCGATCTCGTTGGGTTAGGAAAGGCGCTGTCATCGGATAAGATTGTGGAGCCGAAGAGGGCTCCT
RR and T ObDMR1    ----------------------------------------------------------------------------------------------------
ObDMR1               S  Q  A  G  A  L  V  A  S  V  L  Q  G  D  L  V  G  L  G  K  A  L  S  S  D  K  I  V  E  P  K  R  A  P
```

```
Genoveser ObDMR1   TTGATTCCGGGCATGGAAGCTGTGAAGAAAGCTGCCATCGCAGCAGGGGCGTTTGGTTGCACGATAAGTGGAGCTGGACCAACTGCGGTGGCGGTGACAG
RR and T ObDMR1    -----------------------------------T--G-------------------------------------------------------------
ObDMR1               L  I  P  G  M  E  A  V  K  K  A  A  I  A  A  G  A  F  G  C  T  I  S  G  A  G  P  T  A  V  A  V  T
```

```
Genoveser ObDMR1   ACAGTGAGGAAAAAGGTAGAGAAATTGGGGAGAAAATGGTGGAGGCTTTTGAGAAAGAAGGGAACTTGAAGGCTTTGGCAATGGTGAGGCAGCTTGATAG
RR and T ObDMR1    ----------------------------------------------------------------------------------------------------
ObDMR1               D  S  E  E  K  G  R  E  I  G  E  K  M  V  E  A  F  E  K  E  G  N  L  K  A  L  A  M  V  R  Q  L  D
```

```
Genoveser ObDMR1   AGTTGGAGCTAGGCTTGTCAGCAGTGTTCCCAGATGA
RR and T ObDMR1    -------------------------------------
ObDMR1               R  V  G  A  R  L  V  S  S  V  P  R
```

Figure 4.1. Nucleotide sequence alignment of homologs of DMR1 for three basil varieties-Genoveser, Red Rubin (RR) and Tigullio (T) (Torre et al., 2016), where dash lines represent same nucleotides. The amino acid within the three varieties is also represented in the figure with one amino acid difference highlighted in yellow.

```
ObDMR1     1  MAAVCLKLNFAAAAAASASATTVANLSSPKPQTHLRFNPSASALSTSAYSKSTEPLPVFS
AtDMR1     1  MASLCFQS-------PSKPISYFQPKSNPSPPLFAKVSVFRCRASVQTL-VAVEPEPVFV

ObDMR1    61  SVKSFAPATVANLGPGFDFLGCAVDGIGDYVSLRVDPDVHPGEVSISNITGAGSKLSKNP
AtDMR1    53  SVKTFAPATVANLGPGFDFLGCAVDGLGDHVTLRVDPSVRAGEVSISEITGTTTKLSTNP

ObDMR1   121  LWNCAGIAAIAVMKMLSIRSVGLSLSLEKGLPLGSGLGSSAASAAAAAVAVNELFGGPLS
AtDMR1   113  LRNCAGIAAIATMKMLGIRSVGLSLDLHKGLPLGSGLGSSAASAAAAAVAVNEIFGRKLG

ObDMR1   181  PSELVFAGLESEAKVSGYHADNVAPSILGGFVLIRSYDPLELMQLKFPHEKSLYFVLVNP
AtDMR1   173  SDQLVLAGLESEAKVSGYHADNIAPAIMGGFVLIRNYEPLDLKPLRFPSDKDLFFVLVSP

ObDMR1   241  EFEAPTKKMRAALPQEITMSHHIWNSSQAGALVASVLQGDLVGLGKALSSDKIVEPKRAP
AtDMR1   233  DFEAPTKKMRAALPTEIPMVHHVWNSSQAAALVAAVLEGDAVMLGKALSSDKIVEPTRAP

ObDMR1   301  LIPGMEAVKKAAIAAGAFGCTISGAGPTAVAVTDSEEKGREIGEKMVEAFEKEGNLKALA
AtDMR1   293  LIPGMEAVKKAALEAGAFGCTISGAGPTAVAVIDSEEKGQVIGEKMVEAFWKVGHLKSVA

ObDMR1   361  MVRQLDRVGARLVSSVPR
AtDMR1   353  SVKKLDNVGARLVNSVSR
```

Figure 4.2. Amino acid sequence alignment of ObDMR1 and AtDMR1. Sequences were aligned using CLUSTALX 2.1 and displayed with BOXSHADE. The identical and similar amino acids are shaded.

(a)

ATGGCCGCCGTCTGCCTGAAGCTCAACTTCGCCGCCGCCGCCGCCGCCTCCGCCTCCGCAACCACCGTCGCCAACCTATCATCACCAAAGCCCCAAACCC

ACTTAAGATTCAACCCATCCGCATCCGCACTATCAACATCCGCTTATTCCAAATCCACTGAGCCTCTA*CCCGTCTTCTCCTCCGTCAAAT*CTTTCGCCCC
                                                                                    DMR1-CRISPR-F →

CGCCACCGTCGCCAACTTGGGCCCTGGCTTCGACTTTCTGGGATGCGCCGTAGACGGAATCGGCGACTACGTCAGCCTCCGAGTCGATCCAGACGTGCAC

                                                                    TARGET 2
                                                    3´–<u>GGG</u>**AAACCTTAACGCGGCCGTAG**–5´
                                                        ||||||||||||||||||
CCCGGCGAA**GTTTCCATTTCCAACATCAC**<u>CGG</u>CGCCGGCTCCAAGCTCAGCAAGAACCCCCTTTGGAATTGCGCCGGCATCGCCGCCATCGCCGTCATGA
          TARGET 1

AAATGCTCAGCATCCGCTCCGTGGGTCTCTCGCTCTCTCTCGAAAAGGGCCTCCCTCTGGGCAGCGGCCTCGGCTCCAGCGCGGCCAGCGCCGCCGCAGC

TGCTGTCGCTGTAAACGAGTTGTTCGGG*GGTCCTCTGTCGCCGTCAGAACT*CGTGTTCGCCGGTCTGGAGTCTGAGGCGAAGGTCTCCGGCTACCACGCG

                            ← **DMR1-CRISPR-R**
GACAACGTGGCGCCGTCGATCTTGGGAGGTTTCGTTTTGATACGCAGCTACGACCCTTTGGAACTGATGCAACTAAAGTTTCCCCATGAGAAAAGCTTGT

ATTTCGTGCTGGTGAATCCGGAATTCGAAGCCCCAACGAAGAAGATGAGAGCGGCGTTGCCGCAGGAAATCACGATGTCGCACCACATATGGAATTCCAG

CCAAGCTGGGGCTTTGGTTGCGTCTGTTTTGCAAGGCGATCTCGTTGGGTTAGGAAAGGCGCTGTCATCGGATAAGATTGTGGAGCCGAAGAGGGCTCCT

TTGATTCCGGGCATGGAAGCTGTGAAGAAAGCTGCCATCGCAGCAGGGGCGTTTGGTTGCACGATAAGTGGAGCTGGACCAACTGCGGTGGCGGTGACAG

ACAGTGAGGAAAAAGGTAGAGAAATTGGGGAGAAAATGGTGGAGGCTTTTGAGAAAGAAGGGAACTTGAAGGCTTTGGCAATGGTGAGGCAGCTTGATAG
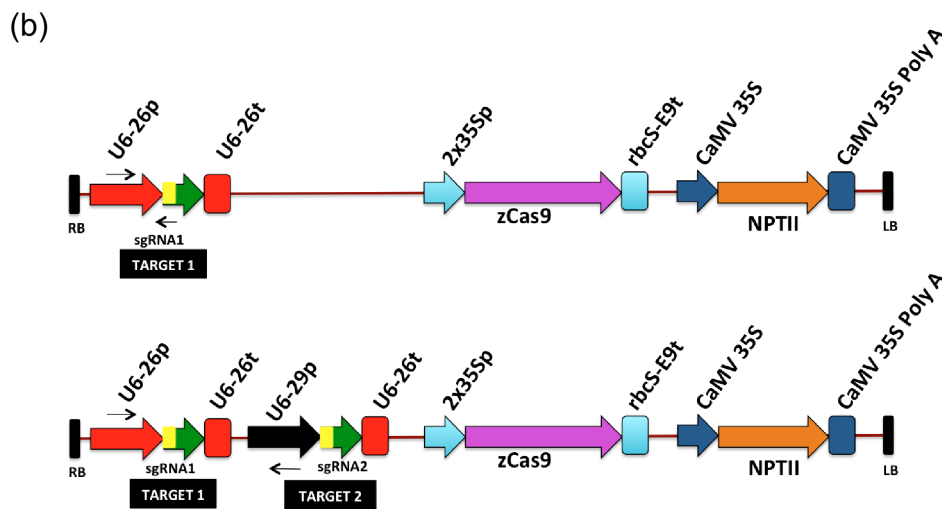
AGTTGGAGCTAGGCTTGTCAGCAGTGTTCCCAGATGA

(b)

Figure 4.3. Target sites and constructs used for targeted mutagenesis of *ObDMR1*. (a) The protein encoding sequence of Genoveser ObDMR1 with two sgRNA target sequences (Target 1 and Target 2) marked in bold and PAM sites underlined. The sequences of the primers (DMR1-CRISPR-F and DMR1-CRISPR-R) used to amplify *ObDMR1* fragment for mutation analyses are marked with black arrows. (b) Schematic representations of expression cassettes within the T-DNA of pKSE401-sgRNA1 and pKSE401-sgRNA1+2. The elements were described in Xing et al. (2014). The primer pairs (U6-26p-F and DMR1-target1-R, U6-26p-F and U6-29p-R) used for detecting the transgene integration in plants transformed with pKSE401-sgRNA1 and pKSE401-sgRNA1+2 are indicated by arrows.
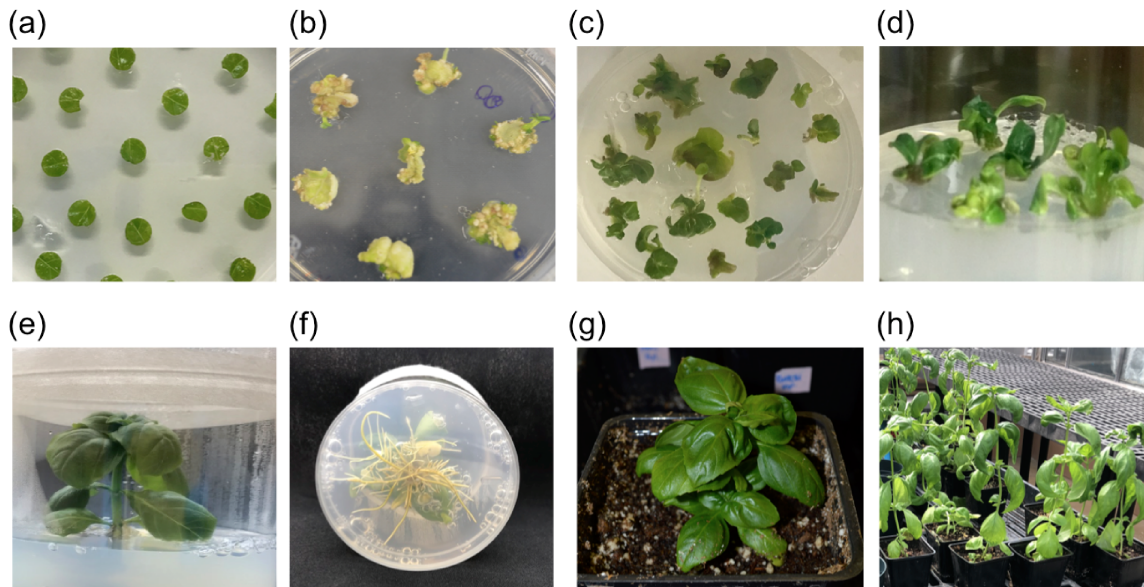
Figure 4.4. Transformation and regeneration of sweet basil. **(a)** Co-cultivation of leaf explants with *Agrobacteria* on callus and shoot induction (SI) media containing acetosyringone in dark for 3 days. **(b)** Callus formation and shoot regeneration on SI media with kanamycin selection after 2 weeks in dark. **(c)** Individual sprouting shoots placed on Root Induction (RI) media with kanamycin for shoot elongation and root development. **(d)** Plantlets formed on RI media with kanamycin. **(e)** and **(f)** Well developed transgenic plants. **(g)** Acclimatization of a plantlet in soil. **(h)** Plants in the greenhouse for seed production.
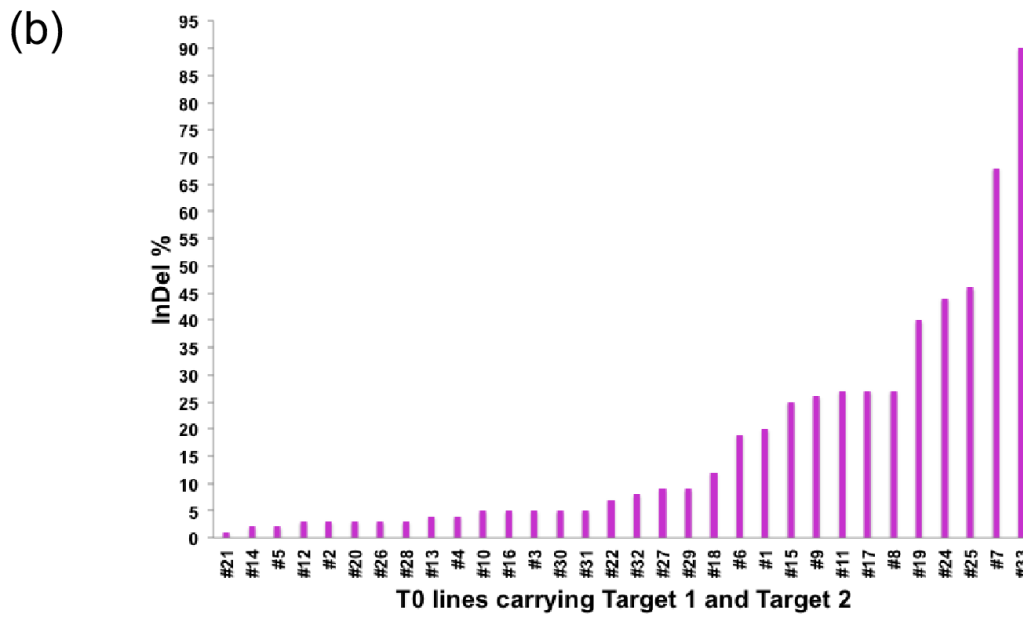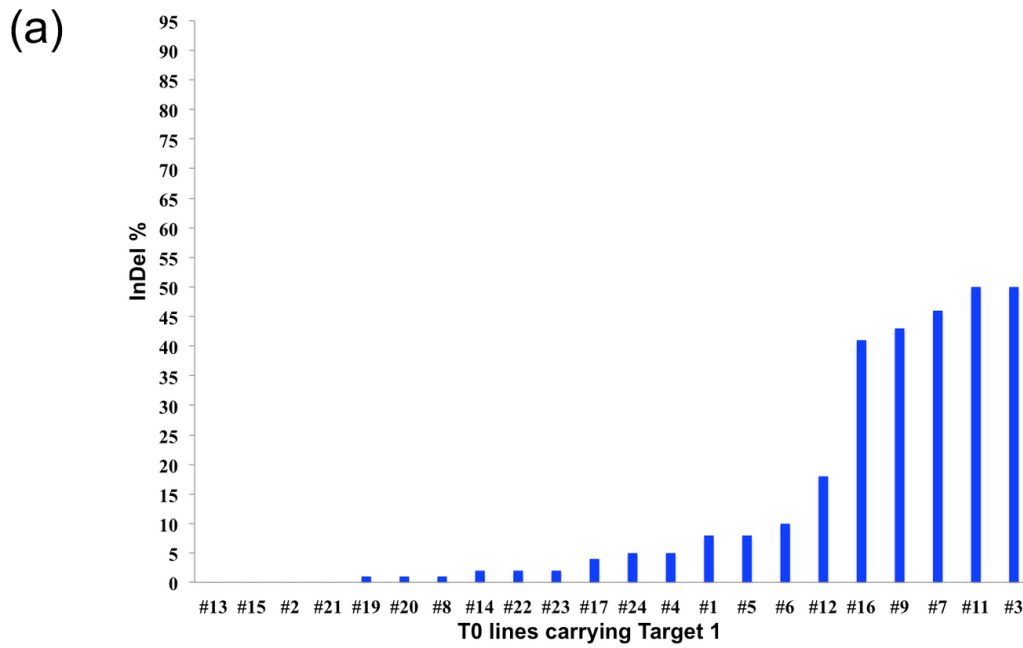
Figure 4.5. Indel frequency (%) at target site 1 in T0 transgenic Genoveser lines transformed with the CRISPR/Cas9 constructs expressing one sgRNA **(a)** or two sgRNAs **(b)**.

```
                TARGET 1          PAM
            GTTTCCATTTCCAACAT-CACCGG
CGTGCACCCCGGCGAAGTTTCCATTTCCAACAT-CACCGGCGCCGG  WT
CGTGCACCCCGGCGAAGTTTCCATTTCCAACATtCACCGGCGCCGG  +1(T)
CGTGCACCCCGGCGAAGTTTCCATTTCCAACATgCACCGGCGCCGG  +1(G)
CGTGCACCCCGGCGAAGTTTCCATTTCCAACATcCACCGGCGCCGG  +1(C)
CGTGCACCCCGGCGAAGTTTCCATTTCCAACA--CACCGGCGCCGG  -1(T)
CGTCCACCCCGGCGAAGTTTCCATTTCCAAC---CACCGGCGCCGG  -2(AT)
CGTGCACCCCGGCGAAGTTTCCATTTCCAA----CACCGGCGCCGG  -3(CAT)
CGTCCACC-------------------------CACCGGCGCCGG   -25
```

	PLANT ID (% READS)				
7(24)	9(51)	11(67)	16(66)	24(51)	
7(46)	9(46)	11(31)			
			16(32)		33(36)
				24(34)	
7(19)	9(1)	11(1)	16(0.6)		33(34)
7(8)					33(14)
7(1)					33(15)
				24(13)	

Figure 4.6. Mutation types at Target 1 site and distribution in six independent T0 transgenic sweet basil lines, determined by amplicon deep sequencing. The different insertions are marked in small case and deletions are indicated using boxed dashed lines. The 20-nt target sequence of Target 1 and the downstream PAM site (underlined) are marked in bold. The identities (IDs) of T0 transgenic plants are shown in numbers, with 9, 11 and 16 carrying one sgRNA, and 7, 24 and 33 carrying two sgRNAs, The percentage of reads corresponding to a mutation type in each line is shown using a number in red in a parenthesis.
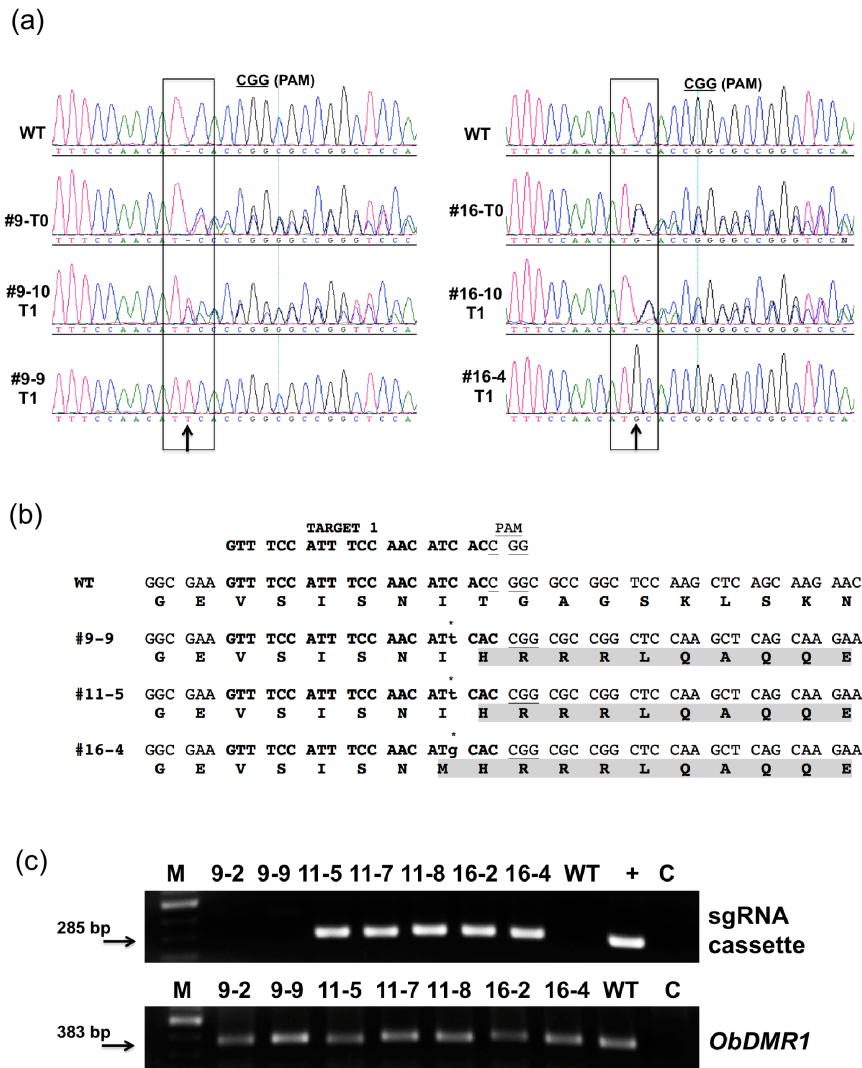
Figure 4.7. Characterization of *ObDMR1* homozygous mutant sweet basil plants in T1 generation. (a) Chromatograms of the *ObDMR1* fragments from the wild-type (WT), T0 lines #9 and #16 (#9-T0, #16-T0) and their derived T1 plants with heterozygous (#9-10, #16-10) and homozygous mutations (#9-9 and #16-4). The inserted 'T' and 'G' are indicated with an arrow. (b) Representation of the frameshift mutation (shaded in grey) of ObDMR1 in homozygous T1 transgenic lines (#9-9, #11-5 and #16-4) compared to WT at target 1. Letters in lower case (below asterisk) indicate mutation at target 1 (bold) where PAM site is underlined. (c) Agarose gel images showing PCR amplification of the sgRNA cassette (upper panel) and *ObDMR1* (lower panel) from WT and indicated homozygote T1 lines. +, pKSE401-sgRNA1; C, no template negative control; M:100bp ladder. The sizes of the corresponding bands are indicated with arrows.

Figure 4.8. Dwarfing phenotype exhibited by T1-homozygous mutant sweet basil lines at young seedling stage in comparison to WT (control). Lines #9-2, #9-9, #11-5, #11-7 and #11-8 contain 1-bp 'T' insertion and #16-4 carries 1-bp 'G' insertion within the *ObDMR1* sequence. 18-days old plants were used to take photographs.
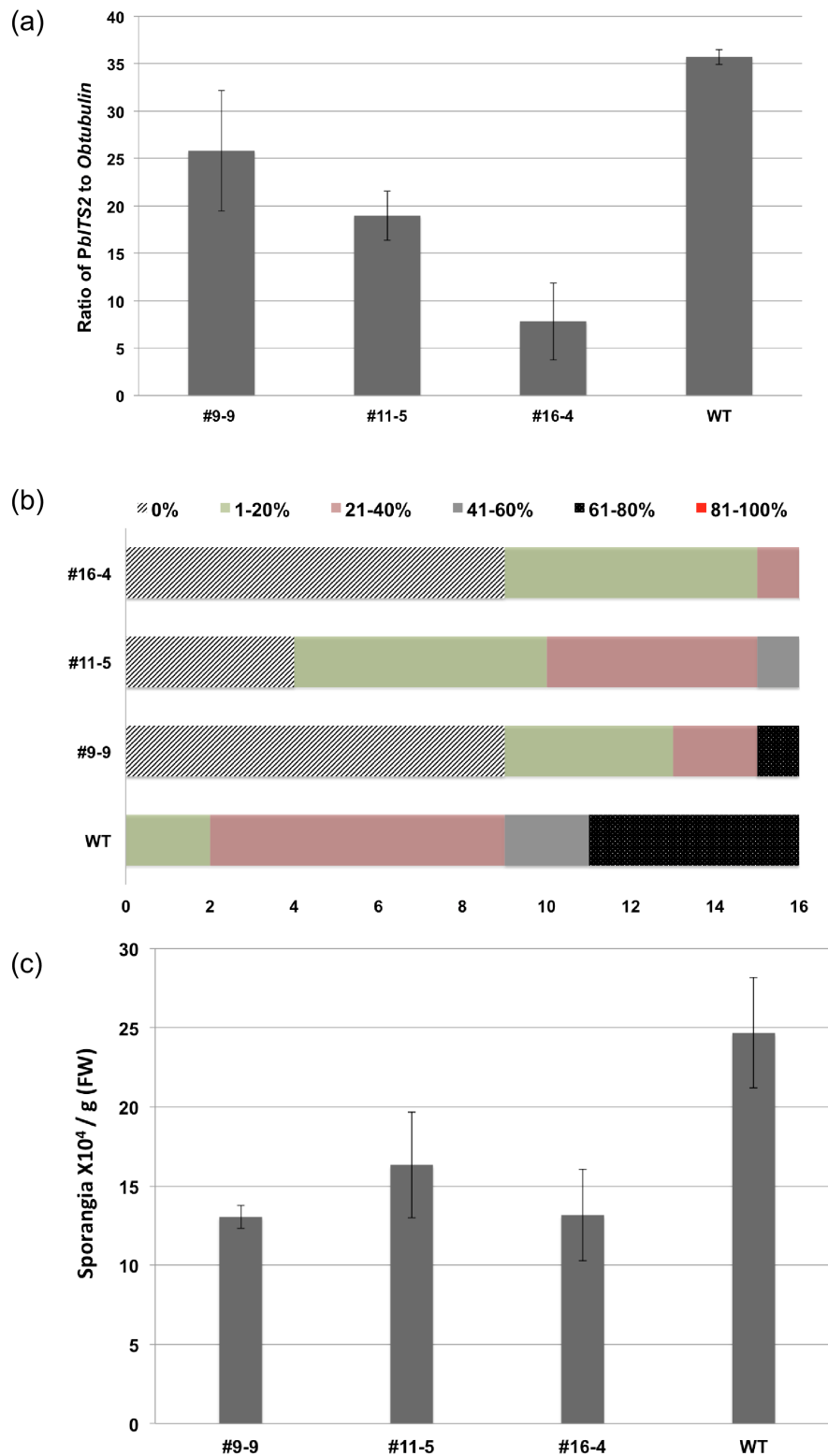
Figure 4.9. Targeted mutagenesis of *ObDMR1* in T2 Genoveser plants reduces susceptibility to *Peronospora belbahrii*. (a) Quantification of pathogen biomass determined by qPCR. Infected leaf samples were collected from the wild-type (WT) and mutant plants at 4 days post inoculation (dpi). The pathogen biomass was quantified as the ratio of

amplification of *P. belbahrii ITS2* relative to *O. basilicum β-tubulin*. Values represent mean ± standard deviation of three biological replicates with each having three technical replicates. This experiment was performed thrice, displaying similar trend as shown. **(b)** The number of leaves with indicated percentages of leaf areas showing sporulation at 7 dpi. **(c)** The abundance of sporangia on inoculated leaves at 9 dpi, calculated as the number of sporangia per gram of fresh weight. Error bars represent standard error of the mean of three sample replicates.
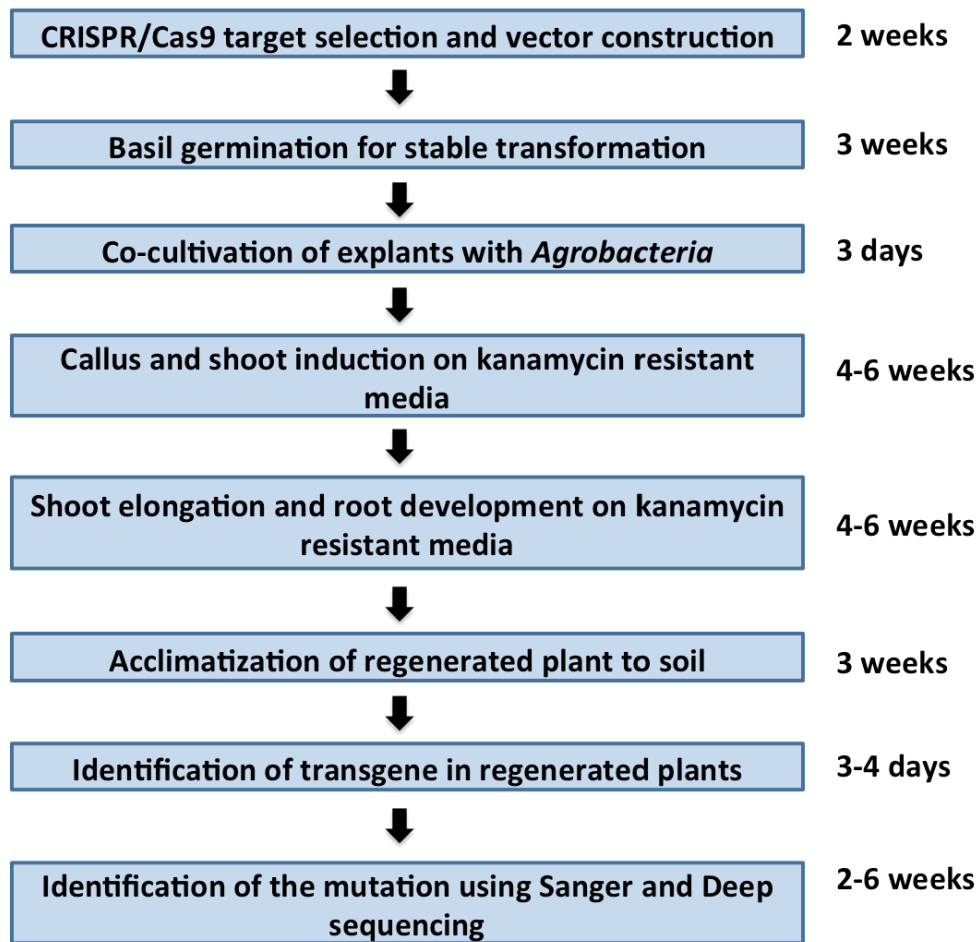
CRISPR/Cas9 target selection and vector construction	2 weeks
Basil germination for stable transformation	3 weeks
Co-cultivation of explants with *Agrobacteria*	3 days
Callus and shoot induction on kanamycin resistant media	4-6 weeks
Shoot elongation and root development on kanamycin resistant media	4-6 weeks
Acclimatization of regenerated plant to soil	3 weeks
Identification of transgene in regenerated plants	3-4 days
Identification of the mutation using Sanger and Deep sequencing	2-6 weeks

Figure 4.10. A flow chart depicting CRISPR/Cas9-based targeted gene-editing in sweet basil using *Agrobacterium*-mediated stable transformation. The entire testing period requires a time-period of minimum 7 months.

CHAPTER 5

Future research prospects

Basil downy mildew has posed a major constraint to basil production worldwide. Developing genetic resistance in economically important herb sweet basil (*Ocimum basilicum*) is essential given the risks posed by repeated use of a limited number of available chemicals and the inconvenience of traditional breeding strategies. In order to achieve this, prior understanding of the complex molecular dynamics of basil-*Peronospora belbahrii* interactions is a prerequisite to utilize knowledge-based engineering approaches for developing resistant varieties. In addition, dissecting the molecular basis of sweet basil resistance and its pathogen *Peronospora belbahrii* virulence at the host-pathogen interface will enable researchers to deploy effective and sustainable control strategies. The study of this pathosystem has been facing challenges owing to the obligate-biotrophic lifestyle of the pathogen, making it recalcitrant to direct transformation. Also, the polyploidy nature of sweet basil adds another layer of complexity. Nonetheless, advancements in science and technology have led to the advent of emerging biotechnological tools enabling the study of plant-pathogen molecular interactions with greater efficiency. The study undertaken in this dissertation work focuses on establishing the essential tools to study sweet basil- *P. belbahrii* interactions and identifying the functions of four genes- two belonging to the host with a potential role in resistance and susceptibility, and the other two being pathogenicity-related genes of *P. belbahrii*.

Oblectin 1 is an L-type lectin domain-containing secreted protein that was identified in a resistant cultivar to be strongly induced during early infection. In contrast, its expression was undetected in a disease-susceptible cultivar. In order to address the functional role of *Oblectin 1* in defense response, four homozygous transgenic lines expressing Oblectin1 in a susceptible cultivar were generated and characterized. The results in this study demonstrate that the ectopic expression of *Oblectin 1* in a susceptible cultivar of sweet basil increased resistance against *P. belbahrii* proliferation. Therefore, secreted lectin-like proteins have the potential to function as a complementary *Peronospora belbahrii* resistance resource among closely related cultivars to provide durable resistance. Since lectin proteins belong to a structurally diverse superfamily, a general consensus to classify them has not been reached yet; therefore, a comprehensive study is required to gather information about Oblectin 1

protein structure and conformation. Oblectin 1 protein detection via immunoblot analysis will reveal protein properties including, size and modification forms since it carries a predicted N-linked glycosylation site for potential post-translational modification. To confirm the predicted N-glycosylation site, a general glycoproteomics assay can be later performed. Also, the homozygous transgenic lines developed in this study can be used to evaluate whether Oblectin 1 is a glycosylated protein by subjecting the total protein extract to enzymatic deglycosylation. Cellular and biochemical evidence is further required to confirm that Oblectin 1 has carbohydrate-binding characteristics using carbohydrate interaction assays. The homozygous transgenic sweet basil lines expressing the double HA-tagged Oblectin1 at the C-terminus can be used as a valuable experimental material for further analysis of the components required for *Oblectin1*-mediated resistance via protein complex pull-down assays. As Oblectin 1 harbors a putative cleavable signal peptide sequence at the N-terminal region indicating it to be secretory protein, determining its subcellular localization before and after pathogen inoculation is believed to provide more clarity about the resistance mechanism.

Due to the lack of an efficient method for the direct transformation of obligate-biotrophic pathogen *Peronospora belbahrii*, the functional characterization of essential pathogen genes has been challenging. In recent years, host-induced gene silencing (HIGS) has shown to be a powerful new strategy for the development of transgenic plants to control diseases and a useful tool to study gene functions in obligate biotrophic pathogens. In this study, our results demonstrated the HIGS is operational to silence *P. belbahrii* gene *PbORCER1* in transgenic sweet basil and generate resistance against basil downy mildew (BDM). These results suggest that PbORCER1 is critical for pathogen development and/or infection, and therefore an ideal candidate to be exploited for disease control. The function of another targeted pathogen gene *PbEC1* was inconclusive due to the inconsistency between its knockdown expression for the chosen time course and reduction in pathogen growth. However, molecular validation of the presence of small interfering RNAs (siRNAs) and/or dsRNAs corresponding to *PbORCER1* and *PbEC1* in the respective homozygous transgenic lines is yet to be performed. A positive correlation between the presence of detectable siRNAs and reduction in pathogen growth after inoculation with *P. belbahrii* in homozygous transgenic lines is required to address the cause-effect relationship between silencing of pathogen genes and impairment of pathogen proliferation. Further assessment of the silencing of targeted pathogen genes at different time courses during infection will shed additional light on the function of pathogen genes. Lastly,

the identities and function of host targets of PbORCER1 and PbEC1 are needed to advance our understanding of how *P. belbahrii* controls host cellular machinery at the molecular level to facilitate infection. In the future, it is highly desirable to target multiple pathogenicity-related factors simultaneously in engineered plants to provide robust and durable resistance against BDM.

Mutations of DMR1 gene have been shown to confer resistance against *Hyaloperonospora arabidopsidis* in Arabidopsis, *Oidium neolycopersici* in tomato and *Phytophthora infestans* in potato; exemplifying the potential robustness of targeting this susceptibility (*S*) gene for generating disease resistance. This study demonstrates the applicability of knocking out the DMR1 homolog, ObDMR1 from sweet basil cultivar Genoveser using CRISPR/Cas9, and the compromised susceptibility of sweet basil to *P. belbahrii* due to ObDMR1 mutations. The results from this study contribute to accelerate basil gene functional analysis, promote molecular breeding and enhance the development of resistant varieties for commercial use. The *ObDMR1*-mutant lines generated and tested in this study showed enhanced resistance against pathogen proliferation but still support a certain level of infection under the current given conditions and inoculum quantity, therefore more inoculation assays in controlled lab, greenhouse and field settings are needed to evaluate further their resistance levels and potential to be used in agricultural production. The transgene-free homozygous *ObDMR1*-mutant lines will be further subjected to greenhouse and field trials along with other susceptible and resistant varieties to assess the resistance capability against BDM. The recent developments in CRISPR/Cas9-mediated gene editing provide an invaluable tool to produce reliable true-knockouts, particularly in polyploidy species. The generation of a complete knockout mutant of *ObDMR1* at T0 generation displays a great potential of using CRISPR/Cas9 for gene functional analysis of the tetraploid sweet basil. Also, the ease of identifying transgene-free plants in the successive second generation with heritable mutations at the target site indicates the potential of utilizing the gene-editing technology to breed sweet basil varieties for commercial production.